Development Of Molecular And Cellular Imaging Tools To Evaluate Gene And Cell Based Therapeutic Strategies In Vivo

2011

Jixiang Xia
University of Central Florida

Showcase of Text, Archives, Research & Scholarship

DEVELOPMENT OF MOLECULAR AND CELLULAR IMAGING TOOLS TO
EVALUATE GENE AND CELL BASED THERAPEUTIC STRATEGIES IN VIVO

by

JIXIANG XIA

B.S. China Pharmaceutical University, 1998
M.S. China Pharmaceutical University, 2001

A dissertation submitted in partial fulfillment of requirements
for the degree of Doctor of Philosophy
in the Burnett School of Biomedical Science,
in the College of Graduate Studies
at the University of Central Florida
Orlando, Florida

Fall Term
2011

Major Professor: Steven Ebert, Ph.D.

ABSTRACT

Molecular imaging modalities are important tools to evaluate the efficacy of gene delivery systems and cell-based therapies. Development and application of these modalities will advance our understanding of the mechanism of transgene expression and cell fate and functions. Physical gene transfer methods hold many advantages over viral vectors among gene therapeutic strategies. Here, we evaluated the efficacy of biolistic ("gene gun") gene targeting to tissues with non-invasive bioluminescence imaging (BLI) methods. Plasmids carrying the *firefly luciferase* reporter gene were transfected into mouse skin and liver using biolistics, and BLI was measured at various time points after transfer. With optimized DNA loading ratio (DLRs), reporter gene expression reached to peak 1day after transfer to mouse skin, and the maximum depth of tissue penetration was between 200-300μm. Similar peak expression of reporter gene was found in mouse liver but the expression was relatively stable 4-8 days post-biolistic gene transfer and remained for up to two weeks afterward. Our results demonstrated BLI was an efficient strategy for evaluation of reporter gene expression in the same animals over a period of up to two weeks in vivo. Different tissues showed different expression kinetics, suggesting that this is an important parameter to consider when developing gene therapy strategies for different target tissues.

We also employed BLI to measure differentiation of mouse embryonic stem (ES) cells into beating cardiomyocytes in vitro and in vivo. A subset of these cardiomyocytes appears to be derived from an adrenergic lineage that ultimately contribute to

substantial numbers of cardiomyocytes primarily on the left side of the heart. At present, it is unclear what the precise role of these cardiac adrenergic cells is with respect to heart development, though it is known that adrenergic hormones (adrenaline and noradrenaline) are essential for embryonic development since mice lacking them die from apparent heart failure during the prenatal period. To identify and characterize cardiac adrenergic cells, we developed a novel mouse genetic model in which the *nuclear-localized enhanced green fluorescent protein (nEGFP)* reporter gene was targeted to the first exon of the *Phenylethanoamine N-transferase* (*Pnmt*) gene, which encodes for the enzyme that converts noradrenaline to adrenaline, and hence serves as a marker for adrenergic cells. Our results demonstrate this knock-in strategy effectively marked adrenergic cells in both fetal and adult mice. Expression of nEGFP was found in Pnmt-positive cells of the adult adrenal medulla, as expected. Pnmt-nEGFP expression also recapitulated endogenous Pnmt expression in the embryonic mouse heart. In addition, nEGFP and Pnmt expression were induced in parallel during differentiation of pluripotent mouse ES cells into beating cardiomyocytes. This new mouse genetic model provides a useful new tool for studying the properties of adrenergic cells in different tissues.

We also identified two limitations of the Pnmt-nEGFP model. One is that the amount of nEGFP expressed within individual adrenergic cells was highly variable. Secondly, expression of nEGFP in the embryonic heart was of low abundance and difficult to distinguish from background autofluorescence. To overcome these limitations, we developed two alternative genetic models to investigate adrenergic cells:

iv

(1) Mouse embryonic stem cells, which have been previously targeted with Pnmt-Cre recombinase gene, were additionally targeted with a dual reporter plasmid which covered both a loxP-flanked cDNA of *red fluorescence protein (HcRed)* and also EGFP. Under the undifferentiated status, cells emit red fluorescence as transcription stops before EGFP coding sequence. After differentiation into beating cardiomyoctyes, some cells switch fluorescence from red to green, indicating that excision of loxP-flanked sequences by Cre since Pnmt had been activated. (2) A surface marker, truncated low-affinity nerve growth factor receptor (ΔLNGFR) was used as the reporter gene as cells expressing this marker can be enriched by magnetic-activated cell sorting (MACS), a potentially efficient way to yield highly purified positive cells at low input abundance in a population. Through a series of subcloning steps, the targeting construct, Pnmt-ΔLNGFR-Neo-DTA was created and electroporated into 7AC5EYFP embryonic stem cells. Correctly targeted cells were selected by positive and negative screening. These cells provide a new tool with which to identify, isolate, and characterize the function of adrenergic cells in the developing heart, adrenal gland, and other tissues where adrenergic cells make important contributions.

I dedicate this work to my dear father, who passed away in 1996. He was not only a

good engineer, but also a knowledgeable educator and a good friend of mine. His

encouragement benefits me in my whole life.

ACKNOWLEDGEMENTS

TABLE OF CONTENTS

LIST OF FIGURES

CHAPTER 1 : INTRODUCTION

Gene therapy continues to hold great potential for treating many different types of disease and dysfunction. Safe and efficient techniques for gene transfer and expression in vivo are needed to enable gene therapeutic strategies to be effective in patients. Currently, the most commonly used methods employ replication-defective viral vectors for gene transfer, while physical gene transfer methods such as biolistic-mediated ("gene-gun") delivery to target tissues have not been as extensively explored. Compared with viral vector [1] based therapeutic strategies, non-viral vectors have the advantages of simple preparations, tissue-specific expression, lower immunogenic responses and less toxicities [2-5]. Among non-viral vector-based gene transfer, physical methods, which employ physical forces to make transgene to target cells can achieve fast expression.

Although these methods are intensively studied, there are still short of accurate and fast evaluation strategies. For example, for the gene delivery into the mouse heart, although naked DNA injection has already been shown as a feasible method to induce transgene expression, however, the evaluation was either based on more qualitative assay such as β-galactosidase activity (LacZ staining) [6] or based on luciferase activities but different animals were used for quantification at various time points after gene transfer [7]. For the latter, there could be difficulties to draw conclusions as discrepancies could occur among individual animal. This inconsistence could be overcome if a technology for evaluation is available to detect the transgene expression

dynamically in a same animal. Bioluminescence imaging (BLI) is such a tool which is based on detection of light emission produced through catalysis of luciferin by firefly luciferase [8, 9]. BLI can efficiently evaluate the efficacy of transgene expression in organs non-invasively, such as cell survival, proliferation and migration after stem cell engraft into mouse myocardium [10-12]. Thus it will be of high interest to evaluate the transfect efficacy of nonviral vector gene delviery, especially by physical forces *in vivo* through BLI. These will highly enrich our knowledge of the characteristics of these physical gene transfer methods, and their advantage and limitations, thus laying the foundations of specific design for each method and further technical improvements to increase the gene expression.

Here, we will use one of the physical gene delivery technology, biolistic delivery "Gene Gun", a method to utilizes the pressurized gas to propel the metal particles which are conjugated with DNA to the target tissues[13-16]. This particle bombardment technique has already been extensively used in both in vitro and in vivo studies [17-20], at the same time, some of the preclinical and clinical trials are undergoing for skin vaccinations and immunizations [21-23]. However, the deeper mechanisms of this gene delivery method are still under exploitation. In the present study, we evaluated the efficacy of biolistic gene transfer techniques in vivo using BLI. We hypothesize that:

Bioluminescence imaging (BLI) can efficiently determine the transfection effects of reporter plasmids, pCMV-Luciferase, which were targeted both *in vitro* mammalian cells and *in vivo* mouse organs (liver and skins).

We will perform the following experiments which are evaluated mainly by BLI to test this hypothesis:

1. Transfection through gene gun can yield relative high level of gene expression compared with other established methods.

2. The optimization of the gene gun parameters, especially the DNA Loading Ratio (DLR) and helium pressure, are critical for the outcome of transfection in vivo.

3. The dynamics of reporter gene expression will be variable concerned with various tissues and organs, here mainly referred to mouse liver and skins, and BLI can accurately recapitulate these processes.

4. The depth of DNA-particles penetration and its relationship with gene expression (determined by β-galactosidase activity) will be determined using mouse skins for further characterization of this delivery method.

5. In order to expand the BLI application in the evaluation of other nonviral gene transfer in vivo, naked plasmid will be injected into mouse heart and the transgene expression is measured continuously for the same animal to monitor the increase and reduction of expression through BLI.

In addition, BLI will also be used to characterize a specific mouse embryonic stem cell line in which the sodium-calcium exchanger-1 (Ncx-1) promoter driven luciferase reporter gene is stably trasnfected.

Catecholamines, including noradrenalin (norepinephrine) and adrenalin (epinephrine) are hormones which exert multiple critical physiological functions. They are mainly produced in chromaffin cells of the adrenal medullae of adult adrenal glands

which are then secreted into the bloodstream during stress conditions [24]. Dopamine β-hydroxylase (Dbh) converts dopamine to noradrenaline, and phenylethanolamine n-methyltransferase (Pnmt) converts noradrenaline to adrenaline. Thus Dbh and Pnm are usually used as markers of noradrenalin and adrenalin producing cells.

However, the locations of catecholamine production are far beyond adrenal glands and sympathetic ganglionic neurons, a variety of tissues and organs can produce and secret catecholamine through paracrine pathway [25-29]. In the developing embryo, however, the major site of production first occurs in the heart [30-32]. These adrenergic-derived cells are largely unknown in terms of their functions. Here, we use Pnmt as a marker for adrenergic cells and generate various genetic models both in vitro and in in vivo to characterize these cells.

We previously described a genetic model where we inserted the cre-recombinase (Cre) gene into exon 1 of the Pnmt gene [33] and when these mice were crossed with ROSA26-β-galactosidase reporter animals, β-galactosidase activity was specifically expressed in the medulla of the adult adrenal gland and in the developing embryonic heart in patterns consistent with those observed for endogenous Pnmt expression in those tissues [30, 31, 33]. However, this strategy has the limitation that both the active adrenergic cells and cells with adrenergic phenotype in the history have been marked at the same time, thus to distinguish those above cells is impossible. In order to fill this gap, in the second part of my thesis, we generate a new genetic model that the reporter gene can track the active adrenergic cells in animals. Our hypothesis is as the following:

Targeting of the Enhanced Green Fluorescent Protein Reporter to the regulatory elements of Pnmt genomic sequences to generate a new knock-in mouse model and this Pnmt-nEGFP model can efficiently mark the active adrenergic cells in both adrenal glands and other organs.

We will set up two aims to test this hypothesis:

1. Verification of this genetic targeting strategy and analysis of reporter gene expression in the adult adrenal gland.

We will determine whether GFP positive cells could be found in the adult adrenal medulla and whether these expressions were tissue specific (only concentrated in medulla instead of cortex), whether these cells are adrenergic such as expressing Pnmt. In addition, if the above questions are answered, then we will further analyze the phenotypes of these GFP positive cells in adult adrenal glands. Questions needed to be answered include:

Whether the GFP expression is localized in the nucleus or in the cellular part;

Whether there're any differences of GFP expression between homozygous and heterozygous animals.

2. Determine whether the cells with GFP expression could be found in the mouse embryonic heart and if possible, further characterize these cells such as their location and dynamics of expression during development.

For this aim, we will mainly use the immunohistochemistry to observe GFP expression from the sections of embryonic mouse hearts. If GFP signal is strong,

Fluorescence-Activated Cell Sorting (FACS) will be used for characterization and sorting of the positive cells. Pnmt-nEGFP pluripotent mouse embryonic Stem Cells (mESCC) will also be differentiated into cardiomyocytes and the expression of both Pnmt and GFP will be determined.

Dependent on the sensitivity of Pnmt-nEGFP genetic animal model, the adrenergic cell populations during heart development [30, 31, 33, 34] could be characterized based on green fluorescence. However, the alternative strategies will also be generated if this genetic model can't identify these transiently expressing cell populations. Considering the small number of these cells and other uncertainty of reporter gene expression based on GFP [35, 36], other strategies are created. The first alternative will be as follows:

For Pnmt-Cre pluripotent mESC cells, a dual fluorescence plasmid which includes both the coding sequence of red fluorescence protein (RFP) and GFP will be stably transfected, the whole RFP codons are conjugated with stop sequences and floxed by LoxP site on both ends [37]. Thus for this model, we will test the following aims:

1. A Stable mESC cell line can be created which incorporate the dual fluorescence indicator, thus red fluorescence emission from cell clones after antibiotic screening.

2. These positive clones can differentiate well into cardiomyocytes, and at some specific stages of cardic differentiation, portion of the cells, especially inside or

close to the beating loci will show fluorescence switch and green fluorescence could be detectable.

For the second alternative, we will take the advantage of a powerful cell separation technology: Magnetic-Activated Cell Sorting (MACS) for the same purpose listed above. MACS is based on immunogenic reaction between magnetic beads and cell surface specific antibodies, which can be purified from the negative populations under the proper magnetic field [38]. It has been reported that mESC cells keep their self-renewal and diverse differentiation capabilities after sorting. In addition, the yield and the purity of the enrichment are very high compared with other methods [38-40]. Therefore, we will choose low-affinity nerve growth factor receptor (ΔLNGFR) as a surface marker to generate a new in vitro model to isolate and characterize the adrenergic cells during cardiac differentiation [41, 42]. The aims are as followings:

1. Through a series of subclone procedures, generate the targeting construct which has ΔLNGFR as reporter gene. The construct is referred as Pnmt-ΔLNGFR-Neo-DTA, which can knock in the ΔLNGFR cDNA into Pnmt genomic locus by homologous recombination.

2. Generate the target mESC cell clones with the above targeting construct by electroporation into 7AC5EYFP pluripotent ES cells. Target cells are screened by antibiotics and biochemistry identification.

Our long term goal is to efficiently enrich the cardiac adrenergic cell populations during fetal heart development determine the destinations of these cell, such as differentiation into various components of different chambers and conduction systems or

others such as apoptosis, and finally explore the exact functions of these cells, the mechanism of their function such as how they regulate the cardiac growth or adaption to hypoxic environment during this period. The electrophysiological properties of these cells will also help us identify their function. These information will greatly help researchers appreciate the detailed process of fetal heart development and provide useful clues for the cell regeneration therapies after myocardial infarction.

CHAPTER 2 : EVALUATION OF BIOLISTIC GENE TRANSFER METHODS IN VIVO USING NON-INVASIVE BIOLUMINESCENCE IMAGING TECHNIQUES

2.1 Introduction

Gene therapy is a promising strategy for correcting both genetic and acquired diseases [43, 44]. There are a variety of gene delivery methods currently available, with the main purpose of any given strategy being to efficiently transfer and express the target gene(s) of interest without adverse side-effects. Development of improved gene delivery strategies is critical for application of effective gene therapies, yet evaluation of the effectiveness of these strategies is often hampered by difficulties in detecting transgene expression in real-time in vivo. Non-invasive bioluminescent imaging (BLI) has been successfully used for evaluation of cell and gene therapies in small animal models [8, 10, 12, 45], though it has not yet been systematically applied to analysis of physical gene transfer methods. The purpose of the present study is to evaluate the effectiveness of biolistic gene transfer in different types of tissue in mice using non-invasive in vivo bioluminescence imaging (BLI).

Vectors for gene delivery can be divided into two general categories: viral and non-viral. Viral vectors are widely employed for gene therapy as they are highly efficient, and the effects can be sustained over periods of weeks, months, and sometimes years [1, 46]. A number of different viral vectors have been utilized for gene therapy approaches based on cell/tissue-type preferences. Some of these include adeno- and

adeno-associated virus, herpes virus, retrovirus, and lentivirus, among others [47, 48]. Each has its own advantages and disadvantages depending on application and tissue type. In general, recombinant replication-defective (ie, crippled) viral vectors are used for this purpose to minimize threats of infection, immune responses, and other potentially adverse conditions. In the past, serious consequences have resulted from the use of viral vectors for gene therapy in humans [9,10]. Most notably, the death of 18-year old Jesse Gelsinger due to immune complications arising in response to adenovirus vectors essentially halted clinical trials using viral vectors for gene therapy for many years[49-51]. More recently, other viral vector-based gene therapy approaches have come into question because of associated genomic instability and activation of proto-oncogenes[52, 53]. Thus, it is becoming increasingly clear that there is an inherent risk of serious adverse side effects with some viral-based gene therapy strategies.

Alternatively, non-viral gene therapy strategies pose less risk of infection and/or adverse immune responses. Non-viral gene transfer techniques typically involve either chemical or physical methods. Chemical methods such as calcium-phosphate or liposome-based approaches have achieved much success for in vitro applications in cell cultures, but have been of more limited utility in vivo due to low transfection efficiencies and toxicity issues[4, 54, 55]. Physical methods are diverse and include direct injection of DNA, electroporation, ultrasonic-based, and biolistic approaches in addition to a variety of other techniques. In most cases where chemical or physical methods are employed, purified plasmid DNA is used for delivery. When effective, this typically

results in transient expression in target tissues since the "naked" DNA is eventually degraded by host nucleases [6]. Thus, these methods are currently limited to specific applications where transient expression of a transgene is warranted (*e.g.,* induction of angiogenesis) [56-59].

In the present study, we chose to use physical methods of gene transfer to avoid complications associated with viral and chemical strategies. In particular, we explore the use of biolistic methods of gene transfer due to its widespread applicability and low toxicity. Biolistic gene transfer has been used for many years primarily for the study and production of transgenic plants [13-16]. It is, in fact, the preferred and most commonly used method for gene transfer in plants due to its versatility and effectiveness. Due to their tough outer cell walls, plants typically require helium pressures well in excess of 1000 pounds/square inch (psi), and the procedure is usually performed under vacuum using a stationary biolistic gene delivery chamber. Animal cells, in contrast, cannot tolerate bombardment with such high pressure, nor are they amenable to vacuum conditions for the transfer process. In recent years, however, a hand-held device known as the Helios™ gene gun (Bio-Rad Labs, Hercules, CA) has been developed for biolistic gene transfer experiments in animals using lower helium pressures (≤ 600 psi) [60]. No vacuum is required, and the DNA-gold particles can be delivered from a hand-held gun that can be used to target virtually any tissue or organ for direct biolistic gene transfer. This device has been used to successfully perform biolistic gene transfer in a number of mammalian cell-culture and live-animal models [17-19, 61, 62]. In the

11

current report, we use BLI to evaluate the effectiveness of gene transfer via biolistic techniques in vitro and in vivo.

Cardiac gene therapy has passed a significant development period in the past ten to fifteen years as the advancement of molecular biology leading to both deep understanding the mechanisms of gene therapy and resulting in more experimental and therapeutical genes as candidates for gene therapy, at least in animal experimental models. In parallel, the development of new delivery methods which are designed to achieve higher therapeutic gene expression and less side effects also enriched the available technologies as different tissues and organs need different gene delivery strategies based on their specific biological properties. As we mentioned in the first section, vectors for gene therapy can be divided into non-viral and viral vectors. The viral vectors actually are the most focused strategies by researchers mainly because they own high transduction efficiency. Although the improving the performance of current viral vectors and discovery of new vectors never stops, there're still serious concerns about their inner characteristics which include immunogenic responses, insertional mutations and proto-oncogene activation, just as we discussed in the first section. On the other side, the non-viral vectors have many advantages, their functional mechanisms are still yet fully uncovered. For some specific situations, non-viral vectors are even preferred concerned with its relatively shorter transgene expression, such as the induction of angiogenesis during heart failure.

Previous views on naked DNA as a mean for cardiac gene therapy are mainly negative. Although the naked DNA can access to the target organs quickly, they're not

easily penetrate to the target cells because 1) DNA are prone to degraded by DNAase, and 2) Without additional protective coverage to facilitate uptake, the entrance to cell membrane by negative charged DNA is limited. However, when considering the advantage of naked DNA, which includes but not limited to: low cost of production, very low immunogenic response and the following toxicity, heat stability and good solubility, it needs for further tested to best utilized from these advantages [63]. There is demanding need to further evaluate this method, especially direct naked DNA delivery to determine its effectiveness in vivo. Therefore, complementary technologies designed to assist naked DNA's performance while reducing its defects are hot research fields. For myocardium gene delivery, which is often used for some purposes such as induction of angiogenesis and treatment of heart failure, many ways can be used to meet this requirement. Some researchers use catheter based direct injection [64]. Recently, DNA loaded microbubbles destruction in the heart by ultrasound is employed as a high efficient way to achieve transgene expression in the myocardium [65, 66]. However, direct injection into myocardium is still an efficient way for short term transgene expression, and is at least a good standard for comparison with other naked DNA delivery techniques. In this section, we use direct injection to the myocardium without thoracotomy with luciferase reporter plasmid and check the gene expression with non-invasive bioluminescence imaging (BLI) and determine whether BLI can efficiently detect the dynamic changes of the transgene expression.

Stem cells are promising strategies for treatment of severe cardiovascular diseases including heart failure, myocardial infarction and others. However, despite the

many multi-center clinical trials for the cell based therapies in cardiovascular disease, controversies about the outcome occurred and currently stem cell therapies haven't been extended to large scale trials and practice. These results push both the basic scientists and clinicians to cooperate deeply to explore the mechanism of stem cell based therapies and discover new strategies for improvements [67, 68].

The most two difficult questions in this fields are actually mutual related, first one is what is the best ideal type of stem cell to be transplanted, and the second one is their behavior after engraftment in vivo[69]. Whether the cells are well retained and survival after transplantation, or dead, washed out through circulation systems, and the potential concomitant immunoresponse and toxicity such as teratoma formations are all important questions needed to be answered, and in realities these are intermingled and tough to figure out not just separately but comprehensively.

Therefore, current situations prompt us to discover good technologies to monitor the post-transplanted cells. Cell imaging based strategies are then put the front line to meet this requirement and scientist hope to accurately localize and dynamically monitor stem cells in vivo[70]. Currently, several imaging modalities are paid more attention to track the stem cells very efficiently. They're magnetic resonance imaging (MRI), reporter gene based imaging, including both radioactive probes and fluorescent proteins, and the derivative bioluminescent imaging (BLI). Each modality has its own strength in the application dependent on the specific purpose [70].

Embryonic stem (ES) cells are usually genetic manipulated in vitro for the following reasons. The genetic modification is utilized for lineage tracking and specific

14

phenotypes are desired with modification with respective gene, either by over-expression or removal. The other reason is manipulated ES cells are helpful for in vivo detection by their tagged sequences. Reporter gene is widely used in the genetic modified ES cells as only live cells can actively launch the machinery transcription and translation of the reporter genes, thus allowing the cells could be identified, characterized and even sorted out[71, 72].

For application of reporter gene in ES cell identification, fluorescent protein gene is usually employed to form a target construct, in which these proteins are driven by the promoter from gene of interest. The most often used fluorescent proteins are GFP variants, spanned from wild type GFP to color shift family members CFP (Cyan) and YFP (Yellow). The respective genetic modified versions with higher brightness are also available, named as EGFP, ECFP and EYFP [73, 74]. These reporter genes extremely enriched the methodologies to investigate the specific types of ES cells, for their proliferation, differentiation, purification and in vivo performance tracing.

The reporter genes can also utilize bioluminescence as an alternative way for quantitative comparison of ES cells [75]. Luciferase, which was initially discovered from fire fly which can convert the substrate luciferin to glowing luminescence. Thus Luc gene is engineered in the construct driven by specific promoter, and the regulation by the promoter can be determined from bioluminescent intensities provided the construct is inserted into somewhere in the ES genome. This is very helpful when we want to explore gene's function in ES cells at different status and the therapeutic potential when

transplanted into experimental animals. In this section, a new type of ES cells, with Ncx-1(Sodium-calcium exchanger-1) as the gene of interest, is characterized.

2.2   Materials and Methods

2.2.1 Evaluation of non-viral gene delivery

The hand-held Helios Gene Gun, Tubing Prep Station, Optimization Kit (including gold microcarriers, polyvinylpyrrolidone or PVP, and tubing), and related supplies were obtained from Bio-Rad, Inc. (Hercules, CA).

2.2.1.1 <u>Reagents</u>

Human embryonic kidney (HEK) 293 cells and mouse embryonic stem cells were maintained as previously described [12, 76]. Cell culture reagents including Dulbecco's Modified Eagle Medium (DMEM) and supplements were obtained from Invitrogen, Inc. (Carlsbad, CA). Fetal bovine serum was purchased from Hyclone Labs (Logan, UT). Lipofectamine 2000 and XGAL were obtained from Invitrogen, Inc (Carlsbad, CA). Luciferin for in vivo use was obtained from Caliper Labs (Hopkinton, MA). Bright-Glo^{TM} Luciferase Assay Kit for in vitro assays was supplied by Promega (Madison, WI). All the other chemicals and reagents used in this study were obtained from Sigma-Aldrich (St. Louis, MO).

2.2.1.2 Plasmids

Plasmids used in this study included pCMV-LUC (Clontech, Menlo Park, CA) and pCMV-beta-galactosidase (pCMV-βGal) [77], pNCX1-LUC [78], have been described previously as indicated. All plasmids were purified using Qiagen Maxi-Prep DNA purification kits (Valencia, CA) followed by phenol:chloroform:isoamyl alcholol (25:24:1) extraction, ethanol precipitation, 70% ethanol wash and air-drying. The dried pDNAs were then resuspended in Tris-EDTA (TE, pH 8.0) buffer at a concentration of 1mg/ml. We found that the additional organic extraction and ethanol precipitation/washing steps were critical for achieving efficient coupling of pDNAs to gold microcarriers.

2.2.1.3 Animals

Adult white FVB mice (18-25g each) were used for this study. The mice were housed in the Transgenic Animal Facility at the University of Central Florida (UCF) on a 12:12hr light:dark cycle, and provided food and water ad libitum. All procedures utilizing mice in this study were performed in accordance with approved UCF IACUC protocols consistent with NIH regulations governing vertebrate animal research.

2.2.1.4 Preparation of gold microcarrier-coated cartridges

Preparation of gold microcarrier-coated cartridges was performed according to the manufacturer's instructions (Bio-Rad, Inc., Hercules, CA) as previously described [18, 60]. Briefly, 25 mg of gold microcarriers (1μm diameter average size) were suspended in absolute ethanol containing 0.05 M spermidine. An equal volume of pDNA was added to this mixture, vortexed, and sonicated. Various amounts of pDNA were used to evaluate different DNA-loading ratios (DLRs). By definition, DLR of 1 =

1µg DNA per mg of gold microcarrier particles [60, 79]. An equal volume of 1M CaCl$_2$ was added to the mixture in dropwise fashion, and then precipitated at room temperature for 5 min (the volume of spermidine was always the same as those of plasmid and CaCl$_2$). The solution was microcentrifuged (14,000xg) for 5s and the supernatant was removed. The resulting pellets were resuspended with 100% ethanol and washed three times with same for 15s each. Finally, the pellets were each resuspended in 2.5 ml absolute ethanol containing 0.05% polyvinylpyrrolidone (PVP), and sonicated to achieve uniform suspension of microcarrier particles prior to cartridge loading. Cartridge tubing was loaded into the Bio-Rad Tubing Prep Station, dried with nitrogen gas, and coated internally with the microcarrier suspension during continuous rotation of the tubing. After complete drying, the tubing was cut into 0.5 inch cartridge "bullets" using the supplied tubing cutter, and stored in the parafilm-sealed containers at 4ºC until ready for use.

2.2.1.5 Electrophoresis of microcarrier mixtures

Just before the last centrifugation step to concentrate the microcarriers in absolute ethanol (see preceding paragraph), a portion of the suspension was transferred to microcentrifuge tubes, and dried in a Speed-Vac centrifuge (Savant Instrument Inc, Farmingdale, NY). The pellet was resuspended in electrophoresis loading buffer and immediately subjected to electrophoresis in 0.8% agarose gels containing 0.2µg/ml ethidium bromide. Each well was loaded with approximately equal amounts of microcarriers. The gels were imaged under ultraviolet light.

2.2.1.6 In vitro gene delivery

For biolistic delivery of reporter genes, cells were trypsinized and transferred to six well plates and kept until 80% confluence prior to gene transfer. Immediately before transfection, the medium was gently removed and washed once with PBS, the barrel ring of hand held gene gun was centered at the well and the distance to the cells was about 2 cm. Upon pulling the trigger, the gold microcarriers were shot out of the cartridges by helium with pressures between 100-150 psi (1psi= 6.89 kPa). Fresh growth media was added to the dishes and the cells were recovered in the incubator for another 48h before bioluminescence measurement. As a positive control, some wells were transfected in parallel using lipofectamine according to the manufacturer's instructions (Invitrogen, Inc.; Carlsbad, CA).

2.2.1.7 In vivo gene delivery

Mouse skin and liver were chosen as the targets of bombardment for dynamic gene expression observation. Prior to the procedure, the mice were administered with 2% isoflurane to achieve a surgical plane, and maintained as such using a nose-cone for continuous isoflurane delivery (in oxygen, flow speed = 1L/min). The mice were placed in supine position on a surgical pad, and the abdominal hair was removed by Nair® hair-removal lotion. For biolistic transfer to skin, the barrel ring of the Gene Gun was lightly touching the skin. For biolistic transfer to liver, an abdominal incision was made to expose the organ, and the barrel of the Gene Gun was positioned directly above the target. Following biolistic delivery, the incision was sutured, and the mice were administered buprenorphine (0.05 mg/kg) in the thigh muscle to help mediate pain

or discomfort associated with the procedure. The mice were then removed from anesthesia, returned to their cages, and were ambulatory within a few minutes.

To determine if differences of DLR could affect expression of biolistically-transferred genes, the mice were divided into four groups with six mice per each group, and DLR was varied between 0, 4, 10 and 25. Helium pressure was set to 200 psi, and the microcarrier bombardment was targeted to abdominal skin. In a subsequent series of experiments, the helium pressure was adjusted to 300-400 psi for biolistic delivery to mouse skin since the lower pressure (200 psi) was well-tolerated in the initial group. For biolistic transfer to soft tissue (liver), helium pressure was held at a maximum of 200 psi to minimize tissue damage.

2.2.1.8 Direct injection of plasmid DNA into mouse beating heart and bioluminescence detection in vivo

In this experiment, we injected purified pCMV-LUC plasmid into the left ventricular muscle tissue of the mouse beating heart as follows. The initial preparation of the mouse, including anesthesia and depilation of the abdominal area, was similar to that described above for the biolistic gene transfer experiments in previous sections. An abdominal incision was made on the left side just beneath the lower ribs to expose the diaphragm. With the assistance of a small forceps to stretch the diaphragm gently, the beating heart became clearly visible. We then injected the plasmid DNA solution into left ventricular muscle using a 1cc Tuberculin syringe (27gauge from BD). Mice were divided into three groups: (i) control group (PBS only), (ii) 10μg pCMV-LUC, and (iii)

50µg pCMV-LUC. Following injection, the incision was sutured and mice were given buprenorphine as described above.

Since the second day after injection, mice are checked for their luminescence every day. The protocol is similar with those utilized for biolistic transfer to mouse liver in previous section. Mice are i.p. injected with 150mg/kg luciferin, then anesthetized with isofluane, placed supinely in the nosecone in the stage of IVIS-50$^®$ and height was adjusted for proper distance to the CCD in order for high quality pictures. Five minutes were set as the period of time for capture of bioluminescence.

2.2.1.9 Bioluminescence imaging (BLI)

For in vitro BLI, luciferase assays were performed as previously described [77] except that the results were quantified using an In Vivo Imaging System-50 (IVIS-50) from Caliper Labs (Hopkinton, MA). For in vivo BLI assessment, mice were injected i.p. with D-luciferin potassium salts (Caliper Life Sciences, Hopkinton, MA) at a dosage of 150mg/kg, and maintained for 5 min before imaging. The mice were then anesthetized with 2% isoflurane and placed in the IVIS-50 chamber in supine position where they were maintained with isoflurane administered through nose-cone ports inside the chamber. The chamber temperature was kept constant at 37°C throughout the procedure. Light emission was collected for 5 min, and the intensity was represented as the number of photons per second/ cm^2/ steradian for a designated "Region of Interest" or "ROI". A standard "ROI" template was used for each experiment so that direct comparison of different data sets could be readily managed.   Images were processed using IgoPro Living Image$^®$ software (Caliper Life Sciences, Hopkinton, MA).

2.2.1.10   XGAL histological staining

Following biolistic transfer of pCMV-βGAL to mouse skin as described above, mice were sacrificed three days later by decapitation while under full anesthesia (2% isoflurane). The abdominal skin surrounding the biolistic target area (22 mm diameter) was excised and fixed with 4% paraformaldehyde for 1-2 hrs on ice. The tissue was then transferred to a solution of 30% sucrose in PBS and kept at 4℃ overnight. The skin was sectioned transversely (14µm/section) using a cryostat instrument. The protocol for the XGAL staining with acidified eosin counterstaining was performed as described previously [33].

2.2.2   Characterization of ES cells transfected with luminescence reporter gene by BLI

pNcx-1 is kindly from Donald Menick, [78], pMC1-Neo is from our lab [33], the latter is a neomycin cassette plasmid. The Bright Glow Luciferase assay kit is provided by Promega and described as in the first section of this chapter.

2.2.2.1   Cell culture

7AC5-EYFP from ATCC are derivative of mouse R1 ES cell line, both are germline competent. All the protocols related to ES cell culture are in accordance with guideline of ATCC and are detailed in Chapter Two, the main bulk of this thesis.

2.2.2.2   Screening and Characterization of positive clones by BLI

Cells were cotransfected with pNcx-1 and pMC-1 neo by electroporation. G418 (Geneticin, In vitrogen) were added on the second day after trasnfection at 350µg/ml.

Around 10days after electroporation, colonies were picked up and transferred to 48 well plates covered with Mitomycin treated mouse embryonic fibroblasts (MEF). Drugs were included during the whole selection process. Cell clones are compared for their luciferase activity by BLI with IVIS-50® after lysed by Glo-lysis Buffer, also provided by Promega. Cells were through two round screening until 2-3 stably transfectant and with highest bioluminescence came out. One of the clones was chosen for all the following experiment.

2.2.2.3 Correlation between the cell numbers of pluripotent Ncx-1 reporter mESC and bioluminescent intensities

Different numbers of puripotent Ncx-1 cell clones were seeded into 24 well plates covered with gelatin. The number ranged from 0, 1000, 5000, 10,000, 50,000, 100,000, 200,000, 50,000 and 1,000,000. 4hs after being seeded, after check the cells are completely attached, their Luciferase activities were determined through Bright-Glo Assay. Light production was measured by BLI and then confirmed with scintillation counting (Liquid Scintillation Analyzer, TRI-CARB2900TR, Packard). Standard curve was made to represent the correlation between cell number sand their respective Luciferase activities.

2.2.3 Statistical Analysis

Results are expressed mean values ± standard deviation. One-way analysis of variance was used to determine if statistically significant differences occurred, with $p < 0.05$ required to reject the null hypothesis.

2.3 Results

Our initial experiments were designed to test the functionality of the biolistic gene transfer with BLI methods. To accomplish this, we bombarded two different cell types in culture with gold (Au) particles coated with or without LUC reporter plasmid DNAs driven by different promoters. As shown in Fig. 1A, HEK cells blasted with gold particles coated with pCMV-LUC produced a strong bioluminescent signal in the presence of the luciferin substrate. In contrast, cells blasted with gold particles alone (Au) or coated with LUC reporter plasmids driven by the cellular promoter from the sodium-calcium exchanger 1 (NCX1) gene generated no measurable bioluminescent signal. In parallel, we performed an analogous transfection experiment using an established in vitro transfection method using lipofectamine [80]. The results were similar to those achieved with the biolistic method except that CMV-LUC activity was much more robust in the lipofectamine sample compared with the biolistic sample in HEK cells. In contrast, biolistic gene transfection produced brighter bioluminescence than lipofectamine for CMV-LUC in mESC (Fig. 1 C and D). The pNCX1-LUC construct did not produce measurable bioluminescence when transfected by either method, and thus was not explored further in this study.
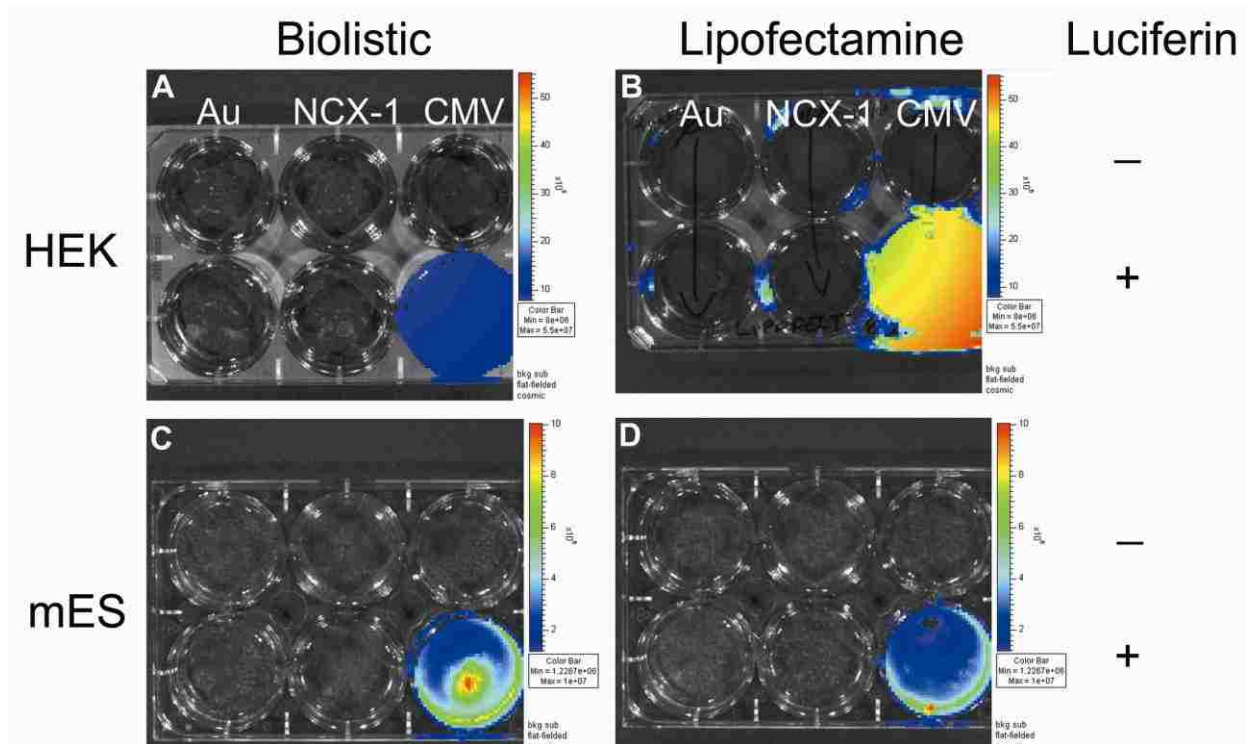
Figure 2-1. Luciferase expression in transfected cells in culture.

(A&C) HEK 293 and (B&D) mouse ES cells transfected using either lipofectamine 2000 (A&B) or the Helios Gene Gun (C&D). The top row in all sets of plates shown did not receive the luciferin substrate whereas it was provided to all wells in the bottom row of each plate shown. The leftmost column of each plate contained mock-transfected cells. The middle column was transfected with pNcx1-LUC, and the rightmost column of each plate was transfected with pCMV-LUC.

To perform biolistic transfer of LUC reporter plasmid DNA in vivo, we next evaluated the effectiveness of physical coupling of plasmid DNA to gold microcarrier particles. The gold microcarriers were 1μm in diameter, on average, and increasing DNA loading ratios (DLRs) were evaluated by agarose gel electrophoresis. As shown in Fig. 2A, increasing the amount of pCMV-LUC in the coupling reactions led to greater retardation of the plasmid through the gel, thereby indicating that more of the plasmid DNA was being coupled to the microcarriers. As the DLR increased from 4 to 10 or 25, however, increased amounts of uncoupled plasmid were

observed ("supercoiled" and "relaxed" bands, arrows, Fig. 2A), possibly indicating that some

saturation of binding had occurred. When the DLR was increased from 10 to 25, most of the

plasmid did not enter the gel presumably because higher order DNA-gold coupling had occurred

such that the complexes were now too large to enter the gel. Less of the "free" supercoiled and

relaxed plasmid DNA was present with a DLR of 25 compared to that observed with a DLR of

10. Macroscopic inspection revealed some "clumping" of gold particles at the highest DLR of 25,

which is consistent with the idea that higher order coupling likely occurred in this group.

To evaluate the efficacy of these different DLRs for biolistic gene transfer, we employed

the Helios gene gun to deliver the gold microcarriers into mouse skin in vivo. Reporter gene

expression from the pCMV-LUC vector was then measured using BLI. Quantitative analyses of

these results are shown in Fig. 2B. Expression appeared highest 24h after biolistic delivery,

and then declined steadily over the next few days. Surprisingly little difference was observed

with the different DLRs. Representative images of in vivo BLI for mice in these experiments are

shown in Fig. 2, panels C-F. In the absence of plasmid DNA, no BLI was apparent (DLR = 0,

Fig. 2C). In contrast, the BLI results for panels D-F (Fig. 2) showed similar levels of

bioluminescence activity under the conditions used for these experiments. No significant

differences in bioluminescence were seen using microcarriers with DLRs = 4, 10, and 25

($p \geq 0.05$), though there was a trend towards increased bioluminescence with increasing DLR

after day one.
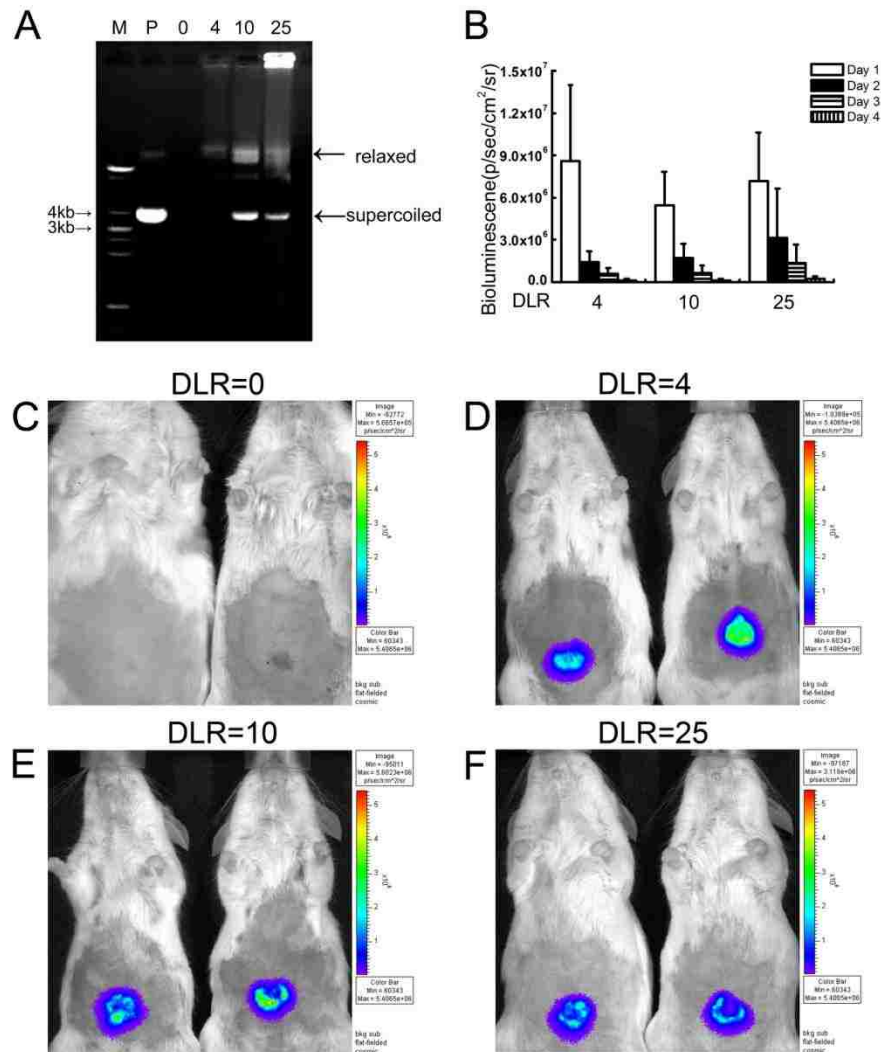
Figure 2-2. Evaluation of DNA-Loading ratio (DLR).

Picture of ethidium bromide-stained agarose gel showing plasmid DNA-gold microcarrier coupling. The amount of microcarriers calculated to contain 100 ng of plasmid DNA was loaded per lane. Lanes: M, marker (1 Kb ladder; P, plasmid DNA (pCMV-LUC) alone; 0, 4, 10, 25 refer to DLRs for the respective lanes indicated. (B) Luciferase activity in mouse skin following biolistic transfer of pCMV-LUC at different DLRs. BLI was performed daily for four days after gene delivery (n=6). (C-F) Representative pictures from different DLRs one day after biolistic gene transfer.

To maximize gene transfer effectiveness and consistency, we chose the middle DLR of

10 to compare the efficacy of biolistic gene transfer into different tissue types in vivo. In this

27

series of experiments we used BLI to measure reporter gene activity following biolistic transfer into either superficial (skin) or internal (liver) tissue in vivo, as shown in Fig. 3. Peak BLI activity was observed at the 2d time-point following biolistic gene delivery into both tissues, with skin showing much greater BLI activity than liver at this point. Over time, however, BLI activity in liver was sustained much longer than that seen in skin. For example, relatively strong BLI activity persisted through 8d after gene transfer into liver, whereas BLI activity in skin was nearly undetectable by the 8d time-point. BLI activity remained relatively stable in the liver between 4-8d following gene transfer, and then began to steadily decline over the next week (Fig. 3G). The last time-point measured in these experiments was 13d post-delivery, and there was still a small but measurable amount of BLI activity present in the liver group. These results show that while biolistic gene transfer was effective for both liver and skin, the dynamic features of reporter gene expression in these two different tissues varied over time.
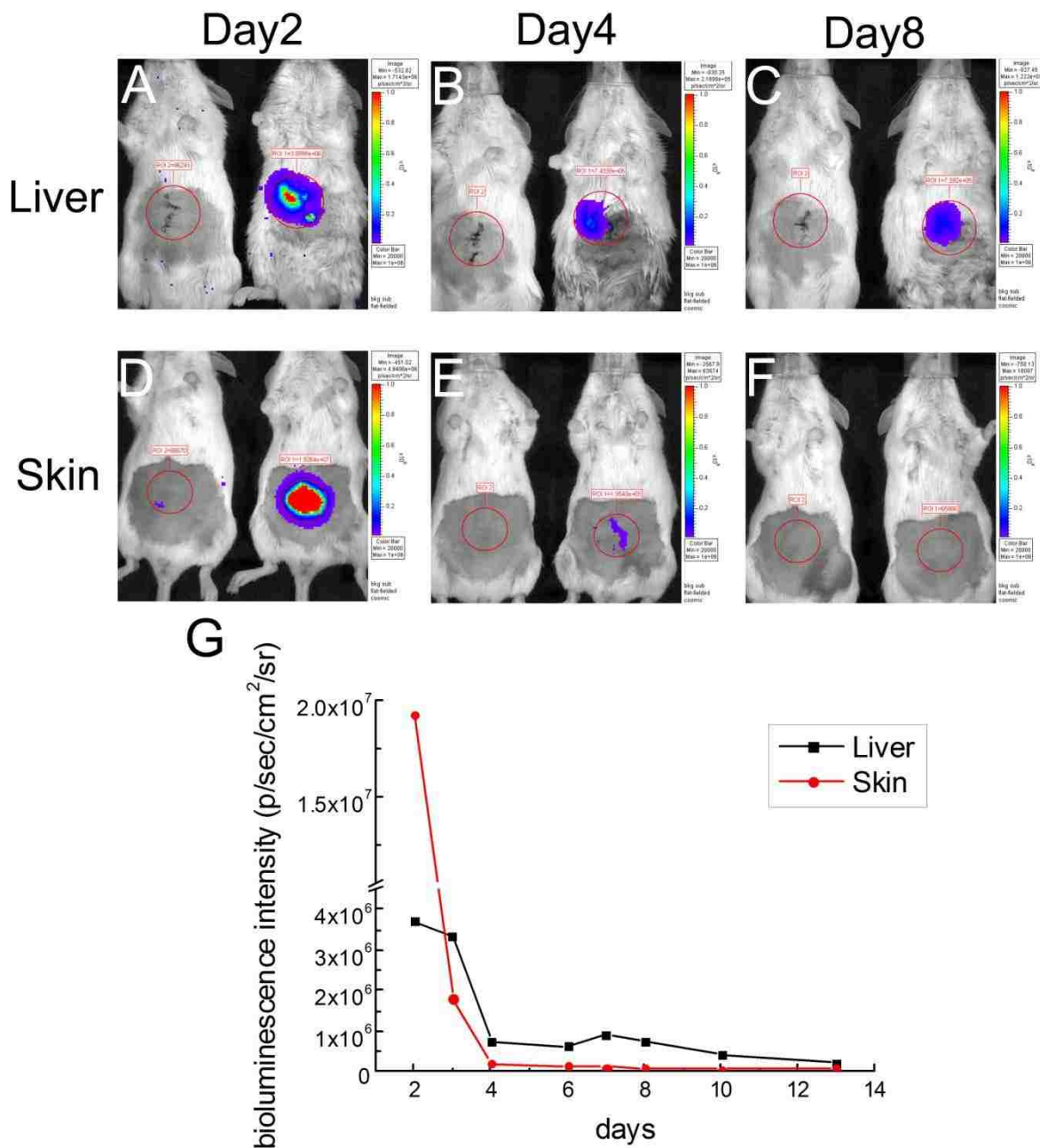
Figure 2-3. Comparison of BLI following biolistic reporter gene transfer into mouse liver or skin.

Representative mice are shown at day 2 (A and D), 4 (B and E) and 8 for (C and F) following biolistic gene transfer. Pictures in A through C are for liver and those in D through F for skin. In each panel, the mouse on the left was transfected with gold microcarriers alone, and the mouse on the right was transfected with gold microcarriers conjugated with pCMV-LUC (DLR=10). Quantitative assessment of these data is shown in panel G.

To determine the depth of gold microcarrier penetration following bombardment of mouse tissue, we performed histological assessments of abdominal skin 3d following biolistic gene transfer. In these experiments, we used pCMV-βGAL reporter plasmid (DLR = 10) to facilitate observation of reporter gene activity in histological sections. The gold microcarriers were readily observed in histological sections (Fig. 4, arrows). Many of them were found in the outermost layer of skin (epidermis), but there were clearly clusters of these particles found in deeper layers. Most of these particles were found approximately 100µm from the surface of the skin, though some were observed as deep as 200-300µm from the surface. In contrast, reporter gene activity, as visualized by blue XGAL staining, was mainly found near the surface of skin, though patches of cells expressing βGAL were seen as deep as ~150µm from the skin surface (Fig. 4, arrowheads). These results indicate that biolistic gene transfer was effective at or near the tissue surface under the conditions employed in these experiments.
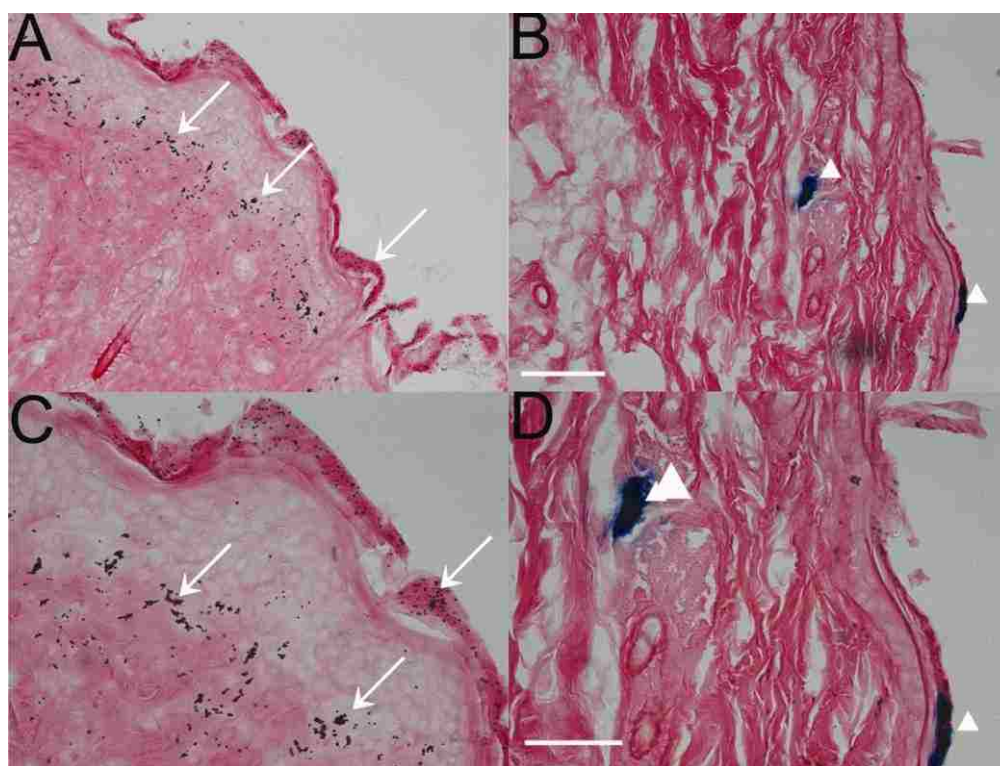
Figure 2-4. Identification of transfected cells *in vivo* following biolistic delivery of gold-coupled pCMV-βGal into mouse skin.

(A-C) Low-magnification (20X objective; scale bar, 100 μm) and (D-F) Higher-magnification (40X objective; scale bar, 60 μm) views of transverse sections of mouse skin collected three days after biolistic gene transfer. The sections were stained with XGAL (blue) and eosin (pink). Examples of microcarriers are indicated by arrows, and transfected cells were identified by blue XGAL staining (arrowheads).

To determine if BLI could effectively monitor cardiac gene expression in vivo, we injected pCMV-LUC plasmid DNA directly into the left ventricular muscle of the beating heart. BLI activity was then assessed over a 10d period following injection. Representative mice from these experiments are shown in Fig. 5, where it can be seen that peak BLI activity was observed ~3d after injection of 50μg of pCMV-LUC. BLI activity then decreased steadily over the next week until it became undetectable by 10d. In one set of experiments, we also tried 10μg of pCMV-LUC per injection. BLI activity

was observed over a similar time-course as that observed for the 50µg injections, though the intensity of the activity was substantially less than that observed when we used 50µg of pCMV-LUC (not shown). In both cases, BLI activity first appeared 2d after the injection. These results demonstrate that BLI can serve as a useful monitor of reporter gene expression in the heart as well as in the liver or skin. Thus, BLI can be used as an effective non-invasive tool for evaluating the effectiveness of gene transfer in vivo using a variety of delivery strategies.
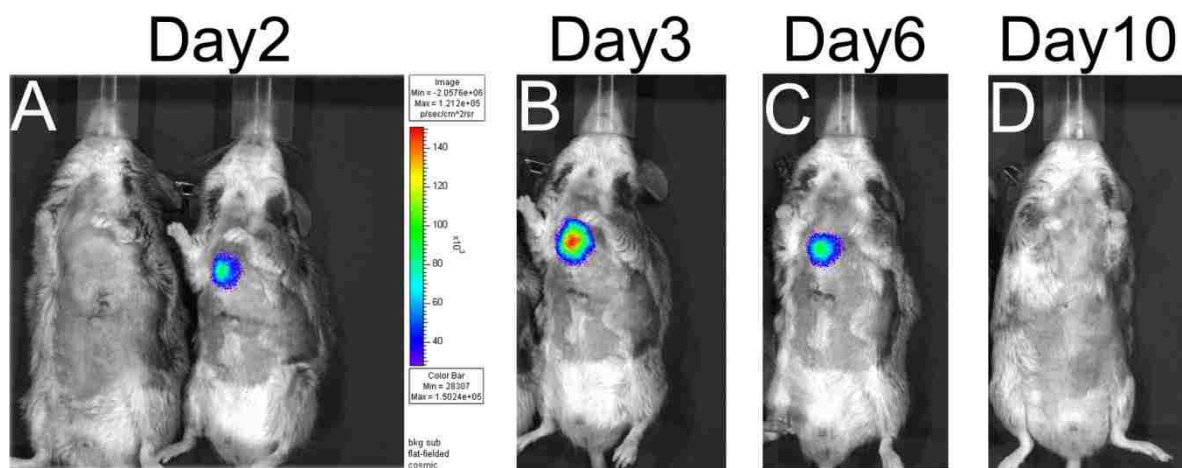
Figure 2-5. BLI of adult mice following direct injection of pCMV-LUC into ventricular myocardium.

Mice were imaged at days 2, 3, 6, and 10 (panels A-D, respectively) post-injection with 50 µg pCMV-LUC. A control mouse that received only vehicle (PBS) injection is shown on the left side of panel A. No BLI activity was observed from vehicle-injected controls at any of the time-points evaluated.

We initially picked up 144 positive clones after electroporation with Ncx-1 and MC1-Neo plasmid together. Not all the clones survived even after pick up, some of them are dead, some of them didn't show convincing Luc activities. Thus after first round selection with G418, there're around 20 clones left for secondary screening, and till the end of this drug selection and Luc activity measurement, there're three clones left for further identification. Finally, Ncx-43 was chosen as candidate for the next following in vitro and in vivo experiments because after in vitro differentiation into cardiomyocytes the baseline Luc activity increased around 2.5 folds.

The correlation of the input cell numbers and their accumulated luminescence were shown in Fig.6. Basically, the quantified luminescence faithfully correlates with the respective pluripotent ES cell numbers, that just confirms within specific window (higher than threshold but lower than saturation level), BLI is a reliable tool for quantification of population of same cells. On the other hand, it also indicates the cloned cells are stable transfectant, instead of mixed population with both trasnfected and untransfected cells, and it is mostly possible that cells in the population have been inserted with even copies of reporter gene. Combined with other data that the transcript level (mRNA) also faithfully correlates with luminescence, the total data suggest the basic characteristics of this engineered reporter ES cells includes nearly even copy insertion and stable incorporation into single cells. These reporter cells provide a new potential for therapeutic applications in myocardial infarction model.
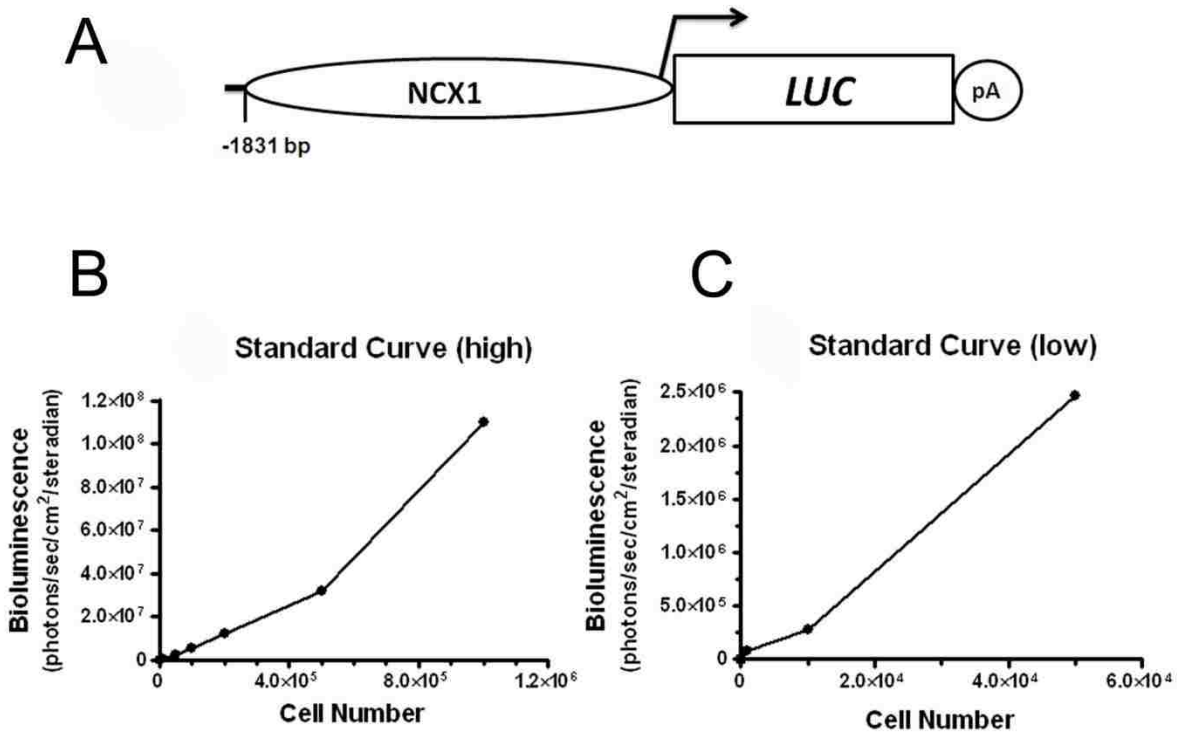
Figure 2-6. Standard curves showing the relationship between BLI and pluripotent Ncx-1 mESC number.

(A) Schematic illustration of the Ncx-1-LUC construct used to transfect mESC. (B) Pluripotent *Ncx-1* -43LUC cells were seeded into 24-well Petri dishes at various concentrations per well (in 1 mL of culture medium): 0, 1,000, 10,000, 50,000, 100,000, 200,000, 500,000, and 1,000,000 cells. The cells were allowed to settle and attach over a 4-h incubation period. They were then evaluated for LUC activity using the Promega Bright-Glo Assay. Light production was measured by BLI using the IVIS, and confirmed using scintillation counting. (**B**) Standard curve for the high concentrations of cells. (**C**) Standard curve for the low concentrations of cells.

2.4   Discussion

In the present study, we have shown that different types of tissues display differential kinetics of transgene expression following physical gene transfer in vivo. We evaluated biolistic gene transfer in external (skin) and internal (liver) tissue. In each case, we were able to

effectively monitor and quantify reporter gene expression using BLI. The main advantage of this approach is that expression of the gene transferred could be evaluated repeatedly in the same animals over a period of several days using non-invasive imaging (BLI) methods. Thus, this strategy requires fewer animals, reduces variability inherent in comparing different animals, and is more economical both in terms of time and money compared with more traditional approaches for analysis of gene therapy methods because fewer tissue samples need to be processed for analysis. Of the tissue types evaluated, decline in transgene expression was most rapid in the skin (3-4d) and most stable in the liver (10-14d). Thus, the principal finding of this study is that transgene expression kinetics are highly tissue-dependent.

Biolistic gene transfer methods are standard for plants, but relatively fewer studies have explored this method of gene transfer in animals. One of the key parameters that we initially evaluated was the DLR, which represents the amount of DNA used for coupling to a set amount of gold microcarriers. We analyzed various DLRs over a range recommended by the manufacturer of the Helios gene gun. Despite clear differences in DNA-gold coupling as evidenced by our gel electrophoresis results, there was surprisingly little difference in transfer efficiency in vivo using DLRs of 4, 10, or 25 (Fig. 2). A likely explanation for these results is that the gold microcarriers became saturated with bound plasmid DNA when DLRs of 4 or higher were used, though higher order complex formation resulting in clumping of the microcarriers was observed when DLR was raised to 25. Such clumping can be problematic in that it makes it difficult to apply a uniform coating of the discharge cartridges, potentially leading to inconsistent results. Hence, we chose the next highest DLR of 10 for our experiments to avoid this potential problem. These findings are consistent with previous reports [18] and with preliminary studies in our laboratory where we found that DLRs of 2 or lower appeared to produce less reporter gene expression compared to DLRs of 4 or higher (not shown). Conversely, using DLRs greater than 10 is probably not recommended because most of the

DNA used will be uncoupled or bound up in higher order complexes resulting in clumping. Therefore, the optimal DLR appears to be in the range of 4-10 when using conditions employed in the present study.

Helium pressures used in our study varied between 200-400 psi. Although not systematically evaluated here, we found that pressures of 300-400 psi were well-tolerated in skin. Other studies have used even higher pressures (500 psi and above) for biolistic-mediated gene "vaccinations" in skin and also observed relatively little tissue damage [62, 81, 82]. Maximum recommended helium pressure for the Bio Rad Helios gene gun is 600 psi. It is anticipated that "tough" tissues such as skin and muscle can tolerate pressures approaching this maximum, but that "soft" internal tissues may not. Consequently, we used lower helium pressure (200 psi) for gene transfer to liver, which is similar to what was used in a previous study (250 psi) to deliver the DNA element regulating cytochrome P450 2B1[19, 83]. We were reluctant to try higher pressures in liver for fear of causing serious tissue damage, and there did not appear to be a need to do so anyway because expression in liver was fairly robust under the conditions utilized here. In fact, expression persisted in liver for several days beyond that observed in the skin. The reason for this observation is not clear, but may be due in part to relatively high turnover of epidermis and/or differential nuclease activities in the two tissues. Indeed, histological assessments revealed that most of the microcarriers were localized to the epidermis following biolistic transfer to skin, with a maximum penetration of not more than a few hundred microns representing approximately 20-30 cell layers from the surface even when employing the highest helium pressure (400 psi) used in this study. Taken together, these results suggest that biolistic gene transfer conditions need to be optimized for each different type of tissue targeted.

As we mentioned in the introduction, various methods can introduce the naked DNA into the myocardium, however, direct injection is still the simplest way for transient transgene expression. In this experiment, we intended to choose injection through diaphragm through abdominal cavity instead of thoracotomy for following reasons: 1) Thoracotomy is a more tedious surgery process as it needs the chest open, thus we must use respirator to assist the breath of animal as the thoracic cavity is deflated in this procedure. The surgery itself is risky which sometime can lead to the death of animals. 2) Even under the chest open situation, the fast moving heart is still a challenge for needle position and injection, on the other hand, through the diaphragm, we can still see the heart very clearly, and with multiple preliminary practices we can well control the depth we push forward to the beating heart, thus achieving similar outcome brought by open chest injection. 3) We will make sure the injection is at right place after the whole bioluminescence measurement is finished by post-mortem inspection. The needle track is carefully checked, and we find consistent correlation between bioluminescent intensities and correct needle track, some animals not injected properly also have poor luminescence.

For this type of experiments, we initially design to deliver the transgene to larger animals such as rat and rabbit, as previous reports showed that biolistic delivery to beating heart [17, 84] is feasible and transfected reporter gene can be found efficiently. However, this was not doable for small tissues and organ targeting, especially for mouse heart, with configuration of the current available gene gun from Bio-rad. Although a similar strategy which treated donor rat heart of antisense for particular gene

by high pressure to the recipient rat can reduce the acute cardiac rejection, direct gene delivery to heart of small animals are not reasonable currently.

Consequently, we switched to more classical DNA injection methods for reporter gene delivery to mouse ventricular muscle. Again, BLI proved to be effective at monitoring gene expression even through the closed chest for up to 8 days or so following the initial transfer. A previous study did successfully use biolistic methods to transfer a reporter gene into beating rat hearts [17], which was somewhat more feasible than trying to do similar in mouse hearts because of the larger size of the rat model.

In addition, similar experiments have been done before which luciferse were also determined [6, 7, 85]. However, beside the difference of gene delivery by thoracotomy, these previous reports have to sacrifice the target animals at different time points, and then extract the tissues for in vitro luciferase assay. In contrast, we employed non-invasive BLI to measure reporter gene activity in vivo, which reduced the need for animal sacrifice and obviated the necessity of tissue extraction typically employed in these types of investigations. The animals' individual susceptibility is also reduced to minimal levels as single animal was continuously monitored instead of different animals used at various time points in previous studies[6, 7].

The success of bioluminescence detection with CMV promoter is encouraging for future directions to use mammalian reporter gene into beating myocardium. These are our future plans and we hope to cover more mammalian promoter driven luciferase construct. These include E2F, β-actin, ubiquitin, CA promoter (chicken β-actin promoter with CMV enhancer) and others. The expression driven by mammalian vectors will test

the feasibility of this method more convincingly. Eventually, we will use cardiac specific promoter for application to myocardium gene delivery, such as α-MHC (α-Myosin heavy chain), MLC-γ (Myosin light chain γ) and others. If still functional, this is a very efficient way to deliver non-viral exogenous gene construct into beating heart of experimental animals.

In the second part of this chapter, my colleagues and I established a new reporter mESC line with Ncx-1 and MC1-Neo plasmid stably transfected into pluripotent EYFP mESCs. Serial experiments show that Ncx-1, an early cardiac development marker from feline can successfully drive the luciferase reporter gene expression and this expression is further increased after differentiation into cardiomyocytes. In addition, these differentiated cells well incorporate into the neonatal hearts after direct injection through chest wall. Histology analysis confirmed some, although not many of the transplanted cells wereed positive for cardiomycyte marker sacromeric α-actinin. Thus, we confirm molecular imaging based on BLI as a useful tool to systemically screen engineered mESC line by random insertion of reporter genes both *in vitro* and *in vivo*. If promoter is properly chosen, it is a good tool to explore the mechanisms of cardiogenesis from this simple model as we can analyze the mechanism of different status, such as differentiation , survival and final cell fate, and the cells can be tracked for their behavior after engraft *in vivo*. In addition, specific cell lineage can be quantified and sorted based on the reporter gene or combined with other lineage markers. Overall, this is a useful model and the preliminary data we obtained did show optimistic potential that Ncx-1 ES cells as a good candidate for cell therapy in the experimental myocardial

infarction model and further experiments are under investigations. Other groups also use BLI strategies to engineer mouse and human stem cells [10, 86, 87], and the results are similar with ours which clearly shows the advantage of BLI during this application.

2.5   Limitations and Future Directions

This investigation was limited to two target tissues in vivo: skin and liver. To compare expression from biolistic-delivered reporter genes, we shot the same CMV-LUC gold "bullets" into these tissues and compared the resulting responses over time in vivo using BLI. An advantage of using the CMV-LUC reporter is that it produces strong LUC activity that is readily measured using BLI. This appears to work particularly well for short-term transient expression, and is consistent with earlier work showing that this promoter is strongly expressed in mouse liver following transfection in vivo [88]. On the other hand, the CMV promoter/enhancer has limited and questionable utility for longer-term sustained transgene expression applications. Even though we did not use a viral vector, the presence of the strong viral enhancer/promoter is still a potential concern. It is well known, for example, that CMV and other strong viral promoter are typically silenced by host methylation mechanisms once they integrate into genomic DNA [89, 90]. The site of integration can also be problematic in some cases such as those where nearby proto-oncogenes get activated as a result [14,15]. Future studies will be developed to investigate tissue-specific promoters tailored to the relevant target tissues. The present study focused on short-term transient expression, but future studies could evaluate more sustained expression over time for various gene therapy strategies. The use of homologous human sequences and tissue-specific non-viral enhancer/promoter elements could be directly applied

40

using biolistic approaches. BLI should prove useful for continued evaluation of these approaches in near real-time in vivo.

Despite the wide application of non-viral vectors in gene therapy, non-viral vectors still have lots of disadvantages. Low trasnfection efficiency overall hampers the utilization of this method in conditions in which longer gene expressions are expected. The decline dynamics of transgene in vivo is poorly controllable due to complex degradation systems compared with viral vector systems. Therefore, the application is still limited to short term gene expression and viral vectors are still the best choice for long term purposes.

The second shortcoming is we use CMV promoter reporter gene, which some time can lead to gene silencing from methylation of promoter sequences. Thus sometime it will be difficult for comparison of transfection efficiency with multiple delivery strategies.

The method of plasmid administration also has limitations. As through the diaphragm although the beating heart is visible, but practically it needs exquisite techniques to push forward the needle to the ventricles, the master of this techniques takes some time and not always well learned. In addition, the mouse heart close to the diaphragm is mainly composed of right ventricles, where the myocardium walls are less thinner than left ventricles, so injection through this side makes heart more vulnerable for ruptures which leads to more difficulties and insistences in real operations.

For the experiments in the second part of this chapter, there're also some limitations. First, the Ncx-1 transfection is based on random genome integration of the

reporter gene. Although we established this stable mESC line, we didn't specifically determine where this construct was inserted in the genome. We can only estimate each cell incorporates similar copies of construct, but the detailed information is lacking. As we know, sometimes, the transgene is inserted into the chromosome with pact gene sequences, therefore, the target genes are difficult for transcription as the transcription factor can't easily access to them. The random insertion sometimes results in unknown genetic processes such as silencing of exogenous gene expression. We used another plasmid (α-MHC) for the same purpose in the studies, and the results were beyond expectations as luminescence activities were decreased after cardiac differentiation. The different performances after cardiac differentiation among various promoters might come from the discrepancies of promoters, although α-MHC promoter contains the key elements for myocyte development [91], the relative short size (353bp) of this promoter could limit its function to control the transcription of reporter gene, especially after induction of cardiac differentiation.

Alternatively, to minimize the potential imbalanced expression of the targeted construct for the generation of reporter mESC, we can use one targeting construct instead of two (Ncx-1 and MC1-Neo) hereof. The promoter of this neomycin cassette is derived from β-actin which is ubiquitously expressed. Although the expression of neomycin resistance gene should be similar compared with Ncx-1 luciferase as same dosage used during electroporation, however, the significant differences among the ESC clones concerned with their luminescence indicate that the imbalanced expression of the two constructs may exist. Therefore, if the cDNA of neomycin resistance gene is

inserted into the Ncx-1 construct, then both the antibiotic resistance and luciferase expression are under regulation of the same promoter, thus hypo- or hyper activation of Ncx-1 will be reduced to minimal levels, and the performance of the selected clones will be less divergent and results will be more consistent.

2.6 Conclusions

We have shown that biolistic gene transfer can be efficiently optimized in different tissues using non-invasive BLI to monitor expression in the same animals repeatedly over time in vivo. Of the representative tissue types evaluated, expression peaked within 2-3 days for both, but declined most rapidly in the skin (3-4 days) compared to liver (10-14 days). Thus, tissue-specific expression kinetics should be an important consideration in the design of effective gene therapies using physical gene transfer techniques, which may serve as potentially useful gene delivery strategies compared with existing viral-based approaches. Biolistic gene transfer methods appear to offer an attractive, safe, and effective alternative to viral vectors for gene therapeutic strategies that can be directly applied in the clinic to treat a wide variety of human ailments. So far, biolistic gene transfer applications in the clinical setting have been primarily focused on transfection of cells in culture which are then transplanted to the patient [23, 92-94]. A more recent study [21] directly targeted external tissues such as epidermis for vaccination applications, and it is anticipated that there will be more of these types of applications developing for biolistic gene transfer in the future. The BLI-

based assessment strategy described here should facilitate optimization of biolistic conditions for different tissue types in the pre-clinical setting, thereby providing an efficient means of pre-evaluation of in vivo efficacy in animal models prior to human trials. In the same time, the BLI is also successfully applied for detection of transgene expression in normal animals by other non-viral gene delivery methods, such as naked plasmid injection into the mouse beating hearts. BLI is also an efficient tool to evaluate the function of mouse mESC cells targeted with cardiac specific reporter gene, the difference of bioluminescent activities between pluripotent and cardiac differentiated ES cells. In addition, only cardiac differentiated mESC can result in maintenance of bioluminescence after transplantation in neonatal hearts which shows BLI is a good modality for assisting studies of mechanisms of differentiation during development.

CHAPTER 3 : TARGETING OF THE ENHANCED GREEN FLUORESCENT PROTEIN REPORTER TO ADRENERGIC CELLS IN MICE

3.1 Introduction

Adrenergic hormones are key molecular modulators of physiological stress responses and are essential for heart function during fetal and early neonatal development [24, 95, 96]. The principle adrenergic hormones in mammals are adrenaline and noradrenaline. In adults, they are primarily produced in the chromaffin cells of the adrenal medullae where they can then be secreted directly into the bloodstream during periods of stress [24]. In the developing embryo, however, the major site of production first occurs in the heart [30-32]. In fact, mouse gene ablation studies have demonstrated that this period of expression in the embryonic heart corresponds with the only developmental stage where adrenergic hormones are absolultely essential for animal viability [96].

In addition, adrenergic hormones are produced by neurons in the central and peripheral nervous systems and also by several other cell types including lymphocytes and cells in the retina, kidney, spleen, and testes [25, 27-29, 97, 98]. However, the role of adrenergic hormones in these non-neuronal tissues is at present poorly understood.

Adrenergic cells can be identified by expression of the biosynthetic enzymes responsible for production of adrenaline and noradrenaline. Dopamine β-hydroxylase (Dbh) converts dopamine to noradrenaline, and phenylethanolamine n-

methyltransferase (Pnmt) converts noradrenaline to adrenaline. Thus, Pnmt expression generally serves as marker for adrenaline-producing cells while Dbh expression in the absence of Pnmt expression generally serves as a marker for noradrenaline-producing cells. Using targeted genetic strategies in mice, we previously described a model where we inserted the cre-recombinase (Cre) gene into exon 1 of the Pnmt gene [33]. By inter-breeding these mice with ROSA26- β-galactosidase reporter animals, we showed that the β-galactosidase reporter was specifically expressed in the medullae of the adult adrenal gland and in the developing embryonic heart in patterns consistent with those observed for endogenous Pnmt expression in those tissues [30, 31, 33]. The Cre/ROSA strategy marks cells that actively express Pnmt as well as those that had a history of expressing it sometime earlier in development, thereby identifying all the cells within a tissue that are derived from an adrenergic lineage. A limitation of this approach, however, is that it is impossible to distinguish cells that are actively adrenergic versus those that are not now synthesizing hormones but are descendants of precursor cells that were adrenergic.

To overcome this limitation, we developed a new model by targeting a *nuclear-localized Enhanced Green Fluorescent Protein* (*nEGFP*) gene to the mouse *Pnmt* locus to create *Pnmt-nEGFP* reporter mice. The present study describes the initial characterization of these mice, including verification of genetic targeting and analysis of reporter gene expression in the adult adrenal gland and developing heart. We also characterize the activation of GFP expression and of endogenous Pnmt in mouse embryonic stem cells as they differentiate into beading cardiomyocytes. The results

46

show that the *nEGFP* reporter gene appears to be exclusively expressed in adrenergic cells and thus may serve as a useful model for identifying, isolating, and characterizing viable adrenergic cells from a variety of tissues and developmental stages.

3.2   Materials and Methods

3.2.1   Materials

Andwin Scientific Tissue-Tek* CRYO-OCT Compound was obtained from Fisher Scientific (Pittsburgh, PA). Sheep anti-Pnmt primary antibody was from Chemicon, Inc. (now Millipore).   Texas-Red conjugated anti-sheep IgG secondary antibody was obtained from Jackson Immunoresearch (West-Grove, PA). Vectashield® mounting medium for fluorescence (H-1000) and mounting medium with Propidium Iodide (H-1300) were obtained from Vector Laboratories (Burlingame, CA). Cell culture media (Dulbecco's Modified Eagle Medium) and supplements were from Invitrogen (Carlsbad, CA). Fetal bovine serum was from Hyclone (Logan, UT). TRIzol® and MuLV Reverse Transcriptase were also from Invitrogen. All other chemicals and reagents used in this study were obtained from Sigma-Aldrich (St. Louis, MO).

3.2.2   Pnmt-EGFP construct

The mutagenesis construct was generated essentially as described [8] but replacing the Cre recombinase gene with the cDNA for Enhanced Green Fluorescence Protein (EGFP) tagged with nuclear leading sequence (nEGFP). Thus this construct

fuses Pnmt 5' non-coding sequences and the Pnmt ATG to sequences encoding EGFP. A *frt*-flanked neomycin cassette was inserted behind EGFP for positive selection. The Diphtheria toxin A (DT-A) cassette was placed outside of the homologous arms as a negative selection marker. The linearized Pnmt-EGFP plasmid was electroporated into R1 mouse embryonic stem cell (ESC) line and G418 resistant clones were isolated and their DNAs were analyzed by Southern blotting using probes external to the targeting construct. The correct targeted ESC lines were injected into blastocysts of mouse embryos. Chimeric founder animals were crossed with Jackson Laboratories strain 003946. These animals are transgenic for the *FLP1 recombinase* gene [10], thus allowing us to remove the Neo^R cassette. Subsequently, mice were backcrossed and maintained in a 129X1/SvJ genetic background. Genotyping was accomplished by PCR using a three primer system (5'-CAGGCGCCTCATCCCTCAGCAGCC-3'; 5'-Pnmt-CTGGCCAGCGTCGGAGTCAGGGTC-3'; 5'-GCTCGACCAGGATGGGCACC-3') to identify bands of 200 and 181 base pairs specific for the wild-type *Pnmt* and the *Pnmt::GFP* insertion alleles, respectively.

3.2.3 Fluorescence and immunofluorescence histology

All animal work was done according to NIH and to PHS policy and was approved by the Animal Care and Use Committees of the NICHD and University of Central Florida. Embryos from wild type (*Pnmt$^{+/+}$*), heterogeneous (*Pnmt$^{+/nEGFP}$*), and homozygous mutant (*Pnmt$^{nEGFP/nEGFP}$*) were isolated and dissected at developmental stages described in text with noon of the day of the vaginal plug designated as embryonic day

0.5 (E0.5). The protocols for dissection and immunofluorescent staining are as described [33].

3.2.4 Quantification of EGFP$^+$ cells

For adult adrenal gland, positive fluorescent cells were counted between heterozygous and homozygous strains. For this purpose, pictures were taken from adrenal gland sections using a 20x objective lens. The exposure time and compensations were set same for all the samples in order for comparison and quantification. In order to exclude disturbance from autofluorescence, image under red fluorescence filter from each sample was also captured. A cell with nuclear-localized green fluorescence without red fluorescence was designated as EGFP+. Counting was performed by separate people who were blinded as to genotype of each sample.

3.2.5 Differentiation of mES into beating cardiomyocytes

Both R1 and Pnmt-nEGFP pluripotent mES cells were maintained on mouse embryonic fibroblasts in DMEM medium supplemented with 15% fetal bovine serum plus 1000units/ml Leukemia inhibitory factor (LIF or ESGRO$^®$, Millipore). mES were differentiated by the hanging-drop as described previously [99].

3.2.6 RT-PCR

The total RNA of mES cells at different differentiation stage were extracted by TRIzol$^®$ reagent, and cDNA were synthesized with MuLV Reverse Transcriptase. RT-PCR was processed for analysis of Pnmt mRNA expression with the following primers: forward: 5'-GGTGGCTCAGACCTGAAG-3' and reverse: 5'-GCCATCAGGGTTGCTCAG-3'. The PCR product was detected under agarose gel

electrophoresis. RNA from adult adrenal glands was used as a positive control for Pnmt expression, while absence of input RNA was used as a negative control.

3.2.7 Statistic Analysis

For the quantification of EGFP-positive cells from adrenal glands, the average from five samples of each genotype was calculated and expressed as Mean±S.E.M. Student t-test was used for comparison between heterozygous and homozygous group, with $p < 0.05$ required to reject the null hypothesis.

3.3   Results

3.3.1 Genetic targeting of the nEGFP reporter gene to the Pnmt

To identify and evaluate adrenergic cells in vivo, we inserted the EGFP reporter gene with a nuclear localization sequence (nEGFP) into exon 1 of the endogenous mouse Pnmt gene as outlined in the schematic shown in Fig. 1A. Correct targeting was confirmed by Southern blotting (Fig. 1B) using 5' and 3' probes external to the genomic sequences used to direct the homologous recombination. A correctly targeted clone was used to make the knock-in mice. Through successive breeding, we removed the Flp flanked NeoR cassette and obtained *Pnmt+/+, Pnmt$^{+/nEGFP}$* , and *Pnmt$^{nEGFP/nEGFP}$* littermates for analysis. Note that even though the Pnmt insertion completely abrogates expression of Pnmt and thus eliminates adrenalin, PnmtnEGFP/nEGF animals are

viable, fertile, and show no obvious differences in health, weight, or appearance (data

not shown). Similar results were already reported for the Pnmt Cre/Cre animals [33] .
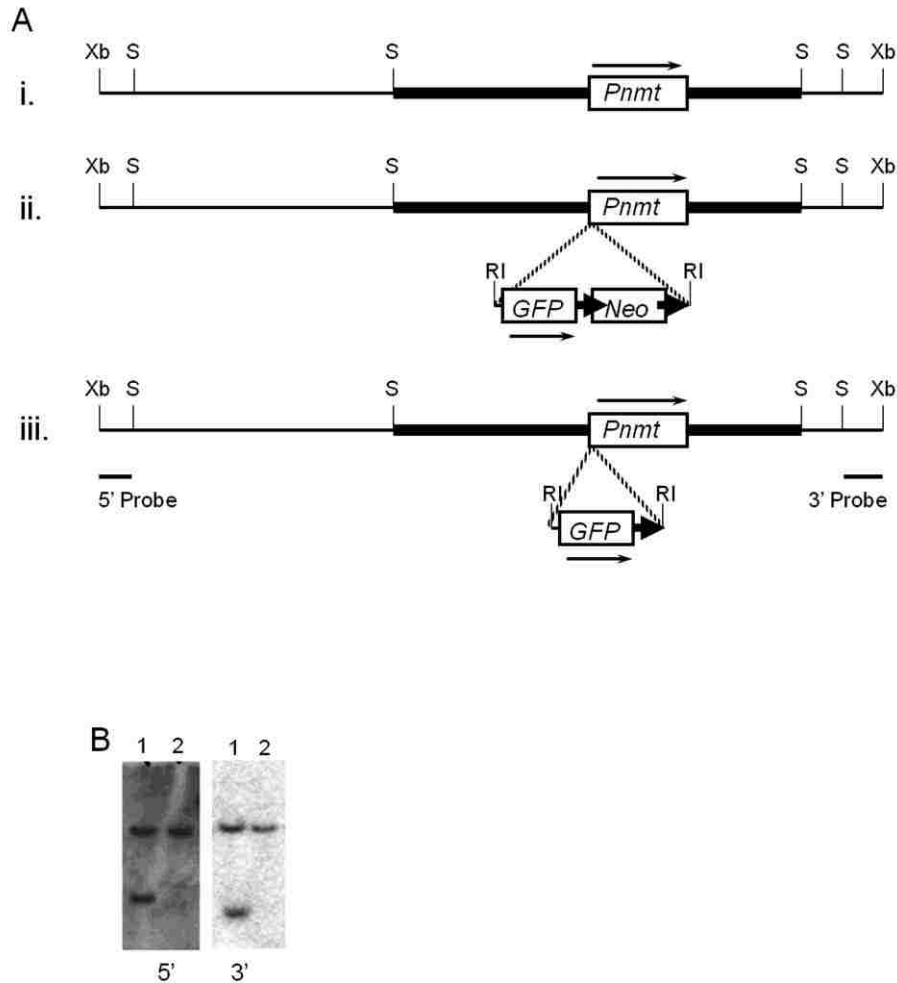
Figure 3-1. Strategies for construction of Pnmt-GFP allele.

A. Skematic depiction of wild type (i), Pnmt-GFP-Neo (ii) and Pnmt-GFP (iii) alleles. The rectangles represent the coding sequences and the thickened lines are used for homologous recombination to introduce GFP and NeoR in front of first exon of Pnmt. B. Southern blot analysis of genome DNA from screened clones shows that correct targeted allele have 8kb (5' probe) and 6kb (3'probe) in addition to the wild type 14kb band. Genome DNA are lysed with EcoRI and XbaI. The left band in both 5' and 3' panel are from Pnmt-GFP knock in sample and right band from wild type. R, EcoRI; S, SacI; X, XbaI. **This figure was by courtesy of Dr. Karl Pfeifer (NICHD; Bethesda, MD).**

3.3.2 Charaterization of EGFP reporter expression in mouse adrenal glands.

The chromaffin cells of the adrenal medulla represent the single most abundant location of adrenalin production and, hence, of Pnmt expression in adult animals. Thus, we examined reporter gene expression in adult mouse adrenal gland tissue sections to determine if EGFP expression was present as expected. In the mouse adrenal gland, the medulla and surrounding cortex are easily distinguishable from each other. As shown in Fig. 2, EGFP expression was observed in the medulla of mice with the targeted $Pnmt^{+/nEGFP}$ allele, but was absent in wild-type ($Pnmt^{+/+}$) controls. In contrast, the low levels of fluorescence in the cortex are indistinguishable in wild type and in Pnmt::GFP animals indicating that GFP expression is specific to the medulla and thus follows the patterns of the endogenous Pnmt gene.
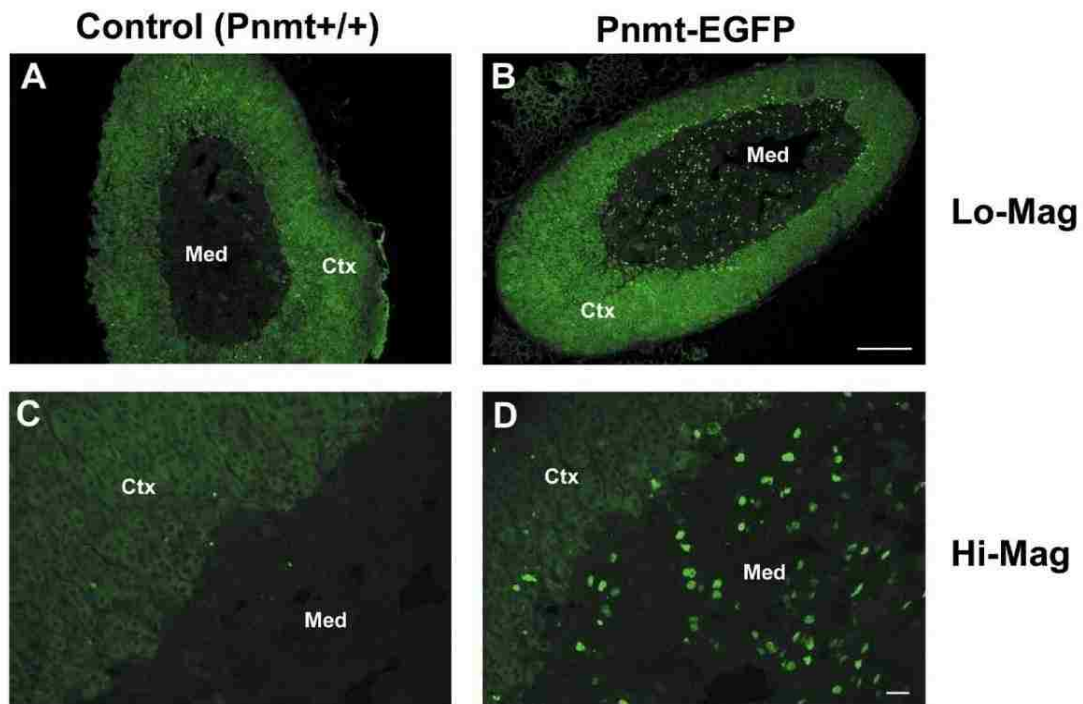
Figure 3-2. EGFP expression in mouse adrenal glands.

(A & B) Low-magnification views of fluorescent imaging of adrenal gland sections from wild-type control and *Pnmt*$^{+/nEGFP}$ mice, respectively. Scale bar, 200 μm. (C & D) Higher magnification of same image. Scale bar, 50 μm. Ctx, cortex; Med, medulla.

To evaluate the specificity of the EGFP reporter gene expression in more detail,

we performed immunofluorescent staining for endogenous Pnmt protein expression

adrenal gland sections from *Pnmt*$^{+/nEGFP}$ mice using a red fluorescent secondary

antibody tag so that we could visualize both Pnmt (Fig. 3A&B) and EGFP (Fig. 3C&D)

expression simultaneously in the same sections. Endogenous Pnmt expression is

mainly cytoplasmic while EGFP expression was restricted to the nucleus of

PnmtEGFP+ cells. Thus, overlay of the red and green fluorescent images shows co-expression in red fluorescent cells containing green nuclei, indicating that EGFP was expressed in the nuclei of Pnmt-expressing adrenal medullary cells (Fig. 3, panels E and F).
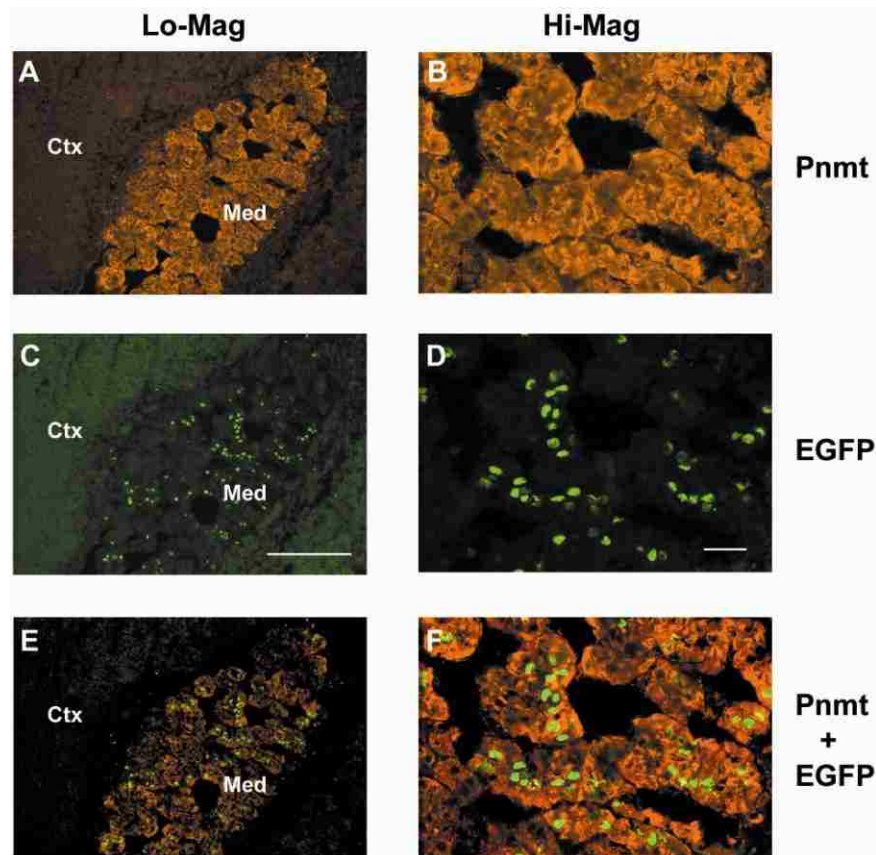
Figure 3-3. Identification of EGFP and endogenous Pnmt in adrenal chromaffin cells.

(A & B) Pnmt immunofluorescent histochemical staining in adult mouse adrenal gland sections as visualized for red fluorescence (Texas Red filter). (C & D) EGFP expression in the same adrenal sections but visualized for green fluorescence (GFP filter). (E & F) Overlay of Pnmt and EGFP staining for each section. (A, C, and E) Lo-mag, low-magnification: Scale bar, 200 μm. Hi-Mag, high-magnification: Scale bar, 30 μm.

Confirmation that EGFP expression was principally localized to nuclei was obtained by co-staining the sections with the red fluorescent nuclear stain, propidium iodide (PI). Within EGFP+ cells of the adrenal medulla, PI labeled the cells in a pattern nearly identical that observed for EGFP (Fig. 4, arrows). Altogether these data demonstrate that EGFP expression is localized to nuclei of adrenal medullary cells in $Pnmt^{+/nEGFP}$ mice.
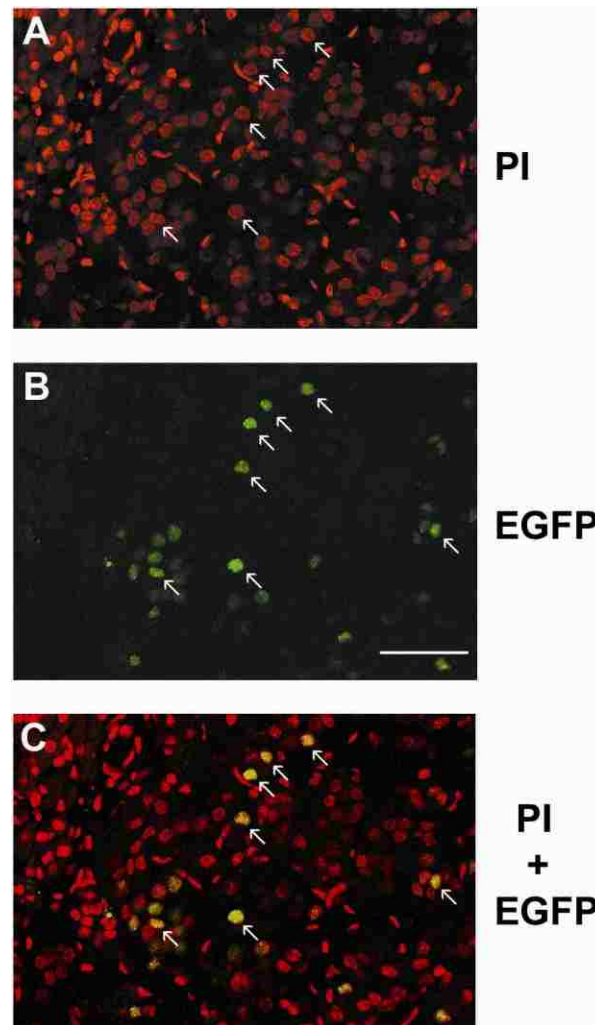
Figure 3-4. Nuclear localization of EGFP expression in adrenal chromaffin cells.

(A) Propidium iodide (PI) staining of nuclei in adrenal chromaffin cells from an adult mouse adrenal gland section. (B) EGFP expression in the same section. (C) Overlay of PI and EGFP staining. Yellow staining indicates regions of overlap. Scale bar, 50 μm.

EGFP expression is always confined to cells that also expressed endogenous Pnmt. It is clear, however, that the EGFP expression was found in only a subset of Pnmt-expressing cells. We did observe that the intensity of EGFP fluorescence was variable in EGFP+ cells (Figs. 2-4), possibly indicating that expression may be limited in some cells. To partially address this issue, we compared EGFP expression in adrenal

56

sections from mice with one EGFP copy ($Pnmt^{+/nEGFP}$) versus those that had two copies ($Pnmt^{nEGFP/nEGFP}$). Representative images of adrenal sections expressing EGFP are shown in Fig. 5 (panels A and B). Quantitative assessment of the number of EGFP+ cells per section revealed that there was a significant two-fold increase in the number of EGFP+ cells found in the homozygous EGFP/EGFP condition compared with those from mice with only one copy (+/EGFP) (Fig. 5C). Altogether, our results indicate that the amounts of GFP stably synthesized in Pnmt::GFP insertion cells is variable from cell to cell and not sufficient to mark all adrenergic cells at any given time point.
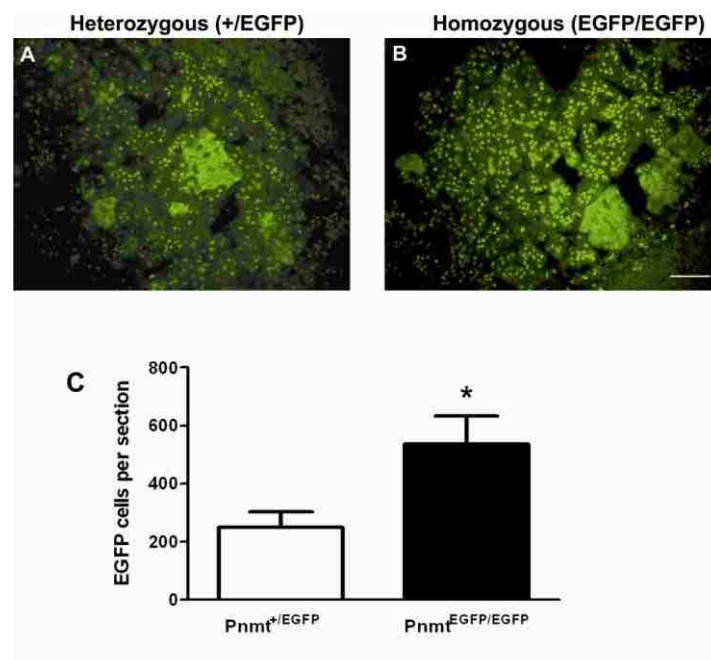
Figure 3-5. Comparison of Pnmt-EGFP expression in heterozygous ($Pnmt^{+/nEGFP}$) and homozygous ($Pnmt^{nEGFP/nEGFP}$) mouse adrenal glands.

(A & B). Representative adrenal gland sections with EGFP expression from heterozygous (A) and homozygous (B) mice. C. Quantitative analysis of average number of EGFP+ cells per section for each genotype ($p < 0.05$, n=5). Scale bar, 100 μm.

3.3.3 Evaluation of EGFP expression during heart development *in vivo* and *in vitro.*

In the heart, Pnmt expression is first detected during early embryonic development at about the time that the heart first starts to beat [30, 31]. To determine if EGFP expression could be identified in cardiac adrenergic cells, we examined embryonic heart sections from $Pnmt^{nEGFP/nEGFP}$ mice for the presence of EGFP+ cells. This was more difficult than anticipated due to the relatively high background autofluorescence in the green spectrum. At low magnification, it was essentially impossible to distinguish EGFP+ cells from non-expressing cells (Fig. 6A). However, at higher magnification, however, characteristic green fluorescent nuclei were evident in cardiac cells (Fig. 6B, arrows) near the atrioventricular junction, a region that has been associated with strong Pnmt expression in the developing rat and mouse embryonic heart from previous studies [30, 33]. Note that the EGFP expression was not visible in the red spectrum, whereas nearby autofluorescent cells showed similar patterns of fluorescence in both the red and green spectra (Fig. 5B&C). These data show that EGFP expression could be identified in presumptive adrenergic cells from $Pnmt^{nEGFP/nEGFP}$ embryonic heart sections.
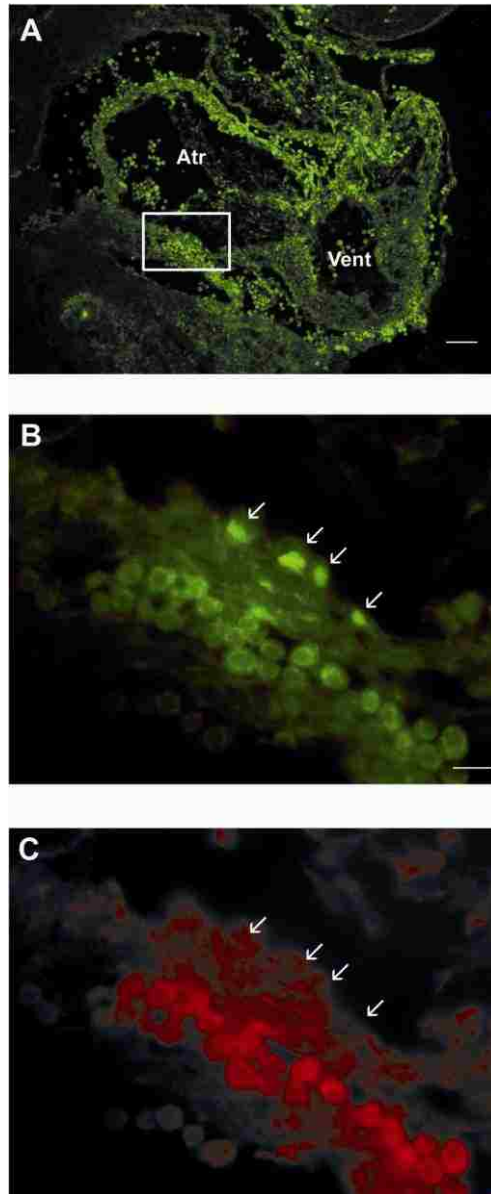
Figure 3-6. Detection of EGFP expression from *Pnmt^{nEGFP/nEGFP}* mouse hearts at E10.5.

(A) Sagittal section of E10.5 mouse heart visualized in the green spectrum, with atrium (Atr) and ventricle (Vent) clearly distinguishable. Scale bar, 100 μm. Although many cells appear to exhibit green fluorescence in this image, most of this fluorescence is due to background autofluorescence. This was determined by comparing fluorescent images in the green and red spectra. An example is shown in panels (B) and (C), respectively. Note that the images shown in panels B & C represent an expanded view of the region of the E10.5 near the A-V junction (boxed region from panel A) representing green and red fluorescent images, respectively. The EGFP+ cells (arrows) were positively identified with the green fluorescence filter showing EGFP expression to be exclusively evident when visualizing green but not red fluorescence. In contrast, autofluorescence was observed similarly in green and red spectra. Scale bar, 20 μm.

59

As an alternative approach to these in vivo assessments, we examined endogenous Pnmt in mESCs and EGFP reporter expression in *Pnmt*[+/nEGFP] mESCs before and after inducing their differentiation into beating cardiomyocytes [99, 100]. As shown in Fig. 7A, Pnmt mRNA was not detected in undifferentiated pluripotent mESCs (lane 1), but appeared subsequent to the onset of contractile activity at 7+3d (lane 2), and continued to be associated with beating cardiac-differentiated mESCs at 7+5d (lane 3). Thus endogenous Pnmt mRNA is restricteded to mESCs that had been induced to differentiate into beating cardiomyocytes, and is not detectable in undifferentiated mESCs.

Evaluation of EGFP expression in these mESCs uncovered small clusters of EGFP+ cells as early as 7+3d (Fig. 7B). We used the same criteria as above (green fluorescence in cell nuclei showing no autofluorescence in the red spectrum), and found no clear EGFP staining in undifferentiated mESCs (not shown). The staining that was observed after induction of cardiac differentiation was observed in a relatively small number of cells, and was often difficult to find. It did not appear that there was appreciable EGFP expression in the beating cardiomyocytes themselves, but small clusters or isolated patches of EGFP positive cells like those shown in Fig. 7B were found adjacent to or near areas of beating activity. These results show that EGFP expression was induced in association with heart development in *Pnmt*[+/nEGFP] embryonic cells both in vitro and in vivo.
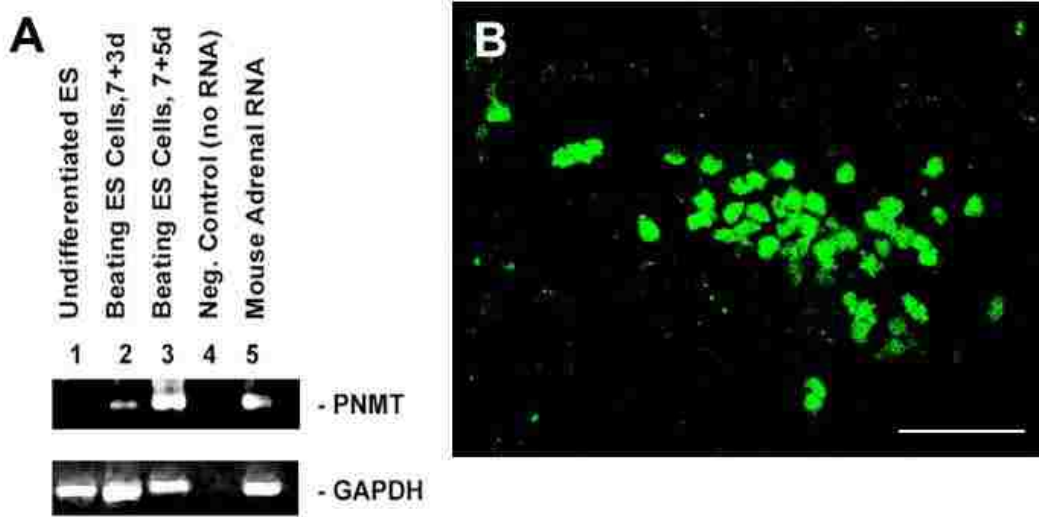
Figure 3-7. Induction of cardiac differentiation and activation of Pnmt and nEGFP expression in mouse ES cells.

(A) Endogenous mouse Pnmt gene expression as detected by RT-PCR before and after induction of cardiac differentiation in mouse ES cells. This procedure takes (7 + n) days. (B) Image of nEGFP+ cells in 7+5d cultures of cardiac-differentiated mouse ES cells. Scale bar, 50 μm.

3.4 Discussion

In this study, we have described the initial characterization of a new mouse model where a nuclear-localized *EGFP* reporter gene was inserted into the endogenous mouse *Pnmt* gene locus to create heterozygous *Pnmt$^{+/nEGFP}$* and homozygous *Pnmt$^{nEGFP/nEGFP}$* mice. Our results showed that *nEGFP* reporter gene expression was specifically found in adrenergic chromaffin cells of the adrenal medulla based on co-expression with endogenous Pnmt protein in these cells. Nuclear localization of the signal was confirmed by co-labeling the cells with the nuclear dye, propidium iodide.

61

We also demonstrated expression of nEGFP near the atrioventricular junction region of the developing mouse heart in vivo, and in association with endogenous Pnmt expression in mESCs after they were induced to differentiate into beating cardiomyocytes in vitro. These initial analyses indicate that the *nEGFP* reporter gene is correctly targeted and expressed in adrenergic cells in the adrenal glands as well as those associated with embryonic heart development. Although further characterization is needed to evaluate reporter gene expression in more detail at different developmental timepoints and in other tissues known to express endogenous Pnmt such as retinal neurons, brainstem neurons, lymphocytes, lungs, liver, spleen, kidney, and testes [7-12], these initial results suggest that nEGFP expression successfully identifies Pnmt-expressing cells in mice.

The *Pnmt*[+/nEGFP] mouse model provides two distinct advantages compared with similar knock-in models that inserted the *Cre-recombinase* gene into the mouse Pnmt locus [33, 101]. First, the *nEGFP* knock-in marks cells actively expressing Pnmt while the *Cre* knock-in marks cells that had a history of expressing *Pnmt* at some point in their development in addition to cells actively expressing *Pnmt*. Second, EGFP can potentially be used to identify and isolate viable adrenergic cells directly using fluorescence imaging and collection strategies such as fluorescence-activated cell sorting (FACS). When comparing the staining results from these models, it appears that the *Pnmt*-driven *nEGFP* expression is restricted to a subset of cells that showed positive expression of *Pnmt*-driven *Cre-recombinase* from previous studies [33]. To identify cells that had expressed *Cre-recombinase*, the mice were crossed with

ROSA26 reporter mice containing the *β-galactosidase* reporter gene. Within the adrenal glands, β-galactosidase staining was restricted to the adrenal medulla. In contrast, β-galactosidase staining in the heart was initially found in the muscle walls of the cardiac chambers of the developing embryonic heart, similar to the nEGFP staining patterns observed in the present study.

It should be noted that the targeting vectors and strategies were similar for both models (*nEGFP* and *Cre*), so we expected some similarity in expression patterns that also matched those observed for endogenous Pnmt staining. The more limited staining observed in the *nEGFP* knock-in model undoubtedly reflects the fact that only active *Pnmt*-expressing cells show *nEGFP* expression compared with the active plus historical expression demarcated by the β-*galactosidase* reporter generated by *Cre*-activation of the *ROSA26* locus [33]. When compared to endogenous Pnmt expression using anti-Pnmt immunofluorescent staining techniques, we also found only a subset of active *Pnmt*-expressing cells that also displayed *nEGFP* reporter expression. Our analysis suggested that this is a sensitivity issue. At any given time, many adrenergic cells have not expressed enough EGFP to effectively mark the nucleus above the fluorescent background. In this regard, the variability in GFP fluorescence between cells is quite interesting as it suggests that the activity of the medullary cells is not uniform. We hope to use our system to characterize this cell to cell variability in future studies.

3.5   Limitations and Future Directions

Although EGFP is widely employed as reporter gene, recent studies show several disadvantages for its application in mouse ES cells and transgenic animals [35, 36]. The spectrum of EGFP fluorescence overlaps with background autofluorescence, which poses challenges for distinguishing EGFP+ cells from non-expressing cells. This is especially true when reporter gene expression is relatively weak or at low abundance, as was the case in the embryonic heart. Improved fluorescence imaging techniques and equipment should help resolve the autofluorescence challenges, which were also partially overcome in the present study by comparing fluorescence images in the red and green spectra. Specific EGFP+ fluorescence was only observed in the green spectrum, whereas autofluorescence has a much broader bandwidth and is evident in both green and red spectra on our microscope.

In addition to the challenges posed by autofluorescence, we also observed considerable variation in EGFP+ cell staining within tissues that express Pnmt. This was most clearly seen in the adrenal medullae where many Pnmt+ cells did not display detectable EGFP expression. Other studies have also noted variable expression for the EGFP reporter in mammalian cells. For example, Swenson did a systemic analysis of GFP transgenic mouse using three different types of GFP mice strains with "ubiquitous" promoters and various methodologies for data acquisition, such as direct fluorescence detection, immunofluorescence and immunohistochemistry with diaminobenzidine, (DAB) deposition. GFP expression characteristics were also determined in various

organs [17]. Notably, GFP expression in different organs varied widely between the three genotypes tested, and the differences from same organs were also significant. No matter which promoter was used to drive GFP expression, not all the cells from examined tissues were GFP+ in any of the three transgenic lines. There may be inherent limitations in the GFP reporter gene itself, perhaps due to toxicity, turnover, nuclear reprogramming, and/or other effects of GFP and its derivatives that have yet to be fully defined. Thus, the main limitations of the model appear to primarily concern the variability of the EGFP reporter and difficulties in distinguishing its expression from background autofluorescence when in low abundance, such as the case observed during embryonic heart development.

3.6   Conclusions

Despite the limitations of the EGFP reporter indicated above, we have nevertheless shown that this reporter gene was correctly targeted to the mouse *Pnmt* gene locus. Further, we successfully created a new mouse genetic knock-in *Pnmt::nEGFP* model that expresses nEGFP exclusively in Pnmt+ cells. In no cases did we find nEGFP expression that was inconsistent with endogenous Pnmt expression. Expression was verified in adult adrenal chromaffin cells as well as embryonic cardiac cells. This model should be useful for identification and characterization of adrenergic cells in a variety of other tissues/cells also known to express Pnmt, such as retina, brainstem, lung, testes, lymphocytes, and others [25, 26, 29, 97, 102-106].

CHAPTER 4 : GENERATION OF NOVEL FLUORESCENT REPORTER CELLS FOR IDENTIFICATION OF CARDIOMYOCYTES DERIVED FROM ADRENERGIC PROGENITOR CELLS

4.1 Introduction

In the chapter III, we used a genetic model to determine whether the specific population of cardiac adrenergic cells occurred during embryonic heart development, in which PNMT regulatory sequences to control the transcription of EGFP, thus enabling us to characterize the live cells with adrenergic phenotypes. Although EGFP is a strong reporter gene under most cases, and we did observe the green fluorescent cells in the embryonic heart, however, as for multiple reasons, the signal was not strong enough to identify these adrenergic cells in addition to other complexities which made it difficult for isolation of these cells, no matter *in vitro* PNMT-nEGFP ES cells or the embryonic hearts of PNMT-nEGFP mice are used. Therefore, genetic models with higher specificities for reporter genes should be developed to improve the shortcomings of the current model.

As our purpose is to study the cell lineage and final destinations of adrenergic derived progenitor cells, so mESCs are very important tools to fulfill the purposes for the following reasons. First of all, pluripotent mESCs have the capability of self-renewal and differentiation to multiple cell types and organs, which include cardiomyocytes [100, 107-109], thus they are good tools to study the gene regulation of cell lineage commitment during embryogenesis, and can give us detailed information of specific

tissue or organ morphogenesis such as cardiac development. Mouse mESC cells are good models to explore the mechanisms of cardiogenesis and also vasculature development [110, 111] .

Secondly, current molecular biology technologies allowed us to do plenty of genetic manipulation of ES cells (knock-in, knock-out and et al) and these engineered ES cells still keep the features of self-renewal and differentiation, even incorporation into embryogenesis when transplanted back into early embryos [112-114]. Thus, we can have variety of genetic engineered animal models in which the gene of interest was altered, therefore, we can identify their phenotypes to determine the function of specific gene at specific tissues, and also at specific time frame. Thus establishing a proper engineered mESC model can help us accomplish our own research objective if the mESC line can provide detailed information about the intrinsic adrenergic derived progenitor cells.

Cre recombinase which was identified in phage P1, can excise the 34bp lox-P site through recombination and results in deletion of the sequences between two lox-P sites [115, 116]. This capability to delete sequences from double strand DNA makes Cre useful in various biological applications, especially in the gene targeting [117]. It can lead to activation or inactivation of specific genes, both endogenous and transgenic, and this process can be through temporal, spatial or cell type specific induction [118], allowing us to explore the functions of these genes at specific milieu. In addition, under proper situations, some specific cell populations can be deleted [119, 120].

67

Recently, a double fluorescent indicator vector was engineered by Hescheler and colleagues [37]. This vector (as outlined below) has several characteristics:
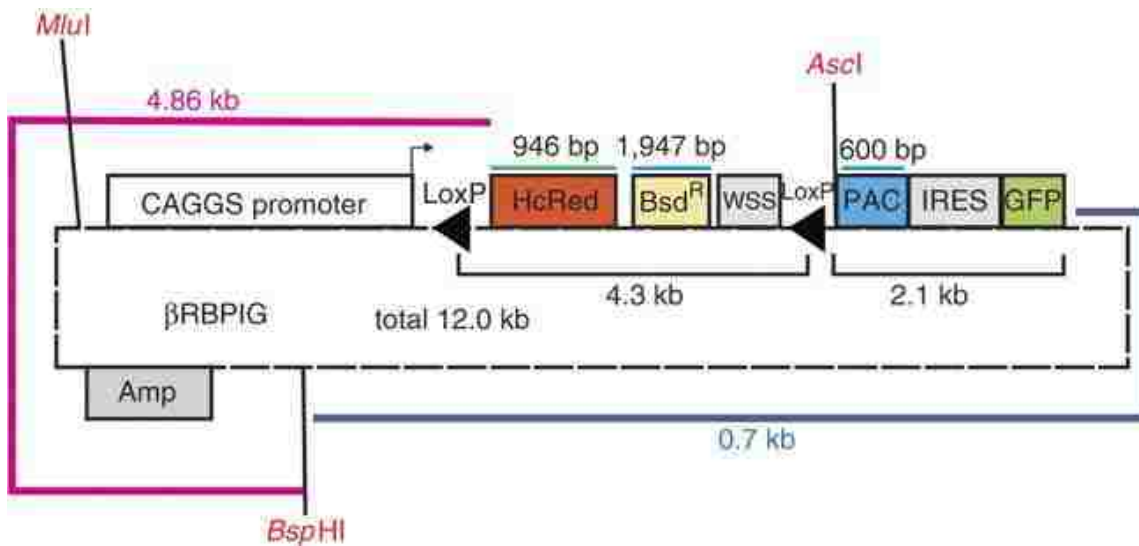
Figure 4-1. Map of the dual fluorescence plasmid βRBPIG.

MluI, AscI and BspHI are the recognized sites of individual restriction endonuclease; CAGGS, chicken β-actin-promoter with CMV enhancer; HcRed, coding sequence for the RFP HcRed1; BsdR, resistance against the antibiotic blasticidin; WSS, Westphal stop sequence; PAC, puromycin acetyltransferase; IRES, internalribosome entry site; GFP, green fluorescent protein; Amp, resistance against ampicillin with bacterial promoter; picture is by the courtesy of Kurt Pfannkuche et al [37].

1. The Multiple cloning sequence (MCS) of the plasmid is divided into two parts: red fluorescent protein (RFP) encoded by HcRed1 gene and enhanced green fluorescent protein (EGFP).

2. The RFP coding sequences is followed by blasticidin resistance and a stop sequence called Westphal stop sequence (WSS), HcRed-Bsd-Wss is flanked by two loxP sites on each ends.

3. Behind the second loxP site, the construct contains Puromycin resistance gene which encodes Puromycin acetyltransferase (PAC) and PAC is linked with elements for internal ribosome entry site (IRES) plus EGFP. The PAC-IRES-EGFP bicistronic expression cassettes will only be expressed when Cre is available and excise the flanked HcRed-Bsd-Wss sequences. Thus, this vector provides the opportunity of discrimination of unrecombined and recombined cell populations dependent on the Cre activity.

4. This vector's promoter is from chicken β-actin and its enhancer from cytomegalievirus (CMV) immediate early gene, the promoter is extremely attractive as it is fully functional in mESCs.In addition, as RFP and EGFP have different antibiotic resistance (blasticidin vs puromycin), it allows us to get high yield of purified either unrecombined or recombined cells by drug selection respectively.

With this powerful Cre indicator vector, researchers can employ it for many ways other than originally designated as a measure for monitoring cell fusion events. For example, if one gene's regulatory elements (including promoter and enhancer) are linked with Cre coding sequence, cells under the regulation of this gene are possibly mapped by introduction of this dual fluorescence vector in cultured cells based on the switches of fluorescence, as only cells with emission of green fluorescence are those regulated by target gene, the activity of which can be illustrated by excision of loxP sequences from Cre. In addition, this specific type of cells can be enriched by administration of puromycin.

Based on our previous results, Pnmt mRNA was only expressed in mESCs after differentiation into cardiomyocytes. Thus in this section we developed a strategy \that the pluripotent mESCs knocked in with Pnmt-Cre were utilized as the starting materials, the Cre indicator vector was stably transfected into this mESC line. Therefore, after in vitro differentiation of these engineered mESCs into beating cardiomyocytes, fluorescence changes will be tracked to determine the activity of this conditionally expressed Cre. This is a simpler *in vitro* model to fulfill the purpose of characterizing adrenergic progenitor cells, and if the hypothesis performs well, we have the opportunity for enrichment of the cells with adrenergic phenotypes which we can use for further identification of their physiological properties.

4.2   Material and Methods

4.2.1 Materials

All the medium (DMEM, high glucose, containing L-glutamine and sodium bicarbonate) and supplements such as Non-essential amino acids (NEAA), L-alanyl glutamine (GlutMAX^{TM}), β-mecaptoethanol, Pen-Strep were from Invitrogen, 0.05% and 0.25% trypsin both with EDTA were also from Invitrogen, Fetal bovine serum defined grade from Hyclone (SH30070.03), ESGRO$^{®}$(LIF) Supplement (10^7 Units) and gelatin were from Millipore, Blastidicine S Hydrochloride (15205, ≥99.0%), Puromycin dihydrocholoride (P7255, ≥98%), Mitomycin C (M5053) were from Sigma. Glass-bottom dishes, P35G-1.5-14-C was from Mat Tek corporation. Regular 96, 48 and 24 well

plates and tissue culture dishes with 20mm grid were from Falcon, regular 10cm, 6cm petri dishes and T25, T75 flasks were from Corning Corporation.

4.2.2 Primary cultures and maintenance of mouse embryonic fibroblasts (mEF)

All the procedures were in accordance with ATCC cell culture protocols with minor adjust. For primary cultures of mEF, mouse fetus at post-cotium 11.5 to 13.5 from 129sv strain pregnant mice were antiseptically removed from opened uterus and transferred to sterile PBS containing petridishes. After removal of placenta and all visible membranes, viscera and other clear organs such as head and tail of fetus were also taken out and then transferred to another petri dish. The remaining tissues were minced with dissection scissors as small as possible, and then put to 50ml cornical tube. Trypsin (0.25%)/EDTA was added to the tube and tissues were dissociated by pipetting, incubated at 37C for 5 to 10mins dependent on the numbers of fetus. The digested product were neutralized with DMEM full medium (10% FBS) and settled for 5mins to precipitate large and undigested pieces. The supernatant were then transfered to 2-3 10cm petri dishes. Cells were incubated at 37°C for 24h and processed with medium change thereafter. After incubation for another 24h, cells were split with 0.05% trypsin at the ratio of 1 to 3 and cells at this passage were marked at P1. mEF at P2 and P3 were frozen for future usage. Usually, the mEF kept good proliferation rate until their 7 to 9 passages and after stop proliferation they were not used as feeder layers.

4.2.3 Mitomycin C treatment of mEF as feeder layers fro mESC

After the mEF were 90% confluent in either petri dishes or tissue flasks, they should be treated with mitomycin C to stop their proliferation thus become ideal feeder

layers for mESC. Medium was changed and Mitomycin solution (0.5mg/ml) was diluted with DMEM to final concentration of 10µg/ml. Cells treated with drugs were incubated at 37°C for 3 to 3.5hr, then rinsed with PBS twice and trypsinzed and collected. Usually we use condensation ratio at 1:1.2 to 1:1.5 to reseed the re-suspended mEF to either 6cm petri dish or T25 flasks. Condensation ratio was designed as the ratio of the whole covered surface areas before Mitomycin C treatment with the whole growth areas after treatment. The reason for thicker seeding densities after drug treatment was because some of mEFs would become less healthy after this process thus higher density was required. Since being seeded, mEF could be ideal feeder layers for two weeks.

4.2.4 Mouse embryonic stem cells culture

Mouse ES cell line used in current part was pre-engineered R1 mESCs with Pnmt-Cre [33]. Standard culture protocol for ES cells includes medium change every day and split at ratio of 1:5 to 1:7 regularly every other day. The medium should contain mouse leukemia inhibitory factor (LIF or ESGRO®) at 1000 units/ml. Most of the time, mESC should be cultured on mEF feeder layers as these are the most close *in vivo* growth milieu for them. For some cases, such as differentiation, ES cells can grow on gelatin (0.1%) coated culture dishes for couple of passages but not for long term maintenance. When grown on mEFs, 0.25% trypsin/EDTA was used to split mESCs when cells were 70% confluent, however, 0.05% trypsin/EDTA was used for ES cultured on gelatin.

4.2.5 Generation of stable double fluorescent indicator ES cell line

4.2.5.1 <u>Linearization of RBPIG plasmid</u>

The RBPIG Cre/loxP vector was digested with MluI overnight at 37°C, confirmed for complete digestion by running small amount digest product through agarose electrophoresis. There should be only one 12kb band on the gel. The whole 100µl product were then purified and precipitated with 70% ethanol, re-suspended in 30µl sterile electroporation buffer. The total DNA was for one electroporation was around 30-40µg.

4.2.5.2 <u>Electroporation of mESC with linearized RBPIG plasmid</u>

Pnmt-Cre mESCs with lower passages were split one day before electroporation. These cells were trypsinized to single cell suspension. After neutralization, cells were washed twice by PBS through centrifugation, after cell counting with hemocytometer, around 3×10^7 cells were re-suspended in 600µl electroporation buffer, linearized DNA was added and balanced with more buffer to final 800µl. The cell suspension were transferred to 0.4cm cuvette (Biorad), put on the ice for 5min before electroporation.

Here we used more hash parameters for the electroporation as the preliminary studies showed that these parameters achieved to higher cell clones compared with other milder ones. With Bio-Rad Gene Pulser Xcell™ electroporation system, 260V and 500µF capacitance were chosen for elctroporation with the module of exponential decay. The time constant often fell into 10-12msec. Cells were returned on ice for another 5min before being transferred and seeded into 30 6cm feeder layer coated petri dishes. Relevant control groups were also set up which included: 1) Mock electroporation, cells

were electroporated without DNA; 2) Normal cells without electroporation; 3) &4) RBPIG and Mock electroporation but without the addition of drugs (detailed as follows).

4.2.5.3 Screening mESC clones with stable transfection of RBPIG

One day after electroporation, medium was changed with addition of 3µg/ml blasticidin, then medium was changed every other day with fresh blasticidin. The cells looked all dead around day 7 after drug treatment, thereafter, small colonies gradually came out. On day 14, colonies were picked out under the microscrope by pipets and transferred to 96 well plates, dissociated with 0.25% trypsin/EDTA, then transferred to 48 well plates pre-covered with mEF. All the selection procedure contained drugs. When colonies became half confluent in 48wells, they were processed as same above and dissociated cells were switched to 24well plates. During the selection, each colony was marked numerically and caution should be paid to avoid the cross-contamination between colonies.

When cells in the 24wells were half confluent, cells were dissociated and divided into two parts. Half of the cells were frozen and the second half was seeded onto 3.5cm glass-bottom dishes covered with gelatin. As for the slim thickness of the glasses in the center of these culture dishes, cells growing on them were easily detected under the microscope.

We use Spin-disk confocal laser microscope (Perkin Elmer) for the screening of live fluorescence for each individual cell clone. The transfected undifferentiated ES cells should emit red fluorescence, and based on the spectrum characteristics of HcRed1 (Maximum Excitation at around 590nm and emission at 645nm), we chose relevant

fluorescence filter to achieve highest fluorescence yield. During the screening, the exposure time and compensation were set up same for each sample for fair comparison of the fluorescent intensities. Each sample should get a number representing the maximum fluorescent intensities. Pictures were also taken for some clear positive transfectants. In the first round of screening, we mainly relied on the absolute reading and pictures to judge their fluorescent activities. Around 30 different colonies were selected as positive during the first round screening. These colonies went through the same protocol for comparison during the second round live imaging screening and the numbers of highest transfected colonies were narrowed to single digit.

In the same time, the selected colonies were maintained for around 10 passages for observation of their ES characteristics: speed of proliferation, self renewal capabilities and morphology, any colonies with abnormal characteristics, especially with big morphology change (indication of self differentiation or other biological changes) should be excluded. The final two to four clones were chosen and by confocal scanning their 3D structures were taken. In addition, their detailed passage information was kept in records.

4.2.5.4 Purification of RBPIG colonies by single cell clonal analysis

As for some reason the colonies we got above had lower percentage of RFP positive expression (would be explained in detail in the discussion part), we utilized single cell culture to get much purer population of fluorescent positive cells. The two colonies we chose were the start of these purification processes. For each cell line, cells were seeded 1 cell per well theoretically based on the counting from hemacytometer in

48 well gelatin covered plates. The medium also included blasticidin at desired concentration. After two weeks or so, some wells could be found with formation of small colonies, through regular medium change and drug refreshing, some colonies continued to grow, we then used epifluorescence microscope to detect the red fluorescence of these cells. Several wells emit much higher fluorescence than others so cells from these wells were candidates for further purification. Cells from these wells were marked and reseeded at very low densities (around couple of hundred cells per well in 48 well plates). Each subclone had 5 to 7 sub-subclones, for example, cells from clone No.3 of original clone No.34 were reseeded and named Clone 34-3-1, 34-3-2, 34-3-3, etc. These clones were checked for their fluorescence both in 48 well plates and also on the glass-bottom petri dishes to determine the fluorescent intensities. These clones were then seeded on 6cm petri dishes covered with mEF and the spouted clones had much more even distributed fluorescence on average and thus the selection ended at this point. Totally there were 2-3 final candidates which were used for the differentiation studies.

4.2.6 Cardiac differentiation of RBPIG mESC into cardiomyocytes

There are several ways to differentiate mESC into cardiomyctes in vitro [121], such as Haninging drop, the method in the chapter III employed, suspension culture in bacterial-grade dishes and etc. However, Hanging drop method is still the most often used tool which cells were allowed to aggregate to form embryonic bodies (EBs) in the bottom of a hanging drop [107]. In this chapter, we mainly used this method to induce

cardiac differentiation in vitro, although at less frequency rotary suspension culture was used as alternative.

For Hanging drop culture, it is introduced briefly as in previous chapter but will amply described here. Early passage mESCs were split into individual cells and counted, 500 cells per 20µl differentiation medium (without LIF) were put on the lid of 150mm petri dish as a drop, the bottom of the dish was covered with PBS in order to avoid dryness. After finshing dropping, the lid was swiftly reversed and placed on the dish which was then incubated at 37 °C. After 2days, the lid was flipped, and the white EBs were transferred to two 10cm bacterial grade dishes within 10ml differentiation medium. At this moment, there're two ways to continue the culture, one is by stationary culture, dishes were just put back into incubator, the second way relied on a horizontal rotating device located in the incubator to make these dishes rotate at 35rpm during growth. For both ways, EBs were in suspension for 2 to 3 more days and then transferred to gelatin coated cell culture dishes. Medium was changed every other day thereafter, EBs were attached first and then gradually stretched out, mesoderm derived cardiomytes were usually in the middle part of the whole differentiated structures, and these were the main observation fields where beating foci could be found. The beating activity started around 7 to 8 days since start of differentiation, and occasionally these could be delayed by several days. The rate of contraction increased gradually since the start of beating and contraction could last for at least 3weeks, then beatings stopped and cells became almost fully differentiated and cardiomyocytes occupied a big portion of these cells.

For some cases, we use rotary suspension cultures to yield differentiated cells from the beginning. The method was mainly based on the protocol from McDevitt's laboratory but with minor modifications [122, 123]. Basically, undifferentiated ES cells were plated at 4×10^5/ml into bacterial grade dishes within 10ml differentiation medium. As mentioned above, dishes were put on the surface of an orbital rotary shaker at around 35 revolutions per minute. The speed was very critical for the quality of EB formation as cells were inclined to aggregate into big clumps instead of EBs at lower speed, and with speed of 45rpm and above, the numbers of the EBs were sharply reduced plus the size was also much smaller. We tested several suggested speeds and chose the above one for most of the experiments. After two days in suspension, the EBs containing medium was carefully transferred to a sterile 15ml conical tube and settled down for 5mins. The supernatant was then discarded and EBs were gently mixed with new medium and seeded into two new dishes. Medium was changed every other day and the culture was kept for 5 to 7 days in suspension, then EBs were plated into 6cm or 10cm gelatin coated dishes at about 30 and 70 per dish respectively. After being plated, it was treated as above with hanging drop method and EBs' morphology changed from round dark core to more spread out multilayer cells 3-4 days later.

4.2.7 Puromycin treatment of cardiac differentiated mESC clones transfected with RBPIG

Puromycin was dissolved at 10μg/ml at stock and aliquot was kept at -20°C. In order to determine the concentration which kills the non transfectant at minimal amount, a dosage curve was made for undifferentiated mESCs. Confluent mESCs in 6cm petri

78

dishes were treated with puromycin at different concentrations from 0.5, 1, 2, 3 to 5µg/ml in full medium. The morphology change was carefully monitored after drug induction every day. The concentration which killed cells almost completely after 48h was chosen as the base concentration in differentiated cardiomyocytes. The concentration was set between 1-2µg/ml.

Cultured differentiated ES cells by both methods (Hanging drop or rotary suspension) were treated with puromycin at different stages. Initially, we treated 14d differentiated cells in 6cm petri dishes with 2µg/ml and change medium 2days later if cells were not completely dead. Later on, drugs were administrated starting from day 8, 10, 12 and also refreshed every other day. Comparison of morphology was made between Pnmt-Cre cells and mESCs transfected with RBPIG.

4.3   Results

Initially we picked up 204 colonies into 48 well plates, some of which still survived the antibiotic treatment, around 100 colonies were cultured in 24 well plates, again the resistant clones were further cultured in 3.5cm petri dishes for fluorescence screening by microscope. We screened about 90-100 colonies by checking fluorescence under both green and red fluorescence filters. The maximal emission spectrum of HcRed1 is around 645nm, so a specific fluorescence filter, rather than regular red fluorescence, was chosen for fluorescence detection. Among the screened samples, 24 colonies

which were red fluorescent based on same evaluation rule (detailed in materials and methods) were screened for the second time, with both fluorescence intensity and morphology taken into consideration. For example, some clones show positive red fluorescence, however, there were some cells undergoing self-differentiation with "dendrite" like cells stretching out from main mESC cell clusters. Clones like the above described won't be designated as a good one and thus excluded. Finally, we chose No.34 and No.46 as the final candidates for the following experiments, both showed well above-background red fluorescence and good morphology. Representative pictures are shown in Fig.2.
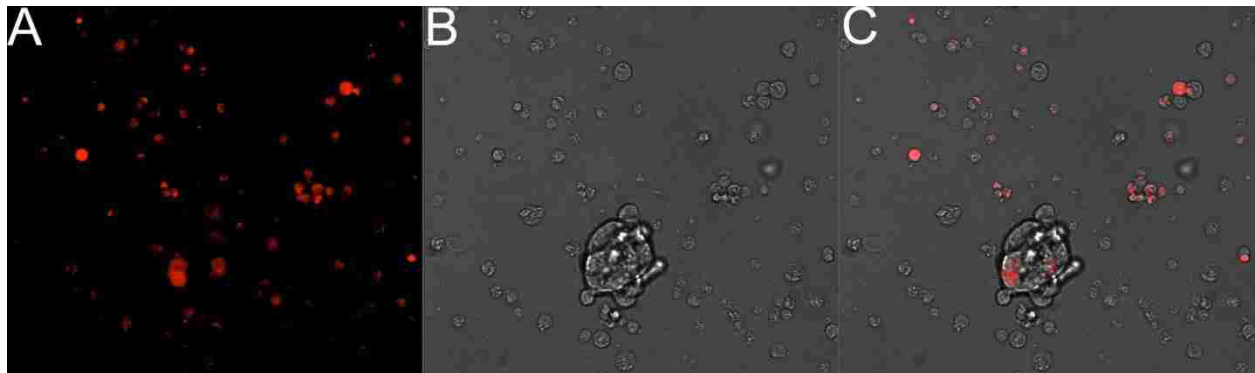
Figure 4-2. Red fluorescence of mESC clones from Pnmt-Cre mESC transfected with RBPIG.

No.34, one of the positive clones from Pnmt-Cre mESCs transfected with RBPIG, showed red fluorescence after blasticidin selection. (A), red fluorescence image; B, phase-contrast and C, overlay of the fluorescence and phase-contrast images. pictures were taken under 10X. Scale bar: 26μm.

In order to see whether green and red fluorescence could be found after transfection, we used HEK293 cells as a control and transiently tranfected them with pEGFP-N1 and RBPIG respectively to determine whether fluorescence could be detected from these transfected cells. Fig. 3 showed that both GFP and RFP could be detected after transient transfection, thus providing a good control for the identification of green and red fluorescence of mESCs.
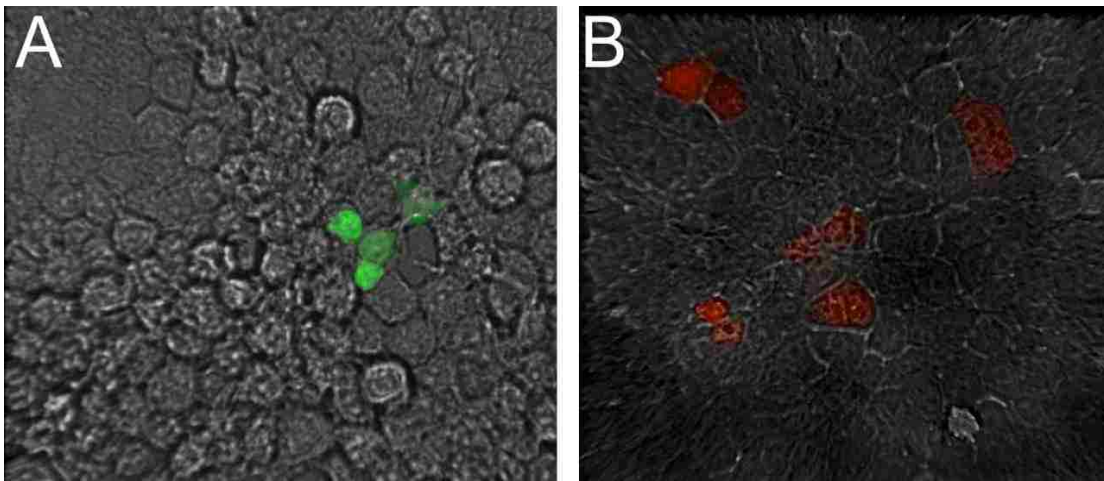
Figure 4-3. Fluorescence of HEK293 cells transiently transfected with pEGFP-N1 and RBPIG respectively.

HEK293 cells were tranfected with pEGFP-N (A) and RBPIG (B) by calcium phosphate precipitation in 3.5cm bottom glass petridishes. 48hrs after transfection, fluorescence was determined by confocal laser scanning microscopy. Pictures were taken at 25X and showed as overlay of phase-contrast and fluorescence.

Then No. 34 and No.46 RBPIG clones were differentiated into caridomyocytes by hanging drop. After 2-3days in stationary suspension, EBs were attached to gelatin coated petri dishes. They started to beat on average 7-8 days since differentiation. The overall beating activity was consistent, with the majority of the seeded EBs could occupy at least one beating loci, albeit the number and physical size of the beating loci highly varialble. We determined their fluorescence 15 days after differentiation and representative pictures were shown as follows.
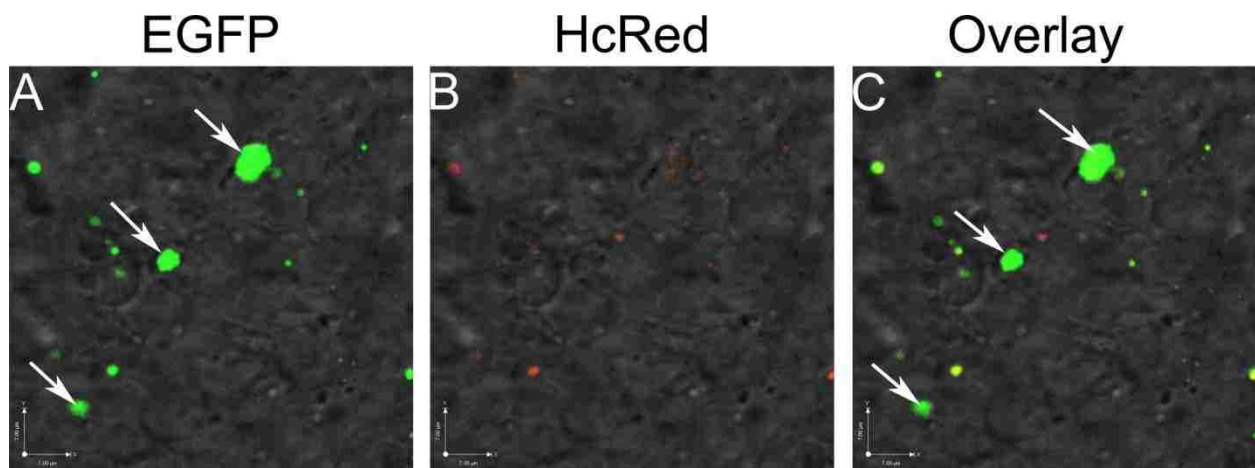
Figure 4-4. Fluorescence switch of cardiac differentiated Pnmt-Cre/RBPIG mESCs.

Images of RBPIG mESCs of clone No.46 on glass bottom culture dishes at 15 days after cardiac differentiation. (A) green fluorescence; (B), red fluorescence; C, overlay of A and B. All the pictures were used phase contrast images as background. Scal bar: 7μm.

Differentiated mESCs from both hanging drop and rotary suspension culture were also treated with puromycin. As for the chosen dosage (0.5-5μg/ml), there were not significant discrepancies of morphology changes between the transfectant and control. Further discussions were in the next part of the same chapter and alternative strategies for enrichment of these green fluorescent cells were also covered.

4.4 Discussion

In this section, we used a dual fluorescence plasmid as the indicator, to monitor the Cre activity by observation of fluorescence switches, this is an straightforward way to determine how does Pnmt exert its function during cardiac differentiation, since the Cre activity is fully controlled by Pnmt.

In the figures we showed above, we successfully established the mESC line transfected with this construct, red fluorescent cells were identified and continuously enriched with antibiotic (blasticidin) inclusion and around 20 or so cell lines were confirmed with positive. After comparison of fluorescence intensities, two out of these 20 were finally chosen as further experimental purposes. They both could differentiate well into beating cardiomyocytes, and representative picture for clone No.46 in figure 4 showed the occurrence of fluorescence switch after cardiac differentiation into partial mature cardiomyocytes (15 days since differentiation). Specifically, these fluorescence emitting cells were located in the beating areas. These results demonstrate that this *in vitro* mESC differentiation successfully imitates the developmental process of cardiomyocyte differentiation *in vivo*. In addition, Pnmt is involved in this molecular process as its regulation is represented by Cre activation and excision of the RFP part of RBPIG, resulting in a portion, although not many of the differentiated cardiomytes with green fluorescence. This is a critical discovery which confirmed our previous data that showed Pnmt expression and participation in the early stages of mouse and rat heart development [30, 31, 33].

Fluorescent protein used in biological science is a revolution as the technology allows us to investigate a variety of biological functions such as the protein localization, dynamic movement and mutual interaction. Among these families GFP was discovered first and also most widely applied in practice. However, red fluorescence protein was used much less for some reasons. One reason was fewer numbers of RFP proteins and their mutant variants available. The other reason originated from the structures of these proteins. RFP was usually tetramers and produced toxicity as there were aggregates in the cells. It was difficult to get RFP expression in murine embryos if the natural forms were not modified.

The most commonly used RFP was DsRed and HcRed. DsRed has gone through several generations of strutcture modifications, such as monomeric RFP (mRFP), which has been successfully applied for generation of mESCs and transgenic mouse [124, 125].

Another far-red fluorescent protein, HcRed, was discovered through site-directed and random mutagenesis on a non-fluorescent chromoprotein (hcCP) isolated from the Indo-Pacific Anthozoa species *Heteractis crispa*. HcRed1 was generated through series of molecular modifications and commercially available by Clonetech as a vector, and this vector provides the cDNA of HcRed1 and was processed through multi-step subclones to form RBPIG. HcRed1 forms dimers instead of tetramers, thus enhancing the performance as a fluorophore. The wavelength is sharply shifted to maximum excitation wavelength at around 645nm [126]. This long wave length fluorophore has several advantages: longer wavelength emissions have lower background

autofluorescence in tissues, thus increasing the tissue penetration and leading to fewer overlays with other fluorophores. When HcRed was just discovered, researchers successfully used it for generation of transgenic embryos and new born mice, however, the long-term survival condition was unknown [127].

Although HcRed1 was already improved compared with those original versions which were tetramers, the dimeric form still has some serious problems. Based on the comparison with other available RFP, HcRed1 still forms obligate aggregates, showing that it is still a not very mature protein tag [126]. In addition to its low brightness compared with others [128], the cytoplasmic background was also higher than others. Those phenotypes possibly explained the practical issues when we transfected mESC with RBPIG plasmid. The transfection efficiency was fairly low during initial screening, only 15 to 20% of the total cells emit red fluorescence. We don't know exactly the reason for the lower transfection ratio at the moment. One of the possible reasons could be from the characteristics of HcRed1 fluorophore itself. On the other hand, the CAGGS promoter was confirmed functional in murine mESCs. This promoter plus CMV enhance should drive the following RFP codons at high expression levels, considering we used a very hush electroporation parameter (260V, 500μF). Although we used single clone analysis protocol to grow one ES cell and tried to get higher population of red fluorescent cells, this adjustment did increase the proportion of red fluorescent cells to some extent (compared with unpurified ES clones), it has to be recognized that positive cells still accounted only a portion of the whole populations instead of 80-90%. Up to now, there was no monmeric version of this fluorophore available, and another modified

dimeric version, tanderm dimers which has two head-to-tail linked HcRed1 molecules, the performance of which was also improved compared with HcRed1 [129]. Thus, the heterogeneity for the RBPIG transfection could be improved by discovery of new version of RFP.

After differentiation in vitro, partial cells will become cardiomyocytes [99, 107, 130]. Cardiomyocytes originate from mesoderm, thus the beating loci usually fell into just outside of EB core. We did see beating loci from different batches of cells after differentiation, and the beating period could last for 3 to 5 weeks since starting. Hanging drop is the major way to let the pluripotent ES cells fully differentiate into beating cardiomyocytes, although other reports suggest other methods, such as orbital rotary suspension culture which make cells aggregate during continuous shaking by outer forces could also yield beating cardiomyocytes [122], however, in our own conditions, the beating loci from the later method were very few, and their morphology were not as fully stretched out compared with those from Hanging drop. Therefore, suspension culture didn't get the same level of differentiation quality in vitro as Hanging Drop did. The other factors, such as difference of each serum lot we used may also play important role. It deserves further effort to optimize the protocol of rotary suspension culture as higher yield of EBs could be achieved, when large scale experiments are demanding. We mainly used suspension culture for drug enrichment experiments as there were almost even numbers of cells in a single culture dish if initial inputs were set at same, therefore, antibiotic selection by puromycin will be more consistent.

However, after puromycin treatment, there were almost no obvious difference for survival cells between RBPIG transfectant and control (Pnmt-Cre) cells. We tested various concentrations, which ranged from 0.5 to 3µg/ml, and the starting time of drug administration was also variable, from around one day to 2weeks after EBs seeded on gelatinized dishes (Earlies at day 6 from starting differentiation). The main purpose of employment of broad time course is to seek a particular window with highest Cre expression. Our results from Pnmt-nEGFP differentiated mESCs demonstrated that Pnmt transcripts could reach to highest level between 10-12 days after cardiac differentiation. The expressions of Pnmt in Pnmt-Cre ES cells should be similar with those from Pnmt-nEGFP. Among all the dosage tested, beating loci could be kept after 1-2 days since puromycin administration, but they were gradually lost, the morphology of which wouldn't be distinguished from the nearby cells which were dead much earlier.

Nevertheless, in each single experiment, there were always some left over cells which looked like alive based on visual observation, especially from 1 to 2µg/ml dosage group, although similar cells, not always, but sometime also were found from the control group. So it deserves a strategy to further identify these differentiated cells, if antibiotic selection can be combined with other methods, such as FACS, which could quantify and isolated the cells with green fluorescence higher than particular intensity, it will be much help full to characterize these differentiated cells with "adrenergic" phenotype, especially for their electrophysiological properties. In addition, to achieve higher population of cardiomyocytes in the whole populations is also an important factor to get the same purpose, as current differentiation method can only achieve less percentage

of beating cells in the whole populations, the majority of beatings are spontaneous. Currently, growth factors, morphogenes, or some other small molecules have already been reported to stimulate cardiac differentiation [131]. The much purer populations of cardiomyocytes will form a more integrated network, and also the higher ratio for cells with green fluorescence, thus when puromycin is introduced, the green fluorescent cells will well resist these drugs and more prone to survive, therefore, the enrichment of the recombinant "adrenergic" cells could be proceeded with higher success rate.

CHAPTER 5 : GENERATION OF KNOCK-IN TARGETING CONSTRUCT WITH SURFACE MARKER AS REPORTER GENE TO ACHIEVE PURE POPULATION OF ADRENERGIC CELLS BY MAGNETIC-ACTIVATED CELL SORTING

5.1 Introduction

The purpose of the project in this chapter was to establish the mESC lines with the features of adrenergic cells which can be purified by MACS. Previous studies have already shown that this was an efficient way to get purified ESCs with high yield even with very low input [38]. This method fits in our practical purpose as adrenergic progenitors only cover a small population of the cell populations during the embryonic heart development based on our hypothesis.

As we mentioned in the Chapter 3, with Pnmt-nEGFP knock-in mouse as genetic model, we did identify cells with adrenergic phenotype during heart development, although practically this type of cells are very hard for identification as for several reasons. However, the same genetic strategy can also be used if other more efficient methods for cell separation or sorting are available. MACS is one of these strategies which is based on affinity based magnetic particle (beads) separation. It has been reported with many advantages compared with other sorting method and currently referred to as the "gold standard" tool for cell separations. In this chapter, we first used molecular biology tools to make the targeting construct in which the transcription of surface marker gene is under the control of Pnmt regulatory elements. This construct

was then electroporated into pluripotent mESCs, and the successful targeted cell clones will give us the capability of enrichment of adrenergic progenitor cells by MACS.

Among various surface makers used for magnetic bead sorting, C-terminal deleted version of low-affinity nerve growth factor receptor (ΔLNGFR) owns many advantages. LNGFR is one of the neurotrophin receptor superfamilies and expressed mainly in central and peripheral nervous systems [132, 133], later on the expression is also found in other tissue and organs such as bone marrow stroma, mescenchymal cells and hair follicle stem cells [134-136]. However, the truncated form of LNGFR is only expressed on cell membrane in addition to its human origin which make it an ideal cell surface marker. Since ΔLNGFR is not expressed in cells except the above mentioned, it will be a good candidate as an exogenous marker to tag the specific cells among mixed populations, then immunogenic magnetic beads conjugated with ΔLNGFR antibody (Provided by Miltenyi Biotech Inc.) can be used for isolation of these cells by MACS. Actually, it has already been reported that ΔLNGFR was used as a tag to monitor gene transduction non-invasively [41, 137] and also a marker for enrichment of specific cell populations by MACS [41, 138] or other methods such as FACS [139]. ΔLNGFR is also used in separation of various stem cells or progenitor cell populations and achieved with higher purities [38, 42, 136]. In addition, no obvious immune responses are found and cells maintain high viabilities and the capabilities of self-renewal and full differentiations.

The establishing of the targeting construct needs several sublcone steps based on the already available plasmids. The purpose of the subclone is to engineer these

plasmids and put the cDNA of ΔLNGFR and neomycin together, which are then inserted into the Pnmt 5' regulatory sequences. The construct will be further engineered by addition of Diphtheria toxin A fragment (DTA) as negative selection marker. Therefore, theoretically any ΔLNGFR positive cells should be transcribed by Pnmt, then the adrenergic cells, no matter on which differentiation status they are, can be characterized and even separated from other cells by MACS. Thereafter, we will target YFP mESCs with this construct and obtained the positive cell clones by both positive and negative selection in order to find the corrected targeted mESCs in which the construct is "knocked-in" into the Pnmt locus by homologous recombination. After confirmation by genetic screen, these cells will be good model to determine the characteristics of adrenergic progenitor cells during cardiac differentiation, and eventually used for further exploration of their biological activities and roles during embryonic heart development.

5.2   Materials and Methods

5.2.1   Introduction of available plasmid constructs for subclone

The purpose of the subclone is to get the correct targeting construct which we will put the Pnmt regulatory sequences in front of surface marker ΔLNGFR. The positive and negative marker should also be added and engineered into the same construct. The plasmids with our hand are as followings:

pMACS-LNGFR, 5445bp, which contains the cDNA of ΔLNGFR is provided by Miltenyi Bitotech.

pPNMT, here referred to p458, which contained mouse genome 5' Pnmt upstream regulatory sequences and also the downstream coding sequence, however, in front of the first base pair of coding sequence, an EcoRI site was created by Promega Mutagenesis kit, thus allowing us to insert the cDNA of interested gene as a marker whose expression would be exactly under the control of Pnmt regulatory sequences. The whole plasmid was 7.6kb which was already cloned as a SacI-SacI fragment, the base vector was pBluescript SK(+) from Clonetech.

pFrt-Neo, here referred to p497, was a Frt flanked Neomycin cassette which was used as seclection marker in our studies. It was subcloned into pBluescript SK(+), with HindIII and SalI as single restriction site in the head and EcoRI in the bottom, all the three sites was used during our following subclone efforts. The whole plasmid was around 5kb and the Neomycin cassette was 2.1kb.

pBJ101-DT, here referred to p8, originally from Knowles Lab of Wistar Institute, was an already subcloned plasmid which included negative selection marker Diphtheria toxin A fragment. The negative selection marker should be placed at one or both ends of the homologous DNA. The DTA sequence was under its own promoter, Herpes simplex Virus thymidine kinase (HSV-tk), which was a very strong promoter to drive the DTA expression. Thus, random insertion other than real homologous recombination was removed as DTA was not cleaved-off and exerting its toxicity. With this strategy, we can

reduce the number of clones for screening as the positive clones were enriched by this selection event [140].
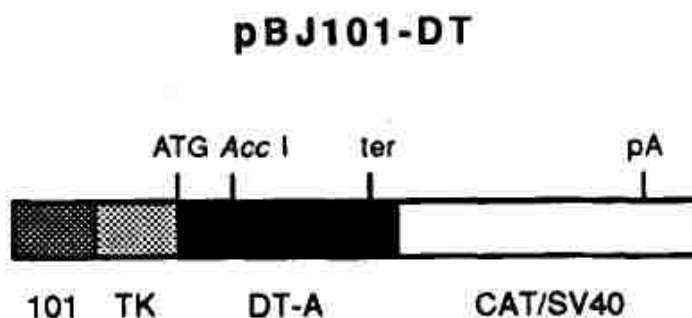
Figure 5-1. Skematic depiction of Diphtheria toxin A genetic component.

EcoRI phosphorylated linkers (Catalog No. 26-3200-09) was from Gene Link ^{TM}, with total amount of 20μg and molecular weight at 3726, the sequence of which is 5'-Pccggaattccgg-3'.

All the restriction enzymes were from New England Laboratory (NEB), T-4 DNA ligase (M0202S), Klenow Fragments of DNA polymerase (M0210S), Antarctic Phosphatase (M0289S), Calf Intestinal Alkaline Phosphatase (M0290S) and λ-HindIII digest (M3012S) were also from NEB. Small amount of plasmid extraction was proceeded by QIAprep Spin Miniprep Kit (Qiagen, Catlog No. 27106), and large amount of plasmid extraction by Qiagen Plasmid Maxi Kit (Qiagen, Catlog No. 12163). QIAquick Gel Extraction Kit (Qiagen, Catlog No. 28706) and QIAquick PCR Purification Kit (Qiagen, Catlog No. 28104) were used for purification of DNA fragments from gel

extraction and enzymatic reaction separately. UltraPure™ Phenol:Chloroform:Isoamyl Alcohol (25:24:1, v/v) was from Invitrogen. Geneticin was from In vitrogen.

XL-1 blue (Catlog No. 200249, Stratagene) competent cells were used for regular transformation with medium sized plasmid. For transformation of ligation product with large size DNA, XL-10 Gold Ultracompetent Cells (Catlog No. 200314) from Stratagene (Agilent Technology) and NEB10-beta competent cells (C3019H) from NEB were used.

5.2.2 Generation of targeting construct Pnmt-ΔLNGFR-Neo-DTA

5.2.2.1 Plasmid engineering to get ΔLNGFR and Neomycin dual cassettes

pMACS-ΔLNGFR was cut with HindIII/XhoI/EcoRI (sequential digestion, first digested with HindIII/XhoI, then EcoRI) to pop up the 1.2kb ΔLNGFR fragment. The digested product was electrophoresed in 0.8% agarose gel and DNA band at 1.2kb was cut under UV, retrieved with the Qiagen gel extraction kit. 1μl of linearized DNA was further electrophoresed for identification of the correct size. Plasmid 497 was also cut with HindIII, blunted by Klenow larger fragment, then dephosphorylated by Antarctic Phosphatase (ARP), then purified by phenol/chloroform/isoamyl alcochol and precipitated in ethanol, finally re-suspended in pure distilled water. The concentration for the vector (497) and insert (ΔLNGFR) should be higher than 30 ng/μl, thus we can clearly see the band when 1-2μl DNA was loaded into the gel.

Ligation reaction was followed the suggestions from NEB and detailed information was in the appendix B. The molar ratio of vector and insert was set between 1:3 to 1:5, thus roughly 100 to 150ng DNA (Including both vector and insert) was added

together with ligation buffer and balanced with distilled water, around 0.2μl concentrated T4 ligase was added in the end to achieve a volume of 20μl for the reaction. The reaction product was incubated at 4°C overnight. On the second day, around 5μl reaction product was transformed into either NEB10-beta or XL-10 gold competent cells. When we got the colonies, we used miniprep to extract the plasmid from bacteria cultures from individual colony and identified their insertion and orientation by restriction digestion.

The first subclone step yielded a plasmid around 6.2kb, with ΔLNGFR/Frt-Neo dual cassette cloned into pBluescript SK(+). Hence we called this plasmid p498. The plasmid was accurately confirmed by double digestion with one restriction site inside the insert (HpaI) and one outside the insert such as SacI or EcoRI.

5.2.2.2 EcoRI site creation upstream of ΔLNGFR cDNA

In the following step, theoretically we would subclone the ΔLNGFR/Frt-Neo fragment into plasmid p458. The insertion site was at EcoRI site, 3369bp downstream of the start of Pnmt regulatory elements. As for the p498, there was one EcoRI site outside of Neo cDNA, and in front of ΔLNGFR, there was only a SalI single restriction site. In consideration it was a large size subclone (3.25kb ΔLNGFR/Frt-Neo ligation with 10.6kb p458), it would be very less efficient for blunt ligation and this was confirmed by our previous efforts. So modification of the plasmid/insert was necessary in order to create cohesive site and its following ligation.

Thus in this step, the p498 was engineered to achieve another cohesive EcoRI site in front of ΔLNGFR cDNA. In order to do this, p498 was linearized by SalI and

blunted by Klenow fragment. The linearized p498 was resuspended in distilled water and the proper amount of EcoRI phosphorylated linker (the linker was dissolved in around 89ul of distilled water to get concentration of 60pmol/μl, or around 225ng/μl.) was added to make the molar ratio of linker to DNA at 50:1, then 2.5ul of 10x ligation buffer was added and the whole reaction buffer was adjusted to 24ul and then T4 DNA ligase was added. Through screening, we got the second plasmid which had two EcoRI site and named it p499.

5.2.2.3 Subclone the ΔLNGFR-Neomycin casettes into Pnmt genomic locus

Plasmid 499 was cut with EcoRI and BcgI (sequential digestion), the 3.25kb dual insert was thus isolated from the gel and purified. p458 was also cut with EcoRI, dephosphorylated and the ligation reaction was set up as mentioned above. The clones were identified by several steps. First, the extracted plasmids and p458 were loaded into gel together. The comparison of the band shift was made as the engineered plasmid with insertion should migrate a little slower than p458. The clones with slower migration were further checked by single digestion with EcoRI for insertion and double digestion with SacI/HpaI for their orientation. The correct clone was named as p461.

5.2.2.4 Generation of targeting construct Pnmt-ΔLNGFR-Neo-DTA with addition of negative selection gene

The negative selection marker was p8 (DTA), which was around 2.8kb as a SalI-SalI fragment. p8 was cut with SalI, retrieved from the gel and purified. The plasmid p460 also had only one SalI site in the Multiple Cloning Site (MCS), as the other SalI site in p497 during previous subclone steps. The p461 was digested with SalI and

dephosphorylated. The molar ratio of the vector and insert was carefully chosen as this was a large size ligation. We tried different ratios from 1:1.5 to 1:2 and 1:3. The final targeting construct was confirmed by multiple restriction digestion, with both single and double enzymes involved. The plasmid was named Pnmt-ΔLNGFR-Neo-DTA, and referred to p462. The length of the final construct was 16.62kb.

5.2.3 Generation of YFP mESCs knocked in with Pnmt-ΔLNGFR-Neo

7AC5EYFP cells (SCRC-1033™, available from ATCC) which was a R1 derived mESC line, was used for the generation of new mESCs with the Pnmt genomic locus knocked in by the above target construct. This mESC line showed yellow fluorescence as cDNA of EYFP was inserted into the genome and also kept the germ line competency which could be used for generation of genetic manipulated mice.

mESC were maintained as described in previous chapters. Cells at early passages were used for electroporation. The p462 was linearized with BcgI and then purified, around 40µg DNA was resuspended in 30µl electroporation buffer and kept sterile. The electroporation parameter and detailed protocol was described in the Chapter 4 with proper control groups included.

Geneticin (G-418 Sulfate) was used for selection of positive clones as it acts similar with neomycin but functional in eukaryotes. The concentration of G-418 during clone selection was 350µg/ml and drugs were added 1d after elctroporation and refreshed every other day. On day 5 to 6, apparently most of the cells were dead. After small patches of cells gradually came out and we will pick them out on day 10. The

criteria for good neomycin resistant clones were clearly reported before [141]. We picked up 84 colonies totally. The colonies were carefully frozen as stock for identification of correct homologous recombination by southern blot and PCR.

5.3 Results

5.3.1 Creation of Pnmt-ΔLNGFR-Neo-DTA targeting construct through series of subclone

The schematic map of the plasmid, which was based on pBluescript SK(+), was described in Fig.2. The total length of the plasmid was 16623 base pairs which was illustrated in the map. Plasmid generated from individual step was characterized in orders by restriction analysis.
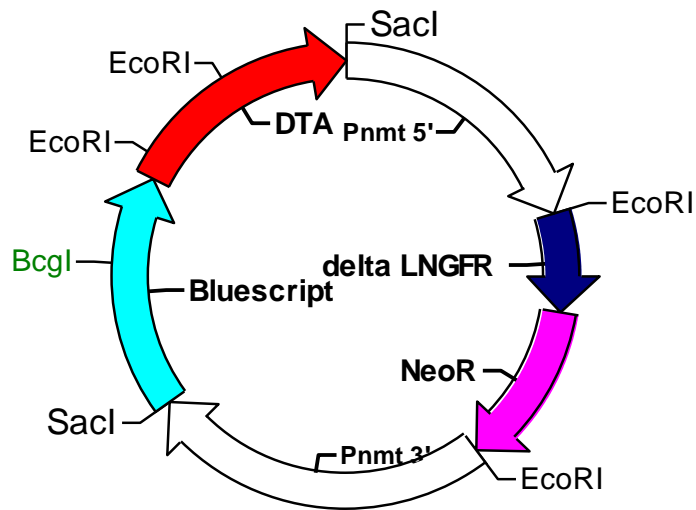
Pnmt-deltaLNGFR-Neo
16623 bp

Figure 5-2. Schematic map of targeting construct Pnmt-ΔLNGFR-Neo-DTA.

The length of each part of the plasmid was scaled to its size, with different colors representative of these component. White: the 5' and 3' of Pnmt genomic sequences; Dark blue; the cDNA of delta LNGFR; Pink, the cDNA of Neomycin resistance cassette; Red, DTA fragment; Light bluel: the pBluescript SK(+) plasmid.

5.3.1.1 Creation of plasmid with ΔLNGFR and Neomycin dual cassettes
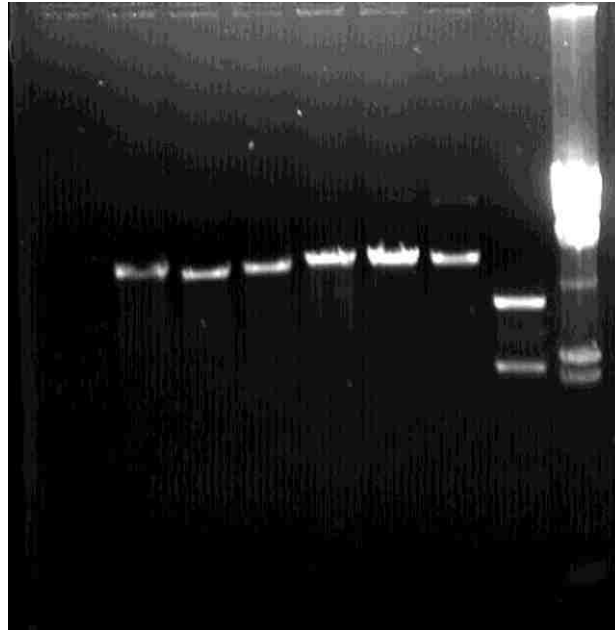
Figure 5-3. Restriction analysis of plasmid with insertion of ΔLNGFR and Neomycin resistance gene.

The 4th through 7th lanes were restriction analysis of engineered plasmid (p498) with ΔLNGFR cDNA insertion. The 4th through 6th lanes are EcoRI, SalI and BamHI single digestion respectively, where the 7th lane was SacI/HpaI double digestion for confirmation of the orientation. The rightmost band was HindIII digest as DNA ladders.

5.3.1.2 Creation of plasmid with EcoRI restriction site on both end of ΔLNGFR and Neomycin cassettes
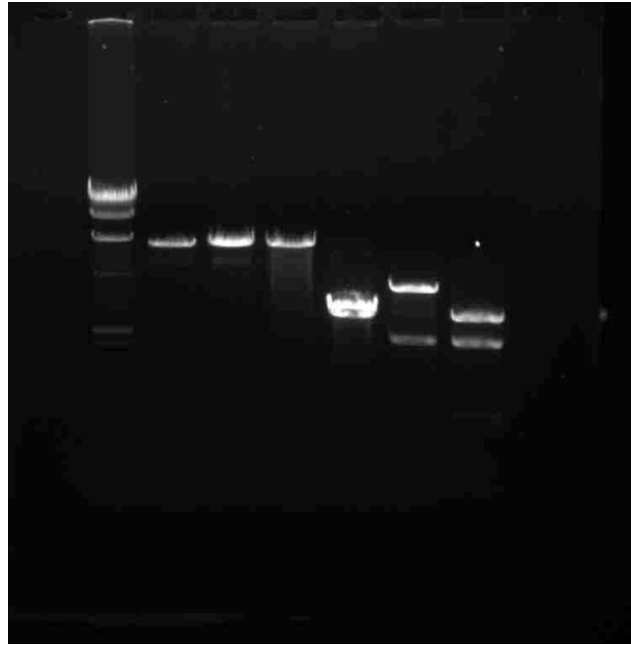
Figure 5-4. Restriction analysis of plasmid with EcoRI site on both end of ΔLNGFR and Neomycin resistance gene.

The first lane was HindIII digest as DNA ladder. The 2nd, 4th and 6th were p498, while the 3rd, 5th, 7th were p499 with correct EcoRI linker modification in front of ΔLNGFR. The 2nd and 3rd lanes were BcgI single digestion, the 4th and 5th were EcoRI single digestion, the 5th lane showed p499 with successful addition of an EcoRI site thus two bands with similar size appeared. The 6th and 7th lanes were BcgI/EcoRI double digestion which made (ΔLNGFR+NeoR) cassette of p499 easily separated from the leftover fragment. This cassette was around 3.25kb.

5.3.1.3 Creation of plasmid with ΔLNGFR and Neomycin insertion into Pnmt genomic locus
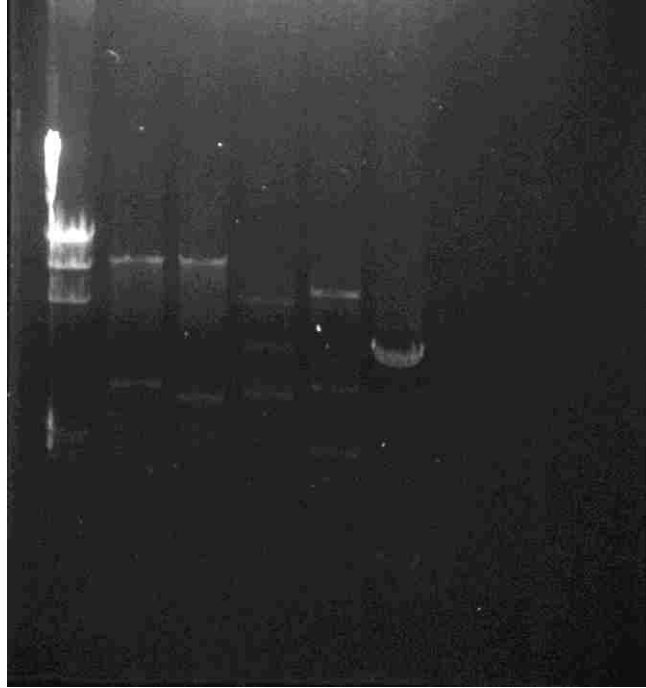
Figure 5-5. Restriction analysis of Pnmt-ΔLNGFR-Neo plasmid.

p461 was analyzed by restriction digestion. The 1st lane was HindIII digest as DNA ladder, the 2nd and 3rd lane were EcoRI and SacI single digestion respectively, the 4th lane was SacI/HpaI double digestion which showed the correct orientation of the plasmid, the 5th was BamHI/HpaI double digestion, and the 6th lane was BglI digestion of p8.

5.3.1.4 Creation of Pnmt-ΔLNGFR-Neo-DTA by addition of DTA
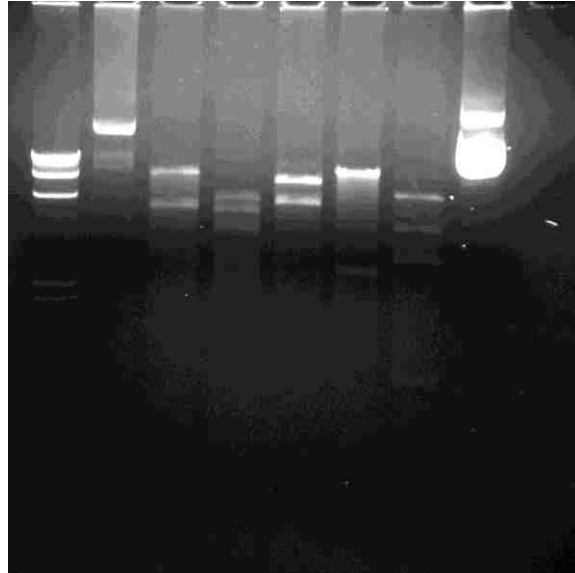
Figure 5-6. Restriction analysis of targeting construct Pnmt-ΔLNGFR-Neo-DTA.

The 1st lane was HindIII digest as DNA ladder, the 2nd lane was undigested plasmid, the 3rd was SacI digestion, 4th SacI/HpaI, 5th XhoI, 6th SalI/NotI, 7th EcoRI, all these analysis were for plasmid p462, and the last lane was undigested p461, the plasmid tested in the above figure.

For the final targeting construct, EcoRI single digestion determined both insertion of DTA fragment and the orientation of the final DTA insertion. Although the DTA has its own promoter and enhancer, its expression during the homologous recombination didn't need to follow the direction of the targeting construct. In this final plasmid, the direction of DTA transcription was the same with that of targeting construct.

5.3.2 Generation of mESC line knocked in with Pnmt-ΔLNGFR-Neo-DTA through homologous recombinations

After electroporation of linearized p462 and screened by G418, we picked 84 colonies, among which 75 colonies were continuously resistant to G418 and kept good proliferation rate. These clones were carefully maintained and each of them was frozen as back up for further identification of correct targeting.

5.4 Discussion and Future Plans

MACS technology is a well established method for cell separations. This technology utilize particular superparamagnetic particles, the diameters of which are around 50 nanometers. These magnetic particles are conjugated with specific antibodies, thus making labeling and purification of target cells available. As these particles are made of biodegradable matrix, so the enriched target cells don't need to be removed from these particles, and these particles usually don't alter the structure and activity of the labled cells. Since its discovery, this technology has already been applied in many types of cells, both from common populations to very rare cells which can't be purified with high yield and purity with other methods such as FACS [38].

MACS technology is based on above mentioned microbeads, and also MACS separator and MACS columns. When MACS column is placed in a separator, magnetic field is formed on the column matrix which can retain the cells labeled with microbeads.

There're mainly two kinds of labeling strategies: the direct magnetic cell labeling for which cells are labeled with magnetic particles conjugated with specific antibodies, usually immunogenic for antigens on cell surface; the indirect magnetic cell labeling will label cells first tagged with primary antibodies which are either unconjugated, biotinylated or fluorochrome conjugated, and then relevant anti-immunoglobulin, anti-biotin, strepatavidin or anti-fluorochrome microbeads are used for magnetic labeling. Since discovery, MACS has been widely employed for separation of many types of cell populations, such as Plasma cells from bone marrow [39], enrichment of specific spermatogonia from testis [142], separation of SSEA-4 (Undifferentiated ES cell surface marker) labeled human embryonic stem cells from heterogeneous populations [143, 144]. In addition, MACS doesn't affect the differentiation status of the initial cell input, for example, sorting of VCAM1 (Vascular cell adhesion molecule 1) positive cells from human ESC and human induced pluripotent stem cells (hiPSC) by MACS both achieved pure populations of VCAM1 positive cells, and these cells can well differentiate into functional cardiomyocytes [40]. In another study when ΔCD4 is used as surface marker, partial differentiated ES cells (day 3 after starting differentiation) could be purified by MACS, and the yield could still differentiate into all three germ layers (ectoderm, mesoderm and endoderm), elucidating the advantage of this strategy. Some reports showed that cells sorted by FACS had higher percentage of apoptotic like phenotypes [145, 146], however, there have been no reports so far for obvious cell damages of sorted cells by MACS.

In our studies, we successfully engineered the targeting construct with ΔLNGFR as the surface marker, the transcription of which is regulated by Pnmt sequences, thus isolation of these rare adrenergic progenitor cells from mixed cell populations will be technically doable. LNGFR (CD271) conjugated microbeads are commercially alavailable from Miltenyi Biotec Company along with the separation kit (column and magnetic separator). The purification of these cells will be feasible if proper amounts of LNGFR microbeads are loaded with fixed number of "knocked-in" cells. Under various differentiation status (pluiripotent, partial differentiated, terminally differentiated into beating cardiomyocytes), cells will be pooled and proceeded with MACS. We hypothesize that the expression of this surface marker would be strong enough to be detected by these antibody conjugated beads and cells would be separated from the column under magnetic conditions by positive selection, and the eluted cells will yield high concentration of positive cells, which can be confirmed by immunostaining and FACS. These sorted cells will be further characterized by their electrophysiological properties to see whether they're matched to various cell types during cardiogenesis, whether they have the features similar to specific populations, such as progenitors from ventricles, atria and conduction systems. In addition, comparisons will be made among these cells, first to see whether ΔLNGFR's expression is dependent on the differentiation status, such as the expression is negative or below detection under pluripotent status, however it will increase after cardiac differentiation, and under which status the expression is highest will also be determined, as this will indicate the peak function of Pnmt during this process. Provided that the in vitro evidence is convincing, the knock-in mouse strain will be established which will be an useful tool for further

identify and characterize the function of adrenergic cells during cardiovascular development and the compound mechanisms of regulation of cardiac growth, differentiation and other unknown functions regulated by Pnmt. Adrenergic cells from other extra-adrenal tissues can also be collected from this animal model, their functions will be uncovered to a deeper level.

CHAPTER 6   : SUMMARY

The general purpose of this thesis was to develop and apply imaging modalities and other relevant tools to evaluate the efficacy of transgene expression in specific tissues *in vivo* and determine the how this transgene expression was correlated with the potential of induction of exogenous gene therapy, or explanation of an important biological phenomena during embryonic development. We will summarize each chapter as follows:

In Chapter 2, we mainly use BLI as a particular non-invasive imaging tool, to determine its capability of evaluation of transgene expression by multiple gene delivery methods, and also characterization of genetic manipulated mESC in which luciferase reporter gene was transfected. Data clearly showed that beyond accurate detection of induced reporter gene expression, BLI possesses the advantage of detection of luminescence continuously in one single animal non-invasively, thus leading to more consistent conclusions for transgene evaluations and cost effectives. BLI has been confirmed useful in measurement of transgene expression in mouse skin, liver and heart introduced with reporter gene by biolistic and needle injection, in addition to the precise correlation of reporter gene expression and the number of pluripotent mESCs cells. Although with some limitations in the studies, BLI is deserved for evaluation of efficacy of other gene delivery methods, especially those with close to clinical applications, such as cardiac gene therapy strategies [63, 85]. With proper design, BLI is also efficient to characterize the engrafted cells, especially manipulated mESCs and hESCs into the damaged tissues, such as their locations, survival or migration patterns,

which are extremely important as cell-based therapies can systematically evaluated with no-bias, thus more convincing results related to this therapeutic strategy come out [147, 148], which will dramatically reduce the conflicted results when ESC based engraftment for cell therapy are applied to repair the injured tissues.

In Chapter 3 through 5, our main purpose was to characterize the catecholamine producing cells in different tissues and at different development stage. As adrenergic hormone deficiency will lead to fetal heart failure, in addition to the broad distribution of catecholamine production in tissues other than adrenal gland, those together prompted us to utilize genetic models to determine the location of these adrenergic cells and try to explore their functions too. We chose the most common reporter gene: EGFP as the tool and generated Pnmt-nEGFP mouse model. This model provided us detailed information for the adrenergic cells in various organs. The EGFP positive cells also expressed Pnmt in adult adrenal medullar chromaffin cells unambiguously demonstrated the accuracy of this genetic manipulation. In extention, we also checked EGFP expression in the fetal heart, although signal was weak and positive cells were also fewer, the positive EGFP cells together with EGFP expression from the Pnmt-nEGFP mESCs showed that cells with adrenergic phenotype did exist during cardiogenesis. In order to further characterize this smaller population of cells, mainly in regard to its function, we relied on other methodologies to improve the resolution to get these cells available. As mentioned in Chapter 4, we used an RFP/GFP dual fluorescence plasmid as the reporter gene and let it stably incorporate into pluripotent mESCs with Pnmt-Cre background. The Cre activation during mESC differentiation

gave us the chance to observe whether the recombination arose, here illustrated by excision of flanked RFP coding sequence through Cre. Through this "Stop then go" strategy, we observed "to go", referred to EGFP expressing cells in beating areas from 15day cardiac differentiated mESCs, which further determined the adrenergic phenotype was tightly associated with cardiac differentiation. Based on these discoveries, systematic experiments are necessary to determine at which stage of differentiation these green fluorescent cells are concentrated, and whether the cell sorting combined with antibiotic resistance selection can yield relatively pure population of these cells. Should these cells available, it will be a big breakthrough as we can determine its function by both electrophysiology, molecular biology and also engraftment *in vivo*.

The lessons from both Chapter 3 and Chapter 4 were focused on one point. The variable expression of targeted cells seemed common when fluorescent reporter gene was employed, although separate target construct was used in each chapter. For Pnmt-nEGFP model, we found less number of EGFP cells compared with those of Pnmt expressing cells in adult adrenal medulla, which we didn't know the exact answer with current data. Similar results were also found from other reports that even more diversified expression patterns existed from GFP transgenic mice with ubiquitous promoters [35]. This is so complicated due to many possible reasons. It's deserved to determine the mechanisms leading to other cells targeted with EGFP but without detectable GFP expression. Gene silencing, inhibition by some post-translational modification such as methylation are among the potential mechanism. The limitations

from the created model from Chpater 4 mainly came from the heterogenicity of RFP expression in pluripotent mESCs. Partial reasons could come from the immature status of the HcRed1 as a protein tag, as other better performed version of HcRed mutants are still under investigation. In addition, more mechanism may also account for this heterogeneous expression pattern. Further characterization of Cre expression since cardiac differentiation will let us know the dynamics of its activity, and more genetic information about the expression of EGFP since differentiation will help us get comprehensive appreciation of this process and also the enrichment of these Pnmt expressing cells.

Nevertheless, the above models show their capabilities in characterization of adrenergic cells, meantime, other strategies are also demanding which can overcome their shortages. Therefore, in the last chapter, I chose other reporter gene as alternative strategy to fulfill the same purpose of the previous two. It has been acknowledged that magnetic associated cell sorting is a far efficient way for isolation of rare population of cells compared with FACS [38], with higher yield and also higher concentration of positive cells when proper cell surface marker was chosen. In this chapter, the cDNA of human ΔLNGFR, a truncated low-affinity nerve growth factor receptor, was chosen as this marker, and engineered into Pnmt genomic locus which will recapitulate its expression *in vivo*, through homologous recombination, the targeted clones were collected and under identification. The correct targeted mESCs will enable us a powerful tool to determine the adrenergic cells during *in vitro* cardiac differentiation. At various differentiation stages (immature, partially mature and fully mature cardiomyocytes), the

111

input cells can be loaded into column under magnetic field and sorted. It will be great helpful if we can successfully sort the positive cells and do the comparison based on their expression of markers of cardiomyocyte, endothelial cells, fibroblast or other type of progenitor cells. As mentioned before, their proliferation, differentiation capability, electrical activity and performance after engraft into animal heart are also deserved for studies. This method is one of the best ways to accomplish the objective and we will eventually draw the convincing conclusion that whether this type of cells expressed in embryonic heart and also in other adult extra-adrenal organs have specific functions should the animal model is available.

All the work in these chapters will lay the ground of basic biological knowledge of Pnmt expressing cells during embryonic development. The data we have and the anticipated results from new genetic models will make us understand more broadly about specific adrenergic cells expressed in tissues other than adrenal gland. These methodologies pave the way to isolated, characterize and determine their individual function in various organs.

The reason of the long term pursuit for these adrenergic cells during embryonic heart development is we want to compare the identical and different features with those established cells which were sorted based on specific markers such as Isl-1, Sca-1, c-Kit, and also other morphogens [69]. Although these cells have been tested and confirmed as origins of cardiac progenitor cells, it's still lacking convincing data that these cells are the real cardiac progenitors, as most of the markers were also found in other type of progenitor cells. Pnmt expressing cells, although transiently expressed

during heart development, might also have some cross-over with expression of those above markers, the distinguishing between those cells and adrenergic cells will help us understand at which specific development stage do adrenergic hormone are involved in the regulation of cardiogenesis, and also the potential as target cells as therapeutic strategies for recovery of myocardium infarction and other cardiac repair.

APPENDIX A: COMPONENTS OF MEDIUM AND BUFFER FOR MOUSE EMBRYONIC STEM CELL CULTURES

Pluripotent ES cell growth medium

DMEM (4.5g/L) 500ml

Fetal Bovine Serum 90ml

Penn/Strep 6ml

Glutamx 5.8ml

Non Essential Amino Acids 5.8ml

2-mercaptoethanol 1.1 µl

LIF   600µl

ES cell differentiation medium

DMEM (4.5g/L) 500ml

Serum 90ml

Penn/Strep 5.8ml

L-glutamine 5.5ml

Non Essential Amino Acids 5.8ml

2- mercaptoethanol 1.1µl

Mouse embryonic fibroblasts (MEF) medium

DMEM(4.5g/L) 500ml

Penn/Strep 5.5ml

Fetal bovine serum: 55ml

ES cell Electroporation Buffer 50ml

10x Hanks 5ml

1M Hepes 1ml

2-Mercaptoethanol 0.1ml

1M NaOH 50μl

Double distilled water 44ml

Filtrate with 0.22μm filter by syringe and keep in -20°C

APPENDIX B: EXPERIMENTAL PROTOCOLS

Suclone for generatation of the targeting construct (Pnmt-ΔLNGFR-NeoR-DTA)

Klenow Filling for p497, pΔLNGFR and p498 (pΔLNGFR+NeoR)

DNA:	30µl
dNTP (10X):	4µl
NEB buffer 2:	1 µl
Klenow Fragment:	4µl

Room Temperature for 20mins, reaction was stopped by addition of EDTA to final concentration of 10mM, then heat inactivated at 70°C for 20mins.

Note: dNTP (N0447S from NEB) stock solution was 10mM, and the working concentration in Klenow filling was 33µM, therefore, stock dNTP solution was first diluted 30 times to get the 10X concentrated solution (330µM) with distilled water and kept at -20°C. This solution was further diluted 10 times during the reaction to yield final working concentration at 33 µM.

p497 dephosphorylation by Calf Intestinal Alkaline Phosphatase (CIP)

DNA after Klenow filling:	5µl
NEB buffer 3:	4µl
dH$_2$O	30µl
CIP	0.2µl

Total reaction volume was around 40µl and the reaction was at 37°C for 30mins, then heat inactivated at 65°C for 45mins, and purified by Phenol/Chloroform/Isopropanol (25:24:1, v/v) and precipitated by ethanol.

Ligation of p497 and ΔLNGFR

Insert	4.2µl
Vector	4.2µl
Ligation Buffer (10X)	2µl
Enzyme	0.8µl
PEG8000 (40%)	4µl
dH$_2$O	5µl

The molar ratio of insert (1.2kb ΔLNGFR and 5kb vector) was set at 5:1, the total amount of DNA in the reaction was less than 200ng. The reaction was incubated overnight at 16°C. On the second day, 5µl ligation product was used to transform into NEB 10-beta competent cells.

During the second step of subclone, when 12bp double strand oligonucleotide (5' phosphorylated EcoRI linker) was ligated with p498, the molar ratio of insert to vector was set at 50:1.

The formula for the ligation of ΔLNGFR+NeoR with Pnmt genomic sequences was similar with the above listed reaction between p497 and ΔLNGFR, the insert/vector ratio was set at 5:1.

The formula for the ligatation of pPnmt-ΔLNGFR+NeoR (461) with DTA was similar with those above, only with the ratio of insert to vector reduced to 1.5-3 to 1, which could increase the frequence of the contact between insert and vector.

β-galactosidase activity assay

This protocol is used for detection of formalin fixed frozen sections, when tissues are transfected with plasmid expressing LacZ, the transfection effects can be detected by assay the activity of gene product of lacZ, β-galactosidase, which can catalyze the hydrolysis of β-galactosides (X-gal) to form the deposition of blue colors.

X-gal Stock Solution (4% in DMF):

X-gal (5-bromo-4-chloro-3-indolyl- β-D-galactopyranoside)	20 mg
DMF (N, N Dimethylformamide)	0.5 ml

Mix till complete dissolved, store at -20°C and protected from light

X-gal Dilution Buffer:

Potassium Ferricyanide Crystalline (5mM)	160 mg
Potassium Ferricyanide Trihydrate (5mM)	210 mg
Magnesium Chloride (2mM)	20 mg
PBS	100 ml

Mix well and stored at 4 ºC, protected from light. Warm to 37°C prior to use.

X-gal Working Solution:

First warm X-gal dilution buffer to 37 ºC to prevent precipitation of X-gal.

Then dilute X-gal stock solution 1:40 in warmed X-gal dilution buffer (keep buffer warm at 37 C before applying to slides).

Procedure:

1.   Cryostat frozen sections and fix with cold 2%formalin (4 ºC) for 30minutes.

2.   Wash slides with PBS for three times with5 minutes each and then rinse in distilled water.

3.   Incubate slides in X-gal working solution at 37°C for 24 hours (Put wet Kimwipes around   the tissue to avoid the slides from).

4.   Rinse sections in PBS for 3x5 minutes

5.   Rinse with distilled water briefly.

6.   Counterstain with acidified aqueous Eosin Y Solution for 2 minutes.

7.   Rinse in distilled water.

8.   Mount the slides with aqueous mounting medium.

LIST OF REFERENCES

1. Kootstra, N.A. and I.M. Verma, *Gene therapy with viral vectors.* Annu Rev Pharmacol Toxicol, 2003. **43**: p. 413-39.
2. Al-Dosari, M.S. and X. Gao, *Nonviral gene delivery: principle, limitations, and recent progress.* AAPS J, 2009. **11**(4): p. 671-81.
3. Mintzer, M.A. and E.E. Simanek, *Nonviral vectors for gene delivery.* Chem Rev, 2009. **109**(2): p. 259-302.
4. Kawakami, S., Y. Higuchi, and M. Hashida, *Nonviral approaches for targeted delivery of plasmid DNA and oligonucleotide.* J Pharm Sci, 2008. **97**(2): p. 726-45.
5. Seow, Y. and M.J. Wood, *Biological gene delivery vehicles: beyond viral vectors.* Mol Ther, 2009. **17**(5): p. 767-77.
6. Huang, J., et al., *Myocardial injection of CA promoter-based plasmid mediates efficient transgene expression in rat heart.* J Gene Med, 2003. **5**(10): p. 900-8.
7. Li, K., et al., *Direct gene transfer into the mouse heart.* J Mol Cell Cardiol, 1997. **29**(5): p. 1499-504.
8. Wu, J.C., et al., *Molecular imaging of cardiac cell transplantation in living animals using optical bioluminescence and positron emission tomography.* Circulation, 2003. **108**(11): p. 1302-5.
9. Hakamata, Y., T. Murakami, and E. Kobayashi, *"Firefly rats" as an organ/cellular source for long-term in vivo bioluminescent imaging.* Transplantation, 2006. **81**(8): p. 1179-84.
10. Cao, F., et al., *In vivo visualization of embryonic stem cell survival, proliferation, and migration after cardiac delivery.* Circulation, 2006. **113**(7): p. 1005-14.
11. Li, Z., et al., *Differentiation, survival, and function of embryonic stem cell derived endothelial cells for ischemic heart disease.* Circulation, 2007. **116**(11 Suppl): p. I46-54.
12. Kammili, R.K., et al., *Generation of novel reporter stem cells and their application for molecular imaging of cardiac-differentiated stem cells in vivo.* Stem Cells Dev, 2010. **19**(9): p. 1437-48.
13. Klein, T.M., et al., *Transfer of foreign genes into intact maize cells with high-velocity microprojectiles.* Proc Natl Acad Sci U S A, 1988. **85**(12): p. 4305-9.
14. Klein, T.M., et al., *Stable genetic transformation of intact Nicotiana cells by the particle bombardment process.* Proc Natl Acad Sci U S A, 1988. **85**(22): p. 8502-5.
15. Daniell, H., *Transformation and foreign gene expression in plants by microprojectile bombardment.* Methods Mol Biol, 1997. **62**: p. 463-89.
16. Daniell, H., et al., *Transient foreign gene expression in chloroplasts of cultured tobacco cells after biolistic delivery of chloroplast vectors.* Proc Natl Acad Sci U S A, 1990. **87**(1): p. 88-92.
17. Matsuno, Y., et al., *Nonviral gene gun mediated transfer into the beating heart.* ASAIO J, 2003. **49**(6): p. 641-4.

18.   Uchida, M., et al., *Transfection by particle bombardment: delivery of plasmid DNA into mammalian cells using gene gun.* Biochim Biophys Acta, 2009. **1790**(8): p. 754-64.

19.   Muangmoonchai, R., et al., *Transfection of liver in vivo by biolistic particle delivery: its use in the investigation of cytochrome P450 gene regulation.* Mol Biotechnol, 2002. **20**(2): p. 145-51.

20.   Amenta, J.J. and G.S. Pitt, *The glitter of gold: biolistic transfection of fresh adult cardiac myocytes. Focus on "normal targeting of a tagged Kv1.5 channel acutely transfected into fresh adult cardiac myocytes by a biolistic method".* Am J Physiol Cell Physiol, 2010. **298**(6): p. C1305-7.

21.   Ginsberg, B.A., et al., *Immunologic response to xenogeneic gp100 DNA in melanoma patients: comparison of particle-mediated epidermal delivery with intramuscular injection.* Clin Cancer Res, 2010. **16**(15): p. 4057-65.

22.   Kim, J.W., et al., *Comparison of HPV DNA vaccines employing intracellular targeting strategies.* Gene Ther, 2004. **11**(12): p. 1011-8.

23.   Mahvi, D.M., et al., *Immunization by particle-mediated transfer of the granulocyte-macrophage colony-stimulating factor gene into autologous tumor cells in melanoma or sarcoma patients: report of a phase I/IB study.* Hum Gene Ther, 2002. **13**(14): p. 1711-21.

24.   Kvetnansky, R., E.L. Sabban, and M. Palkovits, *Catecholaminergic systems in stress: structural and molecular genetic approaches.* Physiol Rev, 2009. **89**(2): p. 535-606.

25.   Bohn, M.C., M. Goldstein, and I.B. Black, *Expression and development of phenylethanolamine N-methyltransferase (PNMT) in rat brain stem: studies with glucocorticoids.* Dev Biol, 1986. **114**(1): p. 180-93.

26.   Ziegler, M.G., et al., *Location, development, control, and function of extraadrenal phenylethanolamine N-methyltransferase.* Ann N Y Acad Sci, 2002. **971**: p. 76-82.

27.   Kennedy, B., T.D. Bigby, and M.G. Ziegler, *Nonadrenal epinephrine-forming enzymes in humans. Characteristics, distribution, regulation, and relationship to epinephrine levels.* J Clin Invest, 1995. **95**(6): p. 2896-902.

28.   Campos, M.B., et al., *Catecholamine distribution in adult rat testis.* Andrologia, 1990. **22**(3): p. 247-50.

29.   Bergquist, J., et al., *Discovery of endogenous catecholamines in lymphocytes and evidence for catecholamine regulation of lymphocyte function via an autocrine loop.* Proc Natl Acad Sci U S A, 1994. **91**(26): p. 12912-6.

30.   Ebert, S.N. and R.P. Thompson, *Embryonic epinephrine synthesis in the rat heart before innervation: association with pacemaking and conduction tissue development.* Circ Res, 2001. **88**(1): p. 117-24.

31.   Ebert, S.N., et al., *Expression of phenylethanolamine n-methyltransferase in the embryonic rat heart.* J Mol Cell Cardiol, 1996. **28**(8): p. 1653-8.

32.   Ignarro, L.J. and F.E. Shideman, *Norepinephrine and epinephrine in the embryo and embryonic heart of the chick: uptake and subcellular distribution.* J Pharmacol Exp Ther, 1968. **159**(1): p. 49-58.

33. Ebert, S.N., et al., *Targeted insertion of the Cre-recombinase gene at the phenylethanolamine n-methyltransferase locus: a new model for studying the developmental distribution of adrenergic cells.* Dev Dyn, 2004. **231**(4): p. 849-58.
34. Huang, M.H., et al., *An intrinsic adrenergic system in mammalian heart.* J Clin Invest, 1996. **98**(6): p. 1298-1303.
35. Swenson, E.S., et al., *Limitations of green fluorescent protein as a cell lineage marker.* Stem Cells, 2007. **25**(10): p. 2593-600.
36. Van Overstraeten-Schlogel, N., et al., *Limitations of the use of GFP transgenic mice in bone marrow transplantation studies.* Leuk Lymphoma, 2006. **47**(7): p. 1392-3.
37. Pfannkuche, K., et al., *Generation of a double-fluorescent double-selectable Cre/loxP indicator vector for monitoring of intracellular recombination events.* Nat Protoc, 2008. **3**(9): p. 1510-26.
38. David, R., M. Groebner, and W.M. Franz, *Magnetic cell sorting purification of differentiated embryonic stem cells stably expressing truncated human CD4 as surface marker.* Stem Cells, 2005. **23**(4): p. 477-82.
39. Cumova, J., et al., *Optimization of immunomagnetic selection of myeloma cells from bone marrow using magnetic activated cell sorting.* Int J Hematol, 2010. **92**(2): p. 314-9.
40. Fujiwara, M., et al., *Induction and enhancement of cardiac cell differentiation from mouse and human induced pluripotent stem cells with cyclosporin-A.* PLoS One, 2011. **6**(2): p. e16734.
41. Qasim, W., et al., *T cell transduction and suicide with an enhanced mutant thymidine kinase.* Gene Ther, 2002. **9**(12): p. 824-7.
42. Zhang, J., et al., *Isolation of neural crest-derived stem cells from rat embryonic mandibular processes.* Biol Cell, 2006. **98**(10): p. 567-75.
43. Kohn, D.B. and F. Candotti, *Gene therapy fulfilling its promise.* N Engl J Med, 2009. **360**(5): p. 518-21.
44. Engel, B.C. and D.B. Kohn, *Gene therapy for inborn and acquired immune deficiency disorders.* Acta Haematol, 2003. **110**(2-3): p. 60-70.
45. Wu, J.C., et al., *Optical imaging of cardiac reporter gene expression in living rats.* Circulation, 2002. **105**(14): p. 1631-4.
46. Heilbronn, R. and S. Weger, *Viral vectors for gene transfer: current status of gene therapeutics.* Handb Exp Pharmacol, 2010(197): p. 143-70.
47. Somia, N. and I.M. Verma, *Gene therapy: trials and tribulations.* Nat Rev Genet, 2000. **1**(2): p. 91-9.
48. *Controversy of the year. Biomedical ethics on the front burner.* Science, 2000. **290**(5500): p. 2225.
49. Grilley, B.J. and A.P. Gee, *Gene transfer: regulatory issues and their impact on the clinical investigator and the good manufacturing production facility.* Cytotherapy, 2003. **5**(3): p. 197-207.
50. Couzin, J. and J. Kaiser, *Gene therapy. As Gelsinger case ends, gene therapy suffers another blow.* Science, 2005. **307**(5712): p. 1028.

51.   Yarborough, M. and R.R. Sharp, *Public trust and research a decade later: what have we learned since Jesse Gelsinger's death?* Mol Genet Metab, 2009. **97**(1): p. 4-5.

52.   Dunbar, C.E. and A. Larochelle, *Gene therapy activates EVI1, destabilizes chromosomes.* Nat Med, 2010. **16**(2): p. 163-5.

53.   Stein, S., et al., *Genomic instability and myelodysplasia with monosomy 7 consequent to EVI1 activation after gene therapy for chronic granulomatous disease.* Nat Med, 2010. **16**(2): p. 198-204.

54.   Niidome, T. and L. Huang, *Gene therapy progress and prospects: nonviral vectors.* Gene Ther, 2002. **9**(24): p. 1647-52.

55.   Nishikawa, M. and L. Huang, *Nonviral vectors in the new millennium: delivery barriers in gene transfer.* Hum Gene Ther, 2001. **12**(8): p. 861-70.

56.   Losordo, D.W., et al., *Gene therapy for myocardial angiogenesis: initial clinical results with direct myocardial injection of phVEGF165 as sole therapy for myocardial ischemia.* Circulation, 1998. **98**(25): p. 2800-4.

57.   Bougioukas, I., et al., *Intramyocardial injection of low-dose basic fibroblast growth factor or vascular endothelial growth factor induces angiogenesis in the infarcted rabbit myocardium.* Cardiovasc Pathol, 2007. **16**(2): p. 63-8.

58.   Choi, J.S., et al., *Efficacy of therapeutic angiogenesis by intramyocardial injection of pCK-VEGF165 in pigs.* Ann Thorac Surg, 2006. **82**(2): p. 679-86.

59.   Lin, C.C., et al., *Delivery of noncarrier naked DNA vaccine into the skin by supersonic flow induces a polarized T helper type 1 immune response to cancer.* J Gene Med, 2008. **10**(6): p. 679-89.

60.   Yang, N.S., et al., *Particle-mediated gene delivery in vivo and in vitro.* Curr Protoc Hum Genet, 2001. **Chapter 12**: p. Unit 12 6.

61.   O'Brien, J.A. and S.C. Lummis, *Biolistic transfection of neuronal cultures using a hand-held gene gun.* Nat Protoc, 2006. **1**(2): p. 977-81.

62.   Matthews, K., et al., *The effects of gene gun delivered pIL-3 adjuvant on skin pathology and cytokine expression.* Vet Immunol Immunopathol, 2007. **119**(3-4): p. 233-42.

63.   Muller, O.J., H.A. Katus, and R. Bekeredjian, *Targeting the heart with gene therapy-optimized gene delivery methods.* Cardiovasc Res, 2007. **73**(3): p. 453-62.

64.   Schwarz, E.R., et al., *Evaluation of the effects of intramyocardial injection of DNA expressing vascular endothelial growth factor (VEGF) in a myocardial infarction model in the rat--angiogenesis and angioma formation.* J Am Coll Cardiol, 2000. **35**(5): p. 1323-30.

65.   Korpanty, G., et al., *Targeting of VEGF-mediated angiogenesis to rat myocardium using ultrasonic destruction of microbubbles.* Gene Ther, 2005. **12**(17): p. 1305-12.

66.   Bekeredjian, R., et al., *Ultrasound-targeted microbubble destruction can repeatedly direct highly specific plasmid expression to the heart.* Circulation, 2003. **108**(8): p. 1022-6.

67.   Schachinger, V., et al., *Intracoronary bone marrow-derived progenitor cells in acute myocardial infarction.* N Engl J Med, 2006. **355**(12): p. 1210-21.

68. Assmus, B., V. Schachinger, and A.M. Zeiher, *[Regenerative therapy in cardiology: how distant is it from reality?].* Internist (Berl), 2006. **47**(11): p. 1177-82.

69. Martin-Puig, S., Z. Wang, and K.R. Chien, *Lives of a heart cell: tracing the origins of cardiac progenitors.* Cell Stem Cell, 2008. **2**(4): p. 320-31.

70. Lau, J.F., et al., *Imaging approaches for the study of cell-based cardiac therapies.* Nat Rev Cardiol, 2010. **7**(2): p. 97-105.

71. Giudice, A. and A. Trounson, *Genetic modification of human embryonic stem cells for derivation of target cells.* Cell Stem Cell, 2008. **2**(5): p. 422-33.

72. Habermann, F.A., et al., *Reporter genes for embryogenesis research in livestock species.* Theriogenology, 2007. **68 Suppl 1**: p. S116-24.

73. Hadjantonakis, A.K., S. Macmaster, and A. Nagy, *Embryonic stem cells and mice expressing different GFP variants for multiple non-invasive reporter usage within a single animal.* BMC Biotechnol, 2002. **2**: p. 11.

74. Hadjantonakis, A.K. and A. Nagy, *The color of mice: in the light of GFP-variant reporters.* Histochem Cell Biol, 2001. **115**(1): p. 49-58.

75. Wilson, K.D., M. Huang, and J.C. Wu, *Bioluminescence reporter gene imaging of human embryonic stem cell survival, proliferation, and fate.* Methods Mol Biol, 2009. **574**: p. 87-103.

76. Knollmann, B.C., et al., *Kcnq1 contributes to an adrenergic-sensitive steady-state K+ current in mouse heart.* Biochem Biophys Res Commun, 2007. **360**(1): p. 212-8.

77. Ebert, S.N., et al., *Egr-1 activation of rat adrenal phenylethanolamine N-methyltransferase gene.* J Biol Chem, 1994. **269**(33): p. 20885-98.

78. Barnes, K.V., et al., *Cloning of cardiac, kidney, and brain promoters of the feline ncx1 gene.* J Biol Chem, 1997. **272**(17): p. 11510-7.

79. Yang, N.S., et al., *In vivo and in vitro gene transfer to mammalian somatic cells by particle bombardment.* Proc Natl Acad Sci U S A, 1990. **87**(24): p. 9568-72.

80. Maurisse, R., et al., *Comparative transfection of DNA into primary and transformed mammalian cells from different lineages.* BMC Biotechnol, 2010. **10**: p. 9.

81. Sundaram, P., W. Xiao, and J.L. Brandsma, *Particle-mediated delivery of recombinant expression vectors to rabbit skin induces high-titered polyclonal antisera (and circumvents purification of a protein immunogen).* Nucleic Acids Res, 1996. **24**(7): p. 1375-7.

82. Larregina, A.T., et al., *Direct transfection and activation of human cutaneous dendritic cells.* Gene Ther, 2001. **8**(8): p. 608-17.

83. Yoshida, Y., et al., *Introduction of DNA into rat liver with a hand-held gene gun: distribution of the expressed enzyme, [32P]DNA, and Ca2+ flux.* Biochem Biophys Res Commun, 1997. **234**(3): p. 695-700.

84. Nishizaki, K., et al., *In vivo gene gun-mediated transduction into rat heart with Epstein-Barr virus-based episomal vectors.* Ann Thorac Surg, 2000. **70**(4): p. 1332-7.

85. Fishbein, I., et al., *Site specific gene delivery in the cardiovascular system.* J Control Release, 2005. **109**(1-3): p. 37-48.

86. Sheikh, A.Y., et al., *Molecular imaging of bone marrow mononuclear cell homing and engraftment in ischemic myocardium.* Stem Cells, 2007. **25**(10): p. 2677-84.

87. van der Bogt, K.E., et al., *Comparison of different adult stem cell types for treatment of myocardial ischemia.* Circulation, 2008. **118**(14 Suppl): p. S121-9.

88. Al-Dosari, M., et al., *Evaluation of viral and mammalian promoters for driving transgene expression in mouse liver.* Biochem Biophys Res Commun, 2006. **339**(2): p. 673-8.

89. Brooks, A.R., et al., *Transcriptional silencing is associated with extensive methylation of the CMV promoter following adenoviral gene delivery to muscle.* J Gene Med, 2004. **6**(4): p. 395-404.

90. Hsu, C.C., et al., *Targeted methylation of CMV and E1A viral promoters.* Biochem Biophys Res Commun, 2010. **402**(2): p. 228-34.

91. Subramaniam, A., et al., *Tissue-specific regulation of the alpha-myosin heavy chain gene promoter in transgenic mice.* J Biol Chem, 1991. **266**(36): p. 24613-20.

92. Roy, M.J., et al., *Induction of antigen-specific CD8+ T cells, T helper cells, and protective levels of antibody in humans by particle-mediated administration of a hepatitis B virus DNA vaccine.* Vaccine, 2000. **19**(7-8): p. 764-78.

93. Moller, P., et al., *Vaccination with IL-7 gene-modified autologous melanoma cells can enhance the anti-melanoma lytic activity in peripheral blood of patients with a good clinical performance status: a clinical phase I study.* Br J Cancer, 1998. **77**(11): p. 1907-16.

94. Sun, Y., et al., *Vaccination with IL-12 gene-modified autologous melanoma cells: preclinical results and a first clinical phase I study.* Gene Ther, 1998. **5**(4): p. 481-90.

95. Kudlacz, E.M., et al., *Adrenergic modulation of cardiac development in the rat: effects of prenatal exposure to propranolol via continuous maternal infusion.* J Dev Physiol, 1990. **13**(5): p. 243-9.

96. Thomas, S.A., A.M. Matsumoto, and R.D. Palmiter, *Noradrenaline is essential for mouse fetal development.* Nature, 1995. **374**(6523): p. 643-6.

97. Ziegler, M.G., B.P. Kennedy, and F.W. Houts, *Extra-adrenal nonneuronal epinephrine and phenylethanolamine-N-methyltransferase.* Adv Pharmacol, 1998. **42**: p. 843-6.

98. Slotkin, T.A., C. Lau, and F.J. Seidler, *Beta-adrenergic receptor overexpression in the fetal rat: distribution, receptor subtypes, and coupling to adenylate cyclase activity via G-proteins.* Toxicol Appl Pharmacol, 1994. **129**(2): p. 223-34.

99. Maltsev, V.A., et al., *Cardiomyocytes differentiated in vitro from embryonic stem cells developmentally express cardiac-specific genes and ionic currents.* Circ Res, 1994. **75**(2): p. 233-44.

100. Sachinidis, A., et al., *Cardiac specific differentiation of mouse embryonic stem cells.* Cardiovasc Res, 2003. **58**(2): p. 278-91.

101. Bao, X., et al., *Epinephrine is required for normal cardiovascular responses to stress in the phenylethanolamine N-methyltransferase knockout mouse.* Circulation, 2007. **116**(9): p. 1024-31.

102. Andreassi, J.L., 2nd, W.B. Eggleston, and J.K. Stewart, *Phenylethanolamine N-methyltransferase mRNA in rat spleen and thymus.* Neurosci Lett, 1998. **241**(2-3): p. 75-8.

103. Davidoff, M.S., et al., *Catecholamine-synthesizing enzymes in the adult and prenatal human testis.* Histochem Cell Biol, 2005. **124**(3-4): p. 313-23.

104. Hammang, J.P., M.C. Bohn, and A. Messing, *Phenylethanolamine N-methyltransferase (PNMT)-expressing horizontal cells in the rat retina: a study employing double-label immunohistochemistry.* J Comp Neurol, 1992. **316**(3): p. 383-9.

105. Josefsson, E., et al., *Catecholamines are synthesized by mouse lymphocytes and regulate function of these cells by induction of apoptosis.* Immunology, 1996. **88**(1): p. 140-6.

106. Pendleton, R.G., G. Gessner, and J. Sawyer, *Studies on the distribution of phenylethanolamine N-methyltransferase and epinephrine in the rat.* Res Commun Chem Pathol Pharmacol, 1978. **21**(2): p. 315-25.

107. Boheler, K.R., et al., *Differentiation of pluripotent embryonic stem cells into cardiomyocytes.* Circ Res, 2002. **91**(3): p. 189-201.

108. Sachinidis, A., et al., *Generation of cardiomyocytes from embryonic stem cells experimental studies.* Herz, 2002. **27**(7): p. 589-97.

109. Prelle, K., N. Zink, and E. Wolf, *Pluripotent stem cells--model of embryonic development, tool for gene targeting, and basis of cell therapy.* Anat Histol Embryol, 2002. **31**(3): p. 169-86.

110. Hescheler, J., et al., *Embryonic stem cells as a model for the physiological analysis of the cardiovascular system.* Methods Mol Biol, 2002. **185**: p. 169-87.

111. Hescheler, J., et al., *Embryonic stem cells: a model to study structural and functional properties in cardiomyogenesis.* Cardiovasc Res, 1997. **36**(2): p. 149-62.

112. Roebroek, A.J., X. Wu, and R.J. Bram, *Knockin approaches.* Methods Mol Biol, 2003. **209**: p. 187-200.

113. Limaye, A., B. Hall, and A.B. Kulkarni, *Manipulation of mouse embryonic stem cells for knockout mouse production.* Curr Protoc Cell Biol, 2009. **Chapter 19**: p. Unit 19 13 19 13 1-24.

114. Haruyama, N., A. Cho, and A.B. Kulkarni, *Overview: engineering transgenic constructs and mice.* Curr Protoc Cell Biol, 2009. **Chapter 19**: p. Unit 19 10.

115. Sauer, B. and N. Henderson, *Site-specific DNA recombination in mammalian cells by the Cre recombinase of bacteriophage P1.* Proc Natl Acad Sci U S A, 1988. **85**(14): p. 5166-70.

116. Ghosh, K. and G.D. Van Duyne, *Cre-loxP biochemistry.* Methods, 2002. **28**(3): p. 374-83.

117. Kuhn, R. and R.M. Torres, *Cre/loxP recombination system and gene targeting.* Methods Mol Biol, 2002. **180**: p. 175-204.

118. Utomo, A.R., A.Y. Nikitin, and W.H. Lee, *Temporal, spatial, and cell type-specific control of Cre-mediated DNA recombination in transgenic mice.* Nat Biotechnol, 1999. **17**(11): p. 1091-6.

119. Lee, E.J. and J.L. Jameson, *Cell-specific Cre-mediated activation of the diphtheria toxin gene in pituitary tumor cells: potential for cytotoxic gene therapy.* Hum Gene Ther, 2002. **13**(4): p. 533-42.

120. Buch, T., et al., *A Cre-inducible diphtheria toxin receptor mediates cell lineage ablation after toxin administration.* Nat Methods, 2005. **2**(6): p. 419-26.

121. Kurosawa, H., *Methods for inducing embryoid body formation: in vitro differentiation system of embryonic stem cells.* J Biosci Bioeng, 2007. **103**(5): p. 389-98.

122. Sargent, C.Y., G.Y. Berguig, and T.C. McDevitt, *Cardiomyogenic differentiation of embryoid bodies is promoted by rotary orbital suspension culture.* Tissue Eng Part A, 2009. **15**(2): p. 331-42.

123. Carpenedo, R.L., C.Y. Sargent, and T.C. McDevitt, *Rotary suspension culture enhances the efficiency, yield, and homogeneity of embryoid body differentiation.* Stem Cells, 2007. **25**(9): p. 2224-34.

124. Vintersten, K., et al., *Mouse in red: red fluorescent protein expression in mouse ES cells, embryos, and adult animals.* Genesis, 2004. **40**(4): p. 241-6.

125. Long, J.Z., C.S. Lackan, and A.K. Hadjantonakis, *Genetic and spectrally distinct in vivo imaging: embryonic stem cells and mice with widespread expression of a monomeric red fluorescent protein.* BMC Biotechnol, 2005. **5**: p. 20.

126. Mudalige, K., et al., *Photophysics of the red chromophore of HcRed: evidence for cis-trans isomerization and protonation-state changes.* J Phys Chem B, 2010. **114**(13): p. 4678-85.

127. Hasuwa, H., et al., *Small interfering RNA and gene silencing in transgenic mice and rats.* FEBS Lett, 2002. **532**(1-2): p. 227-30.

128. Campbell, R.E., et al., *A monomeric red fluorescent protein.* Proc Natl Acad Sci U S A, 2002. **99**(12): p. 7877-82.

129. Fradkov, A.F., et al., *Far-red fluorescent tag for protein labelling.* Biochem J, 2002. **368**(Pt 1): p. 17-21.

130. Maltsev, V.A., et al., *Embryonic stem cells differentiate in vitro into cardiomyocytes representing sinusnodal, atrial and ventricular cell types.* Mech Dev, 1993. **44**(1): p. 41-50.

131. Rajala, K., M. Pekkanen-Mattila, and K. Aalto-Setala, *Cardiac differentiation of pluripotent stem cells.* Stem Cells Int, 2011. **2011**: p. 383709.

132. Ebendal, T., *Function and evolution in the NGF family and its receptors.* J Neurosci Res, 1992. **32**(4): p. 461-70.

133. Hantzopoulos, P.A., et al., *The low affinity NGF receptor, p75, can collaborate with each of the Trks to potentiate functional responses to the neurotrophins.* Neuron, 1994. **13**(1): p. 187-201.

134. Quirici, N., et al., *Isolation of bone marrow mesenchymal stem cells by anti-nerve growth factor receptor antibodies.* Exp Hematol, 2002. **30**(7): p. 783-91.

135. Cattoretti, G., et al., *Bone marrow stroma in humans: anti-nerve growth factor receptor antibodies selectively stain reticular cells in vivo and in vitro.* Blood, 1993. **81**(7): p. 1726-38.

136. Huang, E., et al., *Characterization of rat hair follicle stem cells selected by vario magnetic activated cell sorting system.* Acta Histochem Cytochem, 2009. **42**(5): p. 129-36.

137. Lauer, U.M., et al., *A prototype transduction tag system (delta LNGFR/NGF) for noninvasive clinical gene therapy monitoring.* Cancer Gene Ther, 2000. **7**(3): p. 430-7.

138. Dijkers, P.F., et al., *Forkhead transcription factor FKHR-L1 modulates cytokine-dependent transcriptional regulation of p27(KIP1).* Mol Cell Biol, 2000. **20**(24): p. 9138-48.

139. Mavilio, F., et al., *Peripheral blood lymphocytes as target cells of retroviral vector-mediated gene transfer.* Blood, 1994. **83**(7): p. 1988-97.

140. McCarrick, J.W., 3rd, et al., *Positive-negative selection gene targeting with the diphtheria toxin A-chain gene in mouse embryonic stem cells.* Transgenic Res, 1993. **2**(4): p. 183-90.

141. Tompers, D.M. and P.A. Labosky, *Electroporation of murine embryonic stem cells: a step-by-step guide.* Stem Cells, 2004. **22**(3): p. 243-9.

142. Gassei, K., J. Ehmcke, and S. Schlatt, *Efficient enrichment of undifferentiated GFR alpha 1+ spermatogonia from immature rat testis by magnetic activated cell sorting.* Cell Tissue Res, 2009. **337**(1): p. 177-83.

143. Fong, C.Y., et al., *Separation of SSEA-4 and TRA-1-60 labelled undifferentiated human embryonic stem cells from a heterogeneous cell population using magnetic-activated cell sorting (MACS) and fluorescence-activated cell sorting (FACS).* Stem Cell Rev, 2009. **5**(1): p. 72-80.

144. Schriebl, K., et al., *Stem cell separation: a bottleneck in stem cell therapy.* Biotechnol J, 2010. **5**(1): p. 50-61.

145. Fukuda, H., et al., *Fluorescence-activated cell sorting-based purification of embryonic stem cell-derived neural precursors averts tumor formation after transplantation.* Stem Cells, 2006. **24**(3): p. 763-71.

146. Pruszak, J., et al., *Markers and methods for cell sorting of human embryonic stem cell-derived neural cell populations.* Stem Cells, 2007. **25**(9): p. 2257-68.

147. Terrovitis, J.V., R.R. Smith, and E. Marban, *Assessment and optimization of cell engraftment after transplantation into the heart.* Circ Res, 2010. **106**(3): p. 479-94.

148. Codina, M., J. Elser, and K.B. Margulies, *Current status of stem cell therapy in heart failure.* Curr Cardiol Rep, 2010. **12**(3): p. 199-208.